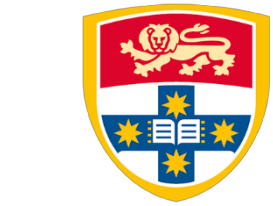

THE UNIVERSITY OF SYDNEY

Developing high performance polymeric nano-composites for tribological applications

A Thesis Submitted to

Faculty of Engineering and Information Technologies

By

Abdulaziz Kurdi

A thesis submitted in fulfilment of the requirements for the degree of

Doctor of Philosophy in the

School of Aerospace, Mechanical and Mechatronic Engineering

University of Sydney

November, 2018

Declaration

I hereby declare that no part of this work has previously been accepted for the award of any other degree in any university or institute. This thesis was completed during my enrolment for degree of Doctor of Philosophy at the University of Sydney, and to the best of my knowledge the material presented is original except where due reference is made in the text of the thesis.

Signature of Student: **Abdulaziz Kurdi**

Authorship attribution statement

*Chapter (2) and part of chapters (1 & 8) of this thesis has been published as [**A. Kurdi**, et al., Recent Advances in High Performance Polymers - Tribological Aspects, Lubricants, 7(1) (2019) 2-31]. I designed the study, identified the key points of discussion and wrote the final paper.*

*Chapter (4) and part of chapter (3) of this thesis is published as [**A. Kurdi**, et al., Comparative tribological and mechanical property analysis of nano-silica and nano-rubber reinforced epoxy composites. 2ed International Conference on Material Engineering and Application (ICMEA 2017), August 2017, Shanghai, China: Applied Mechanics and Materials ISSN: 1662-7482, Vol. 875, pp 53-60]. I designed and performed experiments, interpreted data and wrote the Manuscript.*

*Chapter (5) of this thesis is published as [**A. Kurdi**, et al., Effect of nano-sized TiO2 addition on tribological behavior of poly ether ether ketone composite, Tribology International, 117 (2018) 225–235]. I obtained the experimental results and wrote the final draft of the paper.*

*Chapter (6) and part of chapter (3) of this thesis is published as [**A. Kurdi**, et al., Tribological behaviour of high performance polymers and polymer composites at elevated temperature, Tribology International, 130 (2019) 94-105]. I developed a conceptual framework, identified the findings of study and wrote the Manuscript.*

In addition to the statements above, in cases where I am not the corresponding author of a published item, permission to include the published material has been granted by the corresponding author.

Abdulaziz Kurdi

Acknowledgment

First of all, I would like to express my sincere gratitude and appreciation to my supervisor Dr. Li Chang for his guidance, motivation, encouragement and scientific support during my PhD studies. I could not have imagined having a better supervisor and mentor for my PhD study.

I would like to give very special thanks to Saudi Arabian Cultural Mission (SACM) and King Abdulaziz City for Science and Technology (KACT) for financial support for this research through the scholarship programme.

I would like also to express my thanks to the School Aerospace, Mechanical, and Mechatronic Engineering (AMME) at the University of Sydney to provide me such a wonderful chance to complete my PhD researches. My appreciation is also extended to the Australian Centre for Microscopy & Microanalysis (ACMM) for the help in conducting different types of microscopy techniques.

My sincere thanks also go to Dr. Hongjian Wang for his assistance, guidance and various technical help provided during my researches. My sincere thanks are also extended to Dr. Hamed Kalhori, Dr. Kunkun Fu, Dr. Wen Hao Kan and Mr. Qinghao He for their kind help and advices during my studying.

My deepest thanks and great appreciation go to all my lovely family members: my parents Adel Kurdi and Fatemah Al-Saqaf for their support and encouragement throughout my life and my brother and my sisters for all their love and motivation.

Finally, my greatest thanks to my dear wife Doaa Almalki and my kids (Adel, Omar and Ola) for their patience, understanding and supporting. My words cannot express my feeling toward them

Abstract

Polymers and their composites have been widely applied in different industrial sectors as alternatives to conventional metal-based materials, for the better performance of the system, increasing efficiency and cutting down operational costs. In those applications polymeric materials are sometime subjected to tribological loading conditions where external lubricants are not permissible and polymers' self-lubricating ability is desirable in such tribo-contacts. However, additional problems can arise from the harsh service environments such as high environment temperature, high '*pv*' (pressure-velocity) as well as corrosive medium. In particular, high temperature is often the key factor determining the working conditions of polymers. Hence, high performance polymers (HPPs) have received increasing attention in last decades. On the other hand, engineering polymers are often blended with different types of reinforcing and/or functional elements to further enhance their properties. In particular, there are significant research interests in the use of nano-sized fillers to develop high performance polymer nanocomposites.

In view of above-mentioned facts, the present research investigated the tribological performance of some important engineering polymers and their nanocomposites such as epoxy, PEEK, PPP and PBI. For example, nano-silica (SiO_2), nano-rubber (CBTN) and titanium dioxide (TiO_2) nano-particles have been incorporated in thermosetting epoxy resin and PEEK, respectively, to improve their tribological properties. The results showed that both mechanical and tribological properties of nano-filler blended composites could be effectively improved, compared to neat polymers. However, the

resultant wear properties of polymer nanocomposites were greatly affected by the dispersion of nanofillers, as well as the formation of transfer film layers. Further, the wear properties of HPPs, namely PPP and PBI were also investigated and compared. To explore the effect of harsh environments during sliding wear, pin-on-disk tests of above-mentioned materials were carried out in dry, wet and elevated temperature regimes. The wear testing was followed by the surface and cross-sectional analysis of the wear-tracks with the help of scanning electron microscopy (SEM) with emphasis on the morphology of transfer film layers (TFLs). Further, the thickness and distribution of TFLs were measured using a nanoindentation and as well as possible structural changes of the materials by Fourier transformed infrared (FTIR) technique. The results showed that TFLs play the vital role in determining the deformation and wear of materials during sliding as they may change the nature of the tribo-contact from initial metal-polymer contact to polymer-polymer contacts. Based on the experimental investigation, it was concluded that, intrinsic molecular structure of PEEK synergies tribological responses, together with nano-particles. The process was also strongly dependent on the environmental conditions. In particular, the inbuilt nature of PEEK in contact with water causes matrix relaxation which in turn overshadows the benefit of nanoparticles addition beyond 5% in PEEK composites and overall outcome is the inferior wear-rate of PEEK composites compared to dry tests condition. The effect of temperature on materials' tribological aspects is on two folds. Firstly, all materials are expected to lose their hardness and strength to some extent with the rise of service temperature. Secondly, the development of transfer film greatly affected by temperature and associated with materials' brittle-ductile transition behaviour, depending on the contact temperature risen in testing. Thus, both factors

influence the tribological aspects of HPPs and polymer composites at elevated temperature regimes.

Finally, attempts have been made to establish correlations between the basic mechanical properties of HPPs and their sliding wear behaviour. Various wear models to correlate the tribological aspects of HPPs and polymer nanocomposites with associated mechanical properties were examined along with experimental validation. A number of factors that contribute in wear process were examined including both materials' intrinsic properties and experimental variables. In addition to that, underlying wear mechanisms were taken into account towards model developments. It was concluded that, there is no simple, one-to-one correlation of tribological aspects with materials with their respective mechanical properties for different testing conditions. To develop a quantitative solution for wear prediction, the new computer techniques such as artificial neural network (ANN) may be helpful in the area. Accordingly, the ANN was employed to find the general wear trend of materials.

Acronyms

HPPs	High performance polymers
TFL	Transfer film layer
TL	Transfer layer
PET	Polyethylene terephthalate
CST	Continuous service temperature
PSU	Poly sulfone
PES	Poly ether sulfone
PVDF	Poly vinyl dene fluoride
PEI	Poly ether imide
PPS	Poly phenylene sulphide
PEEK	Poly ether ether ketone
SBC	Styrene butadiene copolymers
PK	Poly ketone
PEK	Poly ether ketones
PPP	Poly para phenylene

PBI	Poly benzimidazole
PTFE	Poly tetra fluoro ethylene
GFRP	Glass fibre reinforced polymer
PI	Poly imide
PTW	Potassium Titanate Whisker
EP	Epoxy polymer
PPA	Polyphthalamide
TPI	Thermo plastic polyimide
PPSU	Poly phenyl sulfone
PC	Poly carbonates
DSC	Differential scanning calorimetry
FIB	Focused ion beam
SEM	Scanning electron microscopy
TEM	Transmission electron microscopy
XRD	X-ray diffraction
TGA	Thermogravimetric analysis

Symbols

p	Pressure
v	Sliding velocity
T_g	Glass transition temperature
Si_3N_4	Silicon nitride
SiO_2	Silicon dioxide
α-FeOOH	Goethite
ZrO_2	Zirconium dioxide
TiO_2	Titanium dioxide
W_t	Time-related depth of wear rate
k^*	Wear factor
t	Test duration
Δh	Height loss of the specimen
φ	Bearing modulus
δS	Solubility parameters of fluid
δP	Solubility parameters of polymer

T_m	Melting temperature
H_c	Composite hardness
A_t	Total projected indentation contact area
A_f	Portions of projected contact areas in film
A_s	Portions of projected contact areas in substrate
H_f	Intrinsic harnesses of film
H_s	Intrinsic harnesses of substrate
h_t	Total indentation depth
h_f	TL thickness
h_s	Indentation depth in substrate
λ	Transfer film efficiency factor
R_a	Surface roughness
H	Hardness
E	Young's modulus
ε	Elongation at break
WD	Volume loss of material by deformation

m	Mass of a single particle
α	Impact angle a single particle
Kmax	Maximum impact velocity of a single particle
εd	Deformation energy factor
WC	Volume loss of material by cutting
ϕ	cutting energy factor
FN	Applied normal load
W	weight loss of material
k	Empirical constants
a	Empirical constants
b	Empirical constants
c	Empirical constants
s	Sliding distance
w	Wear volume loss of material
k1	Proportional constant
h	Initial pin height

Δh	Height loss of the pin
d	Diameter of the pin surface
ρ	Density of the hybrid composites
Ar	Real contact area
μ	Friction coefficient
σ	Tensile yield stress
K_{IC}	Fracture toughness
ρ	Density
c1	Crack length
α_1	Particle shape constant
b_1	Depth of lateral fracture
α_2	Material-independent constant
fv	Volume fraction of reinforcing particles
$\alpha 3$	Material-dependent constant
A_T	Arbitrary mechanical property at a given temperature T
A_0	Arbitrary property at room temperature

List of Tables

List of Figures

Contents

Chapter 1: Introduction

1.1 Background of the Study

Tribology, a multi-disciplinary field across mechanical and materials engineering, has been under ongoing exploration to ensure maximum usage of potential materials where friction and wear are unavoidable. Among different material classes, high-performance polymers (HPPs) and their composites are being investigated by various researchers [1–13] for such applications owing to their high strength/density ratio as well as the structural integrity. A number of the applications, such as seals and bearings, are mainly focused on the tribological performance of HPPs and their composites, especially in non-lubricated, sliding conditions [2–6]. For instance, the exceptional wear behavior of HPPs (commonly against metallic counterparts) without the requirement of lubricants is desirable in a number of applications, such as the textile and food industries, to avoid contamination problems. Further, HPPs have the ability to dampen shock and vibration with excellent corrosion resistance, making them excellent candidates for aerospace, chemical, and offshore applications.

Up to now, different kinds of polymers including both thermoplastics and thermosets are frequently used for various tribological applications [8]. For example, epoxy is a common example of a thermoset, commonly withstanding its fragile and sensitive nature towards microfracture. On the contrary, high performance epoxies, which are normally prepared with high cross-link density, may have high Young's modulus, greater strength, durable bond ability, and outstanding chemical constancy [2–5]. In particular, the mechanical properties, as well as the wear resistance of thermoset

composites can be significantly improved by filling with continuous fibers at high volume contents (> 50 vol.%), e.g., using the conventional autoclave moulding technique. In particular, with the boom of nanotechnology, there were significant research interests in developing high wear resistant epoxy nanocompsoites using various nanofillers [1-13]. Nevertheless, the production time required for thermoset-based composites is rather long, during to the curing process. It has been envisioned that thermoplastics will be increasingly used owing to the more cost-effective injection moulding with particulate and/or short fiber fillers. As noted, neat polymers are commonly 'blended' with different types of fillers to achieve desirable tribological/mechanical properties and other functions. It is important to state that to modify the properties of polymers using fillers, the right term should be 'blended' instead of 'reinforced'. This has been frequently overlooked in the literature. For instance, PTFE is often employed as a solid lubricant to improve the friction performance, but it does not have an effect on improving (reinforcing) the mechanical properties. Towards that, Hunke et al. [14,15] recently indicated the benefits of surface functionalized PTFE powders for better reinforcement capabilities in HPPs. Also, the philosophy of incorporating fillers in the polymer matrix resembles that of metal matrix filled with inorganic oxide/carbide/nitride particles [16]. The type, form, and compatibility of fillers all have major roles in overall material performance.

In literature, polymer composites with various types of fiber-like fillers have been well documented [17-26]. A diverse matrix and fiber materials allow the scheme of composites with exceptional properties for various applications when retention of mechanical properties of materials is of prime concern at different service conditions.

However, compared to injection mouldable neat polymers or particle blended polymers, a drawback of such fiber reinforced composites is that components fabricated from these materials generally necessitate relatively lengthy fabrication times and the complexity of dispersing process, in order to maintain the high length-diameter ratio of fibers. Moreover, alignment and orientation of fibers in fiber blended composite are vital, which is absent in particles blended polymers. Rasheva et al. [27] pointed out the benefits of nanoparticles addition in polymer matrix over short carbon fiber (SCF) type filler blend, as the orientation of fibre type filler significantly influence the wear behavior of the composites and directional loading during sliding. It is also worthwhile indicating that fiber like fillers may not be easily used for the novel additive manufacturing such as the selective laser sinter (SLS) 3D printer.

Over the last few decades, the tribological behavior of nano-particles blended HPPs is receiving more and more attention in the research community [16-21]. The strong mechanical properties of HPPs and their composites lead to the expectation of good wear resistance of them even at high temperatures. Indeed, HPPs are presently being applied as sliding machineries components in machinery or tribo-pairs in various fields where lower friction and wear are foreseen [28-31]. However, the involved wear mechanisms have not been fully understood, particular due to the complex physical and chemical interactions in the wear process. During the wear, material removal occurs due to complex thermo-mechanical reactions, which is dependent on contended polymeric chain structure, types of polymer or co-polymer (thermoplastic/thermoset), the polymeric functional group along with polymeric chain, tactility, molecular weight, curing/setting behavior etc. [28]. Moreover, because of lesser cohesive energy

of polymer compare to those of pairing materials which are generally metals and ceramics, polymers are capable of transmitting and distributing the load effectively across matrix and blended particles which results in significant reduction in wear and friction [32-35]. With the additional nano-fillers, more complicated tribo-chemical reactions might take place in tribo-contact that yields characteristic TLs. The incorporation of nanoparticles into the polymer matrix made these TLs more stable and resilient which may decrease friction and wear significantly. Structure and properties of such TLs differ from system to system and in-depth understanding on that is foreseen to understand the fundamental aspects of tribology of HPPs and their composite. For example, such TLs may offer boundary lubricant effect in tribo-contact, which allow such HPPs composite to be used under high '*pv*' (contact pressure, *p* times sliding velocity, *v*) conditions in unlubricated sliding. It is noted that both the terms, TFL and TL, has been used interchangeably in the literature. However, there is a distinction between them as pointed out by Bahadur et al. [18]. The term TFL is not appropriate when referring material being transfer from a soft polymer interface to a harder metal counterpart. In fact, TFL is most appropriate for continuous and uniform while TL is attributed to irregular and nonuniform along the wear patch or track. To develop high wear-resistant HPPs, it is important to understand the formation mechanism of TFs, as well as its dependence on material properties, the type of fillers and service conditions such as temperature and lubrications.

Another important aspect of friction and wear is that, they not only depend on material properties but also on the tribo-system where the materials are being used, those are 'system responses' [36]. Thus, the environmental conditions such as medium,

temperature, humidity, vibration, etc. also play big roles towards overall performance of the system. For example, in the liquid medium or at high temperatures the abovementioned TLs might get dissolved and unstable, which sometime severely supersede the benefits that were foreseen in dry sliding conditions. Moreover, liquids such as water may be absorbed by the polymers, which interrupt their molecular chain structure and thus deteriorate tribological properties. Such a 'system response' aspect of tribology makes it difficult to study wear behavior of HPPs in isolate without taking consideration of environments and an integrated approach is foreseen to get a complete picture on that. Nevertheless, a whole depiction on tribological behavior of HPPs by taking consideration of material system and environments is not yet available although it is imperatively necessary. There are gaps in the knowledge related to the effects of environment on the tribological performance of such HPPs, and a fundamental understanding related to the role of TLs is absent. Additionally, the most recent progress in this field is not well interconnected in terms of mechanical properties of HPPs and their tribological aspects. To tackle these concerns, wear mechanisms of HPPs and effect of diverse system variables such as, sliding speed, vibration, load and environment temperature on friction and wear development were examined based on the evidence offered in the literature. These understanding will allow the design and selection of tribo-material for particular applications.

1.2 Study Objective

The present work has five main objectives geared towards designing novel polymers and polymeric composites to facilitate selection of materials to be used in research

community and industrial professionals with regards to different sliding conditions as follows:

- To study and understand the role of different kinds of nano-filler (soft/hard) on tribological behavior of thermosetting epoxy-based composites under different sliding settings.
- To explore the friction and wear attributes of PEEK reinforced with titanium dioxide (TiO_2) nanoparticles subjected to dry and water lubricated environments.
- To investigate the tribological behavior of some high-performance thermoplastic polymers and polymers composites under extreme condition.
- To illustrate wear modelling by correlating materials' and system parameters.
- To project wear rate of materials through a well-trained ANN based on present experimental results.

1.3 Dissertation Outline

Chapter 2 of the dissertation will focus on the recent developments on tribological performance of various types of polymers and their composites related to the intrinsic and extrinsic parameters. The materials, experimental procedures and methods used to characterize the presently investigated materials will be presented in Chapter 3. Chapter 4 will explain the effects of reinforcing rigid silica (SiO_2) particles or soft

carboxyl-terminated butadiene acrylonitrile copolymer (CTBN) on thermosetting epoxy composite on tribological performances

Chapter 5 provides details of PEEK polymer focusing on its tribological and mechanical properties strengthened with titanium dioxide (TiO_2) under dry and water lubricated sliding conditions at room temperature.

Chapter 6 focuses on the wear features of three different high-performance thermoplastic polymers PEEK, PPP and PBI. The PEEK composites will also be explained in this chapter subjected to sliding at different temperature regimes.

In chapter 7, a simplified model of wear and coefficient of friction will explored to address the tribological behavior of high-performance polymer and polymer composites developed together with experimental validation and associated with Artificial Neural Network (ANN).

The last chapter of the thesis will summarize the findings and conclusions drawn from the work with suggestion for future research works.

Chapter 2. Recent research on high performance polymers and polymer composites for tribological applications

Several industrial sectors over the past decades have used engineering polymers for tribological applications including physical, chemical, automotive and aerospace. The increasing use of materials for tribological applications has led to the development of high-performance polymers for better efficiency and performance. Despite the fact that the use of these applications has led to the development of better performing polymers, there are new investigations been conducted, aiming at developing polymer-matrix composites under different tribological applications further. Thus, the present chapter reviewed the recent studies on the sliding wear properties of HPPs and their nanocomposites, associated with intrinsic and extrinsic parameters. In particular, the effects of the intrinsic properties of polymer composites (e.g., mechanical properties of the materials and the types of fillers) and external environmental conditions (e.g., service temperature and lubrication medium) on the formation of transfer layers (TLs) were discussed. The latter would govern the overall friction and wear of polymeric materials in steady sliding, against metallic counterparts. In addition, correlations between the basic mechanical properties of HPPs and their sliding wear behavior were also explored.

2.1 Recent developments on tribological aspects of HPPs

Heat distortion, also known as heat deflection temperature (HDT) is a key feature of HPPs. In practice, HPPs are expected to retain their structural integrity over their

continuous service temperature (CST), which is commonly higher than 150 °C by definition [18]. On contrast, commonly used polymers such as polyethylene terephthalate (PET) usually get deformed under 100 °C, which limits their applications under dry sliding conditions substantially, as the contact temperature can be significantly higher [16]. High performance thermoplastics such as polyamides, can be melted into products shape of complex forms, with high physical-mechanical and thermal properties. In fact, polyamides are most widely used structural thermoplastics and characterized by high impact resistance, resistance to fluctuating loads, gasoline and oils [1-8, 37-50]. On the other hand, heat-resistant engineering thermoplastics for special purposes include fluoro-plastics (polyfluoroolefins, fluoropolymers), some of which suffer from low mechanical properties [16, 20]. Fluoroplastics cannot be related to structural plastics, as its physical and mechanical properties are considerably inferior to others such as polyamides. Typical tensile strength of fluoro-plastics does not exceed 30-40 MPa with modulus of elasticity of about 0.4 GPa. Since tribological properties are the actually system responses system, to develop HPPs and their composites as potential tribo-materials, their properties such as chemical resistance, mechanical properties, cohesive strength and the retention of strength and structural integrity at service temperature should be taken into consideration, according to the sliding conditions of the system in which these materials have to function.

2.1.1 Processing characteristics of HPP Materials

High thermal stability, as characterized by HDT, of HPPs normally makes the processing difficult and special instruments are often required for that. Most HPPs are made based on that single property (i.e., heat stability) which makes them moderately expensive [29, 33]. HPPs are thus about 3 to 20 times as expensive as common polymers and plastics [18, 35]. Among various HPPs that are reported in literature, followings are some commonly used in structural applications: Polyamides (PA), Polysulfone (PSU), Polyethersulfone (PES), Polyvinylidene fluoride (PVDF), Polyetherimide (PEI), Poly(p-phenylene) sulphide (PPS), Polyether ether ketone (PEEK), Styrene-butadiene copolymers (SBC), Polyketone (PK), Poly(ether ketones) (PEK), Poly(para-phenylene) (PPP), Polybenzimidazole (PBI) etc. Like normal polymers, HPPs are also made up of the repeating unit of macromolecules that give rise to typical long polymeric chain structure in three dimensions. Fig. 2.1 shows the construction of reiterating unit of PEEK, PPP and PBI that build up the respective polymer structure.

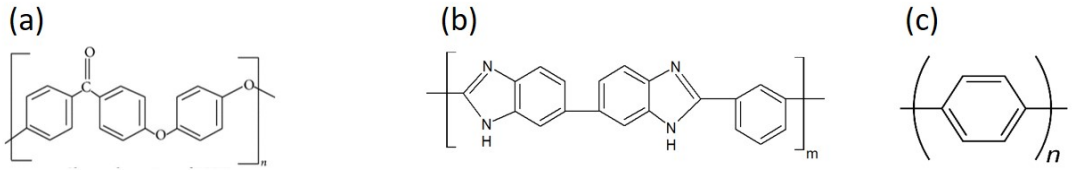

Fig. 2. 1 Reiterating unit construction of (a) PEEK, (b) PPP and (c) PBI [50].

Based on the properties of standard polymers, two approaches are usually taken to further enhance their mechanical and thermal performances: (i) co-polymerization by addition of organic macromolecules and (ii) inorganic nano-fillers in the form of blends. Co-polymerization involves cross-linking of compounding substrates before

hardening with aromatics or other cross-linking agents [51]. As a result, the compounding substrate became chemically incorporated into the network. Aromatics offer a good resistance against polymer chain movement and thus retain strong mechanical properties during sliding. Other commonly used cross-linking agents are SO_2, CO etc. By mixing these different compounds diversity of HPPs has been created with different characteristics [16-28]. According to literature [52-56], the maximum temperature resistance about 260 °C can be achieved with fluoropolymers though their wear resistance may not be necessarily favorable. Mixture of co-polymers gives rise to amorphous and semi-crystalline nature in polymer structure: PSU, PES and PEI are examples of amorphous structure whereas PPS, PEEK, PBI and PPP are semi-crystalline. Semi-crystalline polymers can be used even above their glass transition temperature (T_g), another added advantage against chemical constancy [54]. Various inorganic nano-fillers blends, e.g., silicon nitride (Si_3N_4) [45], silicon dioxide (SiO_2) [49], goethite (α-FeOOH) [19], zirconium dioxide (ZrO_2) [21, 32, 47], titanium dioxide (TiO_2) [32, 45, 48], have been proved to not only contribute towards enhancing mechanical properties but also lower the friction coefficient and rate of wear under various sliding circumstances [57-59]. In particular, PEEK, PPS and PTFE are most widely studied for different tribological applications, and often blended with TiO_2, SiC, Si_3N_4 and carbon fibers fillers. Nevertheless, it is also noted that there are no single polymer or filler or their combination, which provides the best tribological performance in all conditions. Being the "system responses", tribological properties always depend on both intrinsic materials properties and external environmental conditions.

2.1.2 Tribological characteristics of polymers and their composites

In general, wear of polymers under sliding is subjective to certain contact circumstances, depending on the bulk mechanical behaviors and surface profile of polymers, as well as TLs. The effect of lubricants and atmosphere on the wear of polymer is described in stipulations with the chemical interactions among mating contacts. The wear resistance of polymers can be effectively improved with the blended fillers (either nano-particles or traditional fiber fillers). To predict the wear life and rank the wear resistance of materials, time-related depth of wear rate (W_t) is commonly used, which is defined according to Eq. (2.1) [4]:

$$W_t = k^* pv = \frac{\Delta h}{t} (m/s) \tag{2.1}$$

where k^* is wear constant, p is pressure, v is sliding speed, t is the duration of the test and Δh is the loss of height of the specimen. The wear constant, k^* is theoretically a material variable equivalent to the adjustment of the product of p and v. According to Eq. (2.1), 'pv' variable might be assumed as a tribological measure of load-carrying ability of materials, that leads to two evaluation variables [28]: (i) basic wear constant k^*, that remains unchanged in a specific limit of 'pv' parameter and (ii) limiting 'pv' parameter, beyond which the rise of wear rate is excessively fast to be meaningfully used in practical applications. Diminishing the basic wear factor, k^* and boost limiting 'pv' value are the common goals in designing wear resistant HPP materials.

In practice, for the convenience of materials selection, it is commonly assumed that when the limiting 'pv' value is not exceeded the specific wear rate, k* and friction

coefficient are materials parameters and independent of the '*pv'* factor. Nevertheless, to develop new engineering tribo-materials, it is important to systematically evaluate their wear behavior under different '*pv'* conditions, and to understand the effect of '*pv'*, as well as the load-carry capacity of the material under the given environmental conditions [60-65]. Pei et al. [1] observed that with the rise of '*pv'* parameters, a general trend of temperature increases in counterpart and thus concluded that, temperature constancy of polymers would be greatly focused in situations where wear and friction are vital matters. According to Briscoe et al. [66], during the sliding process, polymeric materials can experience a very high temperature which is mainly concentrated at interface region (within depth of around 100 nm). However, rest of the materials, except the contact region, are in test temperature. This high temperature in contact region is significant for tribological features of polymers, as structural failure of the components often starts from this region.

The research has shown that the increase of velocity would mostly affect the tribological properties of polymers by increasing contact temperature, whereas the higher-pressure conditions may change the wear mechanism in different ways depending on the thermal-mechanical properties of polymers. In general, with the increase of pressures, the friction coefficient tends to decrease, which can be explained by the thermal/stress softening effect on polymers. On the other hand, polymer surface could be plasticized trailed under high pressure conditions, which assists to easy separation of surface materials and contributes to acute wear. Zhang et al [60] noted that under higher applied pressure, wear properties of amorphous PEEK might be associated closely to its viscoelastic behavior, which is absent in low load conditions.

However, it is worthwhile indicating that such a correlation between wear and intrinsic material properties remains challenging. Based on the studies of PBI, Friedrich et al. [28] concluded that, the comparative action of hardness or modulus *vs.* impact toughness or ductility stays vague and more work is foreseen to achieve a good understanding on that.

For HPP composites blended with different fillers, some work showed that wear rate could be less dependent as a function of the normal load until a critical value was reached [67]. Fig. 2.2 shows the effect of nano-filler (SiO_2) incorporated PEEK composite as a function of pressure and sliding speed [67]. As given in (Fig. 2.2a), under 1 MPa applied pressure, friction coefficient reaches in stable state rapidly in case of nano-filler incorporated composites. After that, there are fluctuations in the evolution of the coefficient of friction which is absent in case of neat PEEK. This implies the effect of wear debris on friction coefficient. In all cases (Fig. 2.2b), mean friction coefficient is almost half for the case of nano-filler incorporated composites compared to the neat one.

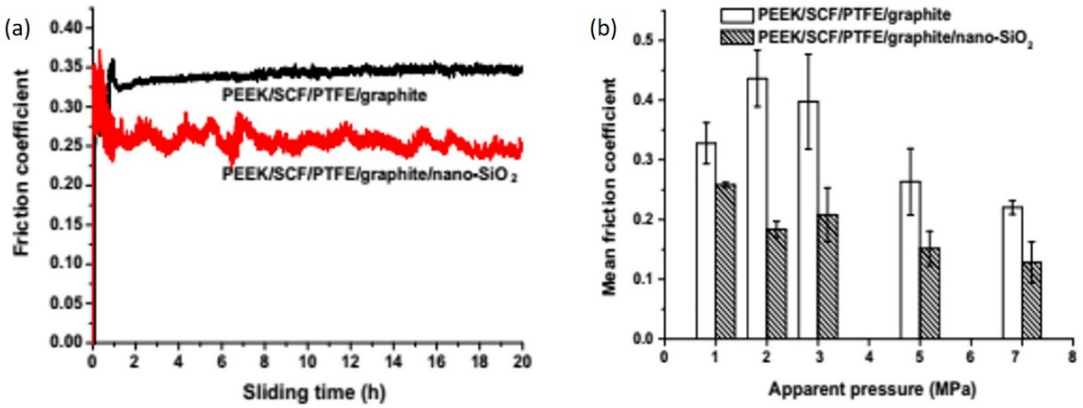

Fig. 2. 2. Typical evolutions of coefficients of friction as a result of nano-filler addition in PEEK composite [67].

Wear behaviour of PEEK composites, as shown in Fig. 2.3, shows mixed behaviour. Under high pressure as well as sliding speed, de-bonding of fillers from the matrix took place which increases wear rate. In addition, detached fillers can graze the matrix material and lead further removal of materials as sliding continues. The grazing effect of broken fillers was reported by the authors [67] as a dominant failure mechanism, and deeper scratch marks were produced by cracked fillers as noted on worn surfaces. The separation of filler/polymer matrix is understood because of interfacial exhaustion happening in several regions where fillers carry extreme loads [5, 61]. Stress transfer and stress concentration among fillers and matrix interface could also lead significant deformation along the direction of rubbing. Owing to repetitions high stress and strain, specific zones lose the load carrying capability and filler pull-out took place.

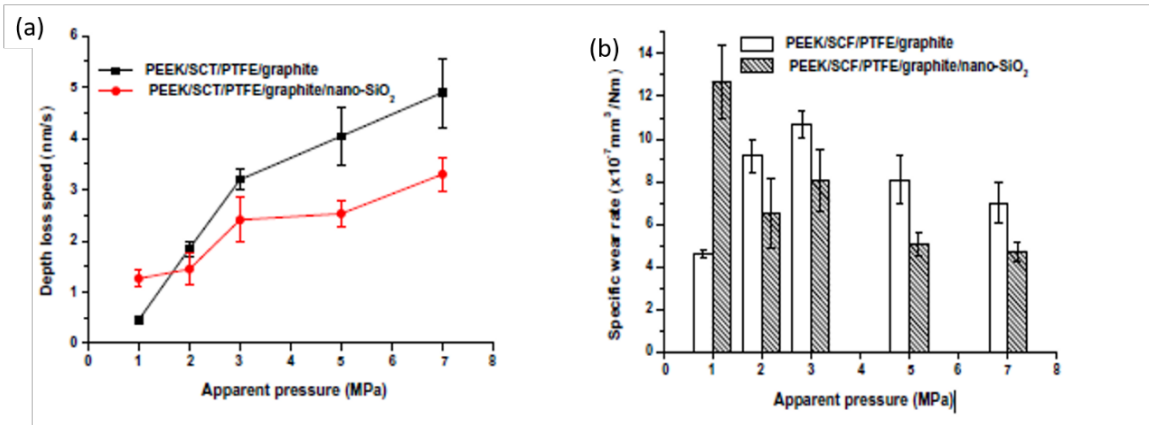

Fig. 2. 3. Typical evolutions of wear rate as a result of nanoparticles addition on polymer composite [67].

This higher stress also generates cracks in filler when the highest stress level of fillers ultimately suppresses its strength [5]. Furthermore, the impact on filler applied by protruding areas of counterpart may also induce filler breakdown when the stress

cannot be effectually transmitted to relatively soft matrix material. This might take place particularly afterward the detachment of filler/matrix. When the pressure exceeds the critical value, agglomerated nano-fillers flattens into lesser ones that will not have their impingement role effectively. Nevertheless, it would be noticed that a change in speed or dispersion situation of nano-filler might alter the limiting pressure level. In addition, the increase in sliding velocity might be associated with greater contact temperature and colliding dynamics applied by protruding areas on the counterpart. The rise in contact temperature declines matrix stiffness and thus initiates acute stress concentration. Greater contact temperature also reduces the shear strength of the matrix and could result in an increased wear rate [67]. The worn surface turns out to be smoother at faster sliding speed and may reduce the coefficient of friction as crushed filler agglomerates incline to alter its movement arrangements to rolling from sliding [58]. These two aspects can lessen ploughing and cutting influences on pulled out nano-fillers and thus reduces further wear. Throughout the sliding procedure, stress transformation takes place from the matrix to nano-fillers in the frictional layer and consequently, stress concentration on nano-fillers can be decreased. This morphology is shaped owing to plastic flow of surface layer because of amalgamation of lower stiffness and higher ductility of polymer matrix [6]. Plastic flow of PEEK matrix is considerably abridged when nano-fillers are integrated in it. Additionally, the improved stiffness of PEEK can diminish the deformation of nano-fillers in tension. In general, this is the wear mechanism of nano-filler incorporated polymer matrix composite regardless of filler and matrix type and composition.

2.1.3 Developing high wear resistant polymer composites filled with nanoparticles

A variety of fillers in the different form such as shape, size, nature, etc. has been added in the neat polymer as reported in the literature with one objective that is enhancing the wear resistance of neat polymers [33, 45, 47, 48, 61-63]. A theory was proposed by Zhang et al. [33], correlating tribological property of PEEK to its viscoelastic property, the effect of interface temperature and strain rate of the surface layers (TLs) - all of which are associated to the friction procedure. Beyond the critical level, nano-fillers protruded through thin TLs and act as third bodies to increase friction coefficient. For the resistance of wear, adding of TiO_2 nano-filler was useful, as an escalation of friction coefficient might happen related to the reduction of the specific rate of wear which might be clarified by the generation of TLs and will be described in later sections as adhesion will be dominant over the abrasion in such situations.

However, in reality, some of the fillers improve wear, but deteriorate friction behavior and also trends in the opposite direction has been reported in the literature. With the increase of nano-filler content, there is a high possibility of particles agglomeration in the polymer matrix and effectiveness of nano-filler addition is suspended. A possible solution of such limitation is that a combination of fillers in neat polymer matrix instead of single one. Such combinations, like a blend of fiber and particle type fillers, is more effective compared to single filler of similar content as reported by Friedrich et al. [4] and shown in Fig. 2.4. There is about 300-time increase of wear resistance of neat epoxy as a result of incorporating a combination of nano-fillers in it. The pronounced effectiveness arias form the fact that, where the addition of fiber type filler increase toughness, the role of particle type filler is more towards the increase of hardness of polymer composite. During wear process, the short fibers can also resist

the exfoliation of surface and accommodate fine wear debris as a form of mess and provide effective and durable TLs. As will be presented in later sections, an effective and durable TLs not only keep the coefficient of friction in manageable scale, but also reduce wear rate, by altering wear mechanism to a greater extent. Österle et al. [64] evaluated the outstanding tribological behavior of a polymer matrix composite incorporated with an amalgamation of micron-sized carbon fibers and nano-sized silica particulates. Silica-based tribo-films firstly prevent severe oxidational wear followed by preventing pull-out and rupture of carbon fibers in the composite by offering a cushioning effect.

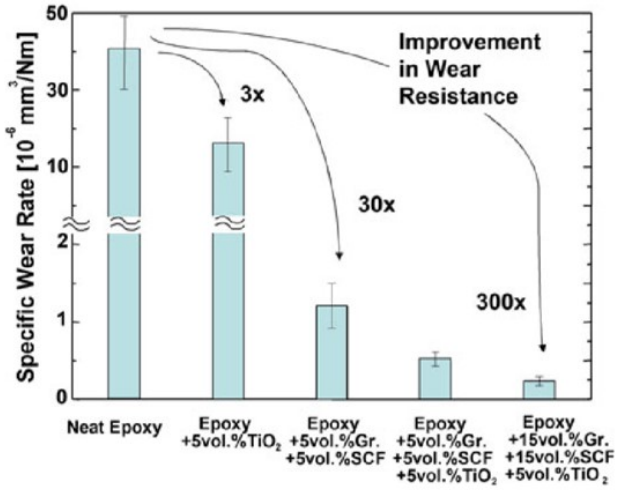

Fig. 2. 4. Specific wear rate for various degrees of the combination of incorporated particles in neat epoxy (Graphite (Gr), short carbon fibres (SCF)) [4].

Xie et al [1] reported that, carbon fiber and potassium titanite whiskers (PTW) functioned synergically to boost wear resistance of hybrid PEEK composite. Furthermore, the carbon fiber transferred the key loads between the contact surfaces and shielded the matrix from additional austere abrasion from the counterpart. Zhang [35, 65] reported that adding up of 20 wt. % nano-silica particulates boosted modulus

and hardness by 78 and 130 %, respectively, compared to that of pure epoxy. In addition, they also emphasis the size of wear debris on TLs formation that was influenced by the quantity of nano-particle in the polymer matrix. Based on the discussions mentioned above, it can be summarized that, a variety of fillers are being used in HPPs to enhance their wear resistance. In general, hybrid type fillers, such as a combination of fiber and particles, is more effective than that of single filler. In that case, particle type fillers provide the strength of the composite, whereas the fiber type fillers contribute towards toughness and modulus. Nanometer-sized fillers are more effective than micron-sized fillers, though the cost-effectiveness is still uncertain. Angularly shaped fillers are more effective than rounded ones, as they are more effective in retaining the transfer layer in places, though there may be relatively higher wear rate during ‘running-in' phase of the process.

2.1.4 Wear mechanisms of polymeric materials under dry sliding condition

2.1.4.1 Transfer film layers (TFLs)

The importance of a TF for the tribological performances of polymers has long been realized and widely studied [68-95]. Transfer film layers (TFLs) is defined as a thin (from nanometre to few microns in thickness) layer (film) of material that form in tribo-contact during sliding as a result of wear. When polymers slide against metal counter faces, wear of polymer as well as counter face generate wear debris, which hold together in a form of adhesive coating in tribo-contact and termed as TFLs. The transfer film formed on a non-polymer counter face is governed by the counter face material and roughness, and of course the sliding conditions. Recently, efforts have been directed to quantitatively characterize TLs, and thus to establish more accurate

correlations between TLs and the involved wear mechanisms. Chang et al. [54] studied TLs formation on different polymer-based hybrid composites scientifically by applying nanoindentation with in-situ AFM examination. Based on the outcomes and analysis, it was noted that the hybrid nanocomposites incorporated with both nanoparticles as well as conventional tribo-fillers were useful to fabricate long-lasting TLs, particularly while used in severe sliding circumstances and subsequently reduce friction coefficient and wear rate. A synergistic action between nanoparticles and TLs is present that might influence significantly to enhance wear characteristics of polymeric hybrid nanocomposites. Generally, a reduction of the coefficient of friction and rate of wear took place with the increase in TLs thickness and even coverage. In utmost tribological uses, TLs controls load transmission and whole wear mechanism significantly and consequently a trustworthy material data for TLs is advantageous [6, 31]. TLs behaviours are often treated as a signature individuality for combinations of polymer/ incorporated particles with its counterpart. Some blends affect the progress of TLs confidently, but some incorporated blends do not have such influence and consequently boosted wear rather than dropping it [31]. It was stated that when the polymeric composites are incorporated with conventional fillers, the composites were more useful to form durable TLs on steel surface related to desired tribological characteristics while sliding [7]. It was also proposed that the brittle-ductile changeover of polymers plays a key role in controlling the development of TLs when the temperature increases [14].

The effect of nano-filler addition, towards enhanced TFLs generation is general more effective than that of micro/macro-filler, as established in literatures [15, 32-34,47-

48]. This is due to the higher surface-to-volume ratio of nano-fillers which inclines to provide the advantage with minute volume fraction than that of micro-filler incorporated blends. TLs broke straightforwardly as wear-debris are comparatively bigger in size and shape for micro/macro-filler incorporated composites. In fact, TLs form as compacted wear remains and greatly associated with the shape/size/nature of nano-filler incorporated blends. TLs generated in the polymer-on-metal sliding process are dissimilar to traditional lubrication films. Thickness of TLs can be estimated by load-displacement curve during nanoindentation based on a relatively simple model as described by Bahadur et al [95-96] and Chang et al [37] where composite hardness, H_c of the film/substrate arrangement while indenting through the film onto the substrate, can be defined from the portion of contact areas [37, 95-96]:

$$H_c = \frac{A_f}{A_t} H_f + \frac{A_s}{A_t} H_s \qquad (2.2)$$

Where A_t is total projected contact area of indentation, A_s and A_f are the projected contact areas in substrate and film respectively, H_f and H_s are intrinsic harnesses of film and substrate respectively. Since $A_t = A_f + A_s$, Eq. (2.2) can be rearranged as:

$$H_c = \frac{(A_t - A_s)}{A_t} H_f + \frac{A_s}{A_t} H_s = H_f + \frac{A_s}{A_t}(H_s - H_f) \qquad (2.3)$$

$$\frac{(H_c - H_f)}{(H_s - H_f)} = \frac{A_s}{A_t} \qquad (2.4)$$

For sharper indenters, for example, Berkovich, indenter contact area is proportionate to the square of indention depth, i.e., $A = k.h^2$ and thus, Eq. (2.4) can be rearranged as:

$$h_f = h_t - h_s = h_f\left(1 - \frac{h_s}{h_t}\right) = h_t\left(1 - \sqrt{\frac{(H_C - H_f)}{(H_s - H_f)}}\right) \qquad (2.5)$$

Where h_t is total indentation depth, h_f is TLs thickness, and h_s is indentation depth in the substrate. The hardness of TLs, H_f, was considered to be similar to the neat polymer matrix hardness. In addition, the variation of hardness between steel counterpart and

neat polymers vary largely. Therefore, the minor deviances in H_f due to the presence of harder minor pieces in soft TL might be overlooked. It is noteworthy that, a strong variation in hardness along the wear trails implies nonuniform allocation of TLs along wear track. On the other hand, a thicker TLs corresponding to lesser magnitudes of H_c. Soft TLs usually pushed out from indentation region, generating a "pile-up" of material nearby the indentation due to the confinement of plastic flow of polymer TLs by hard substrate beneath [37]. As formation of TLs is more qualitative in aspects, transferal film efficiency factor (λ) was found by applying Equation (2.6) [37] to give it a quantitative sense:

$$\lambda = \frac{t}{R_a} \tag{2.6}$$

Where $t = (h_f)$ was average TLs thickness established by nano-indentation and R_a was surface roughness of steel counter surface. Further on equation development and concept of TLs were described in the literature [37].

Gao et al. [19, 46] carries out a detailed investigation on the nature of TLs that form on steel counterpart during sliding against PEEK composite with the help of FIB-SEM and TEM as shown in Fig. 2.5. It was explicitly evident that, the accumulation of TLs on steel counter surface is uneven in nature. Moreover, the selected area diffraction pattern contains both hollow rings as well as dots, which representation of both; amorphous and crystalline nature of the TLs. TLs behave similarly to that of well-established Stribeck curvatures [39] that discuss the reliance of coefficient of friction on liquid lubricating film in the forms of the ratio of lubrication film thickness to the average coarseness between contacting associates. Santer et al. [97] extended this in wear system as a function of relevant factors [97].

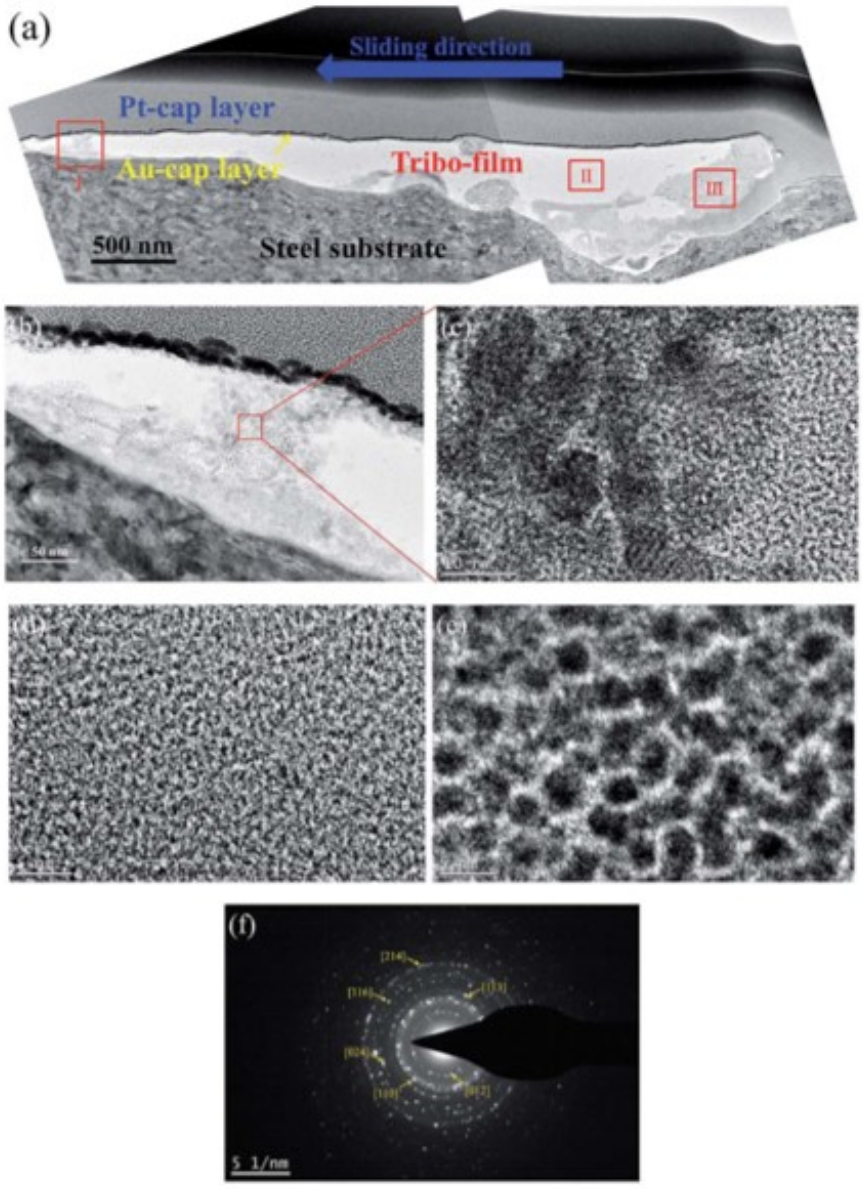

Fig. 2. 5. TEM micrographs of TLs on the cross-section of steel counterpart after sliding on PEEK/10FeOOH at 100 N normal load: (a-e) bright field TEM pictures and (f) selected area diffraction pattern on TLs [19].

TLs share the similar physical meaning of those conventionally applied variables [32], i.e., a higher magnitude of the parameter points out that the characteristics of TLs

further control the frictional property of the sliding arrangement. Despite the desirable wear performance achieved by the presence of TLs, it was also observed that the spreading of TLs was uneven as mentioned earlier. Therefore, during nanoindentation in order to find the thickness of TLs, a sufficiently more significant number of tests should be performed along the wear track for statistical purposes. Under this condition, the discrepancy of average magnitudes of hardness was significantly declined. Though the magnitudes of hardness might be varied broadly between the hardness of virgin steel counterpart and that of the polymer matrix, the average magnitude of hardness exhibited decent replicability and the curves display comparable trends. It is meaningful to notice that, such average magnitudes would not be assumed as the general characteristic of a comparable film, since the film was discontinuous. The 'mean thickness' is generally considered as a quantifiable guide of the total sum of TLs covered on the counterpart for the reason of mathematical modelling. The unevenness of TLs on substrate restricts the accurateness of computed thickness. Additional shortcomings arise due to other parameters for example indenter tip sharpness, the surface finish of sample, pile-up etc. which induce doubts in defining the actual contact area during nano-indentations. Nonetheless, the investigation offers an applied technique to define and compare the TLs generated on a range of materials in various sliding circumstances. Regardless of '*pv'* factor, the common tendency was that the composites incorporated with nano-particles experienced thicker TLs compare to those without nano-fillers in it. The literature indicated that TLs generated by neat polymers has tendency to be thicker at faster speeds but thinner at larger pressures [8, 60]. As pointed by Bahadur et al. [95, 96], wear is dependent on the cohesion of transferal film, bonding of transferal film on counterpart and the safeguard of sliding

polymer surface from metallic asperities by TLs. Friedrich et al. [34] emphasis on the thickness of TLs and according to SEM observation, if the TL is thinner then substrate's roughness, the effect is more dominant, and breakage of TLs is more likely. In the case of the higher surface roughness of mating pairs, more debris is required to fill up the valleys, which results in an initial higher wear rate. In that case, ever after filling the valleys with wear-debris and forming semi-continuous TLs, the detachment of large chunk of TLs is evident, which contribute towards higher wear-rate even after the running-in period.

2.1.4.2 Wear mechanism during steady state sliding wear

As mentioned previously, the TLs would be gradually developed on the metallic counterpart, during the initial running-in phase. Then, the overall friction and wear of the tribo-system become rather steady. In the steady state, with the presence of the TLs, the mode of tribo-contact changes forms initial hard (metal) – on – soft (polymer) to one or more of the subsequent contact couples depending on the thickness, distribution and components of TLs, namely, (a) hard-on-hard (rigid fillers against asperities of steel surface), (b) hard-on-soft (rigid fillers against polymeric TLs) and (c) soft-on-soft (polymer against polymeric TLs). Thus, the mechanisms of contact rely on the spreading and quantity of TLs in actual contact areas. In that respect, the values of transfer film efficiency factor (λ), three different wear - and friction-regimes might be identified as shown in Fig. 2.6 by Chang et al. [37] who has investigated the tribological aspect of various filler incorporated HPPs.

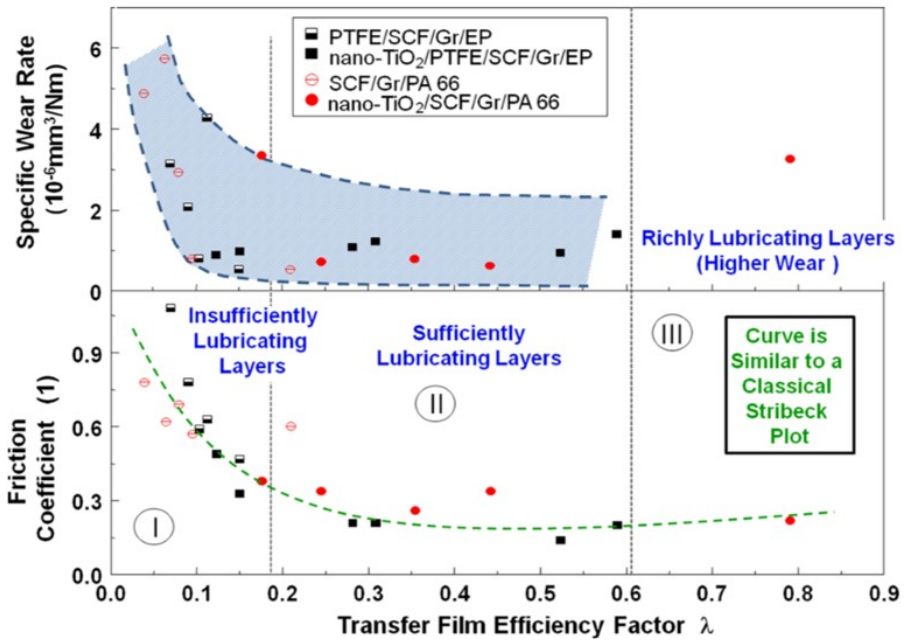

Fig. 2. 6 Evolution of coefficient of friction and specific wear rate based on the transferal film efficiency factor that rise to different boundary regimes [37].

When the magnitudes of λ is comparatively low (< 0.2), the contact is considered as insufficiently lubricated as there is not enough TLs to completely cover the steel counter-face. In this situation, wear behavior greatly depends on sliding circumstances such as '*pv*' factors, as described in section 2.1. When the product of '*pv*' is comparatively small, it is likely for a comparatively thin TLs to shield the surface efficiently because of lower actual contact area and polymer composites might still attain decent wear characteristics with a comparatively smoother worn surface. However, under greater '*pv*' values, actual contact area rises, and additional fillers are uncovered to steel counter surface with insufficient shielding from TLs. The contact type now is in the form of 'hard-on-hard', resulting a greater coefficient of friction. In addition, fillers are more probable to break down and pulled out rapidly. The wear

procedure could be additionally intensified by the thermal assisted mechanical fracture of polymer matrix particularly in the interfacial areas. Therefore, polymer composites risk acute wear loss at severing sliding circumstances. This has somewhat resembled to boundary lubrication situations. With rising magnitudes of λ, TLs might be assumed as adequately lubricated layers where it is capable to shield most of the fillers from direct contact with steel counter-face in every tested situation, that is, in both high and low '*pv'* factors. Wear behavior is developed by a combination of two contact types: (a) contact of the polymer with TLs (soft-on-soft) and (b) contact of hard incorporated particles with TLs (hard-on-soft). Due to the shielding of TLs, acute filler pulls out might be evaded even at higher '*pv'* conditions. Nevertheless, if the quantity of TLs is very high, this might be also related to the rise of wear rate. In this case, TLs can break down in the form of the large chuck of wear debris as a relatively thick TLs may work as a thermal insulator. Hence, localized contact temperature in that thick TLs area might be comparatively high and may raise the adhesion of polymer with TLs, consequential more noticeable transference of compressed wear remains. At the similar period, greater contact temperature may decrease the viscosity of polymeric TLs, which sequentially gives a small coefficient of friction. In view of that, there is no such direct correlation between the coefficient of friction and wear behaviour of material even taking consideration of the role of TLs. However, it can be stated that, at greater quantities of λ, the tribological behaviour of sliding arrangement is mostly controlled by the characteristics of TLs. Therefore, under such circumstances, wear behaviour of HPPs displays lesser dependency on sliding circumstances, producing a steady specific wear rate as well as lower coefficient friction. Though TLs displayed resembling lubrication influence to that of conventional lubrication films, there are

more complex interactions between tribological characteristics of TLs and polymer. One example is that, TLs formed directly by the wear remains of sliding arrangements while the traditional lubrication films are normally formed by an organized external arrangement. Additionally, the rise of temperature in contact due to sliding might significantly affect the characteristics of TLs, which consecutively, influence the tribological behaviour of the sliding arrangement [98]. For example, a small coefficient of friction was attained for PA66 matrix composite with no nano-particles, in the expense surface melting due to high contact temperature. As the thermal conductivity of steel counter surface (around 58 $Wm^{-1}K^{-1}$ [99]) is considerably greater than that of polymers (about 0.25 $Wm^{-1}K^{-1}$ for PA66 [99]), a thicker TL may work as a thermal shield as mentioned before. In case the thickness of TLs is greater than the surface roughness of the steel counter surface, the effect became more significant. The pulped TLs might push towards small coefficient of friction due to lubrication influence but cannot effectively carry the load and failed to protect filler pull-out and resulted higher wear loss. Henceforth, tribological activities of TLs always require to be considered cautiously by the strong knowledge of the wear/contact mechanisms of the system in various sliding arrangements.

The experimental data shows that more durable TLs were expected to form due to adding of more than one type of nano-fillers as incorporated in neat polymers. The outcomes displayed that, lower friction characteristic of nano-filler incorporated composites was triggered by the mechanical collaborations among supplementary nano-fillers, polymeric nature of TLs and contact surfaces [29, 36]. Nano-fillers can contribute towards lower coefficient of friction, because of their ‘spacer’ effects as

well as the capability to rolling [36]. These parameters can realistically clarify the benefits of nano-fillers on the creation of TLs. As the nano-fillers could usually offer enhanced opportunities for wear remains to stay in the worn areas and thus form steady-state TLs on steel counter face. The existence of nano-fillers may also decline the adhesion of TLs with the polymer by decreasing actual contact area. At the similar stage, nano-fillers might be entrenched into soft TLs, instead of pushed away from compressed surfaces. Thus, TLs partly hide the nano-filler incorporate and minimalize their abrasion effect. Such a synergistic interaction between TLs and nano-fillers is useful for an improved wear characteristic of polymeric composites, particularly under acute sliding circumstances.

As frequently discussed in the literature [9], at the microscopic level the contact between mating surfaces during sliding can be resolved as a summation of a number of asperities contact. The nature of continuous/semi-continuous transfer film can be explained in view of such asperities contact, as shown schematically in Fig. 2.7. As the pin (test coupon) travels hard counter surface, the front edge of asperities cut the bulk material from the pin (test coupon) and removed materials being accumulated by front flanks. In the course of that, tail edge of the asperities kept exposed as they do not contact bulk materials. This phenomenon gives rise to characteristic ‘rippler' like appearance of the counter surfaces, as frequently stated in the literature [9]. As the process continues, the space between asperities get filled up with wear debris, and lesser asperities are in contacts and give rise of the transfer layer. This resemble ‘steady-state' phase, where both coefficient of friction and wear rate dropped, in

general, compared to ‘running-in' phases. From this point onward, both wear mechanisms and wear rate are dictated by the retention ability of this transfer layer.

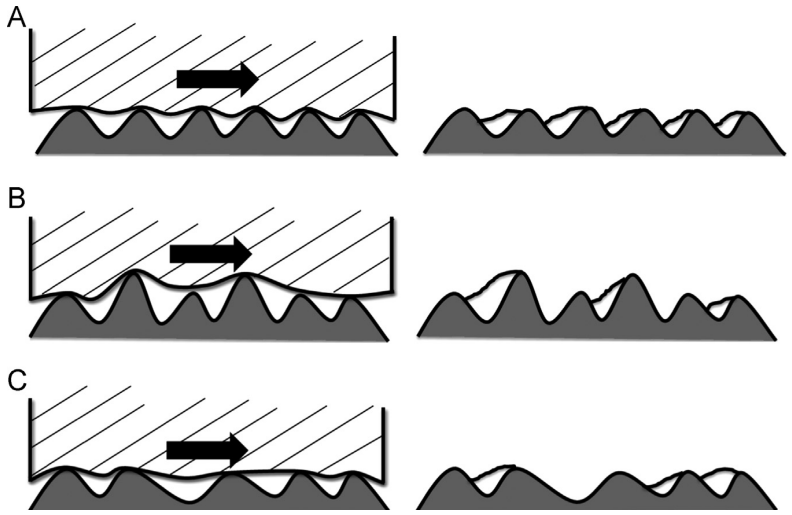

Fig. 2. 7. Schematic of asperity role on transfer layer formation: (a) well-distributed height and spacing of asperity, (b) relatively taller peaks of asperity and (c) asperities with wider gaps [9].

Addition of fillers in the neat polymers does not always yield the positive effect on transfer layer formation as presented by Bahadur et al. [15]. Depending on compatibility and chemical nature, some fillers helps towards better adhesion of the transfer layer with the counter surface and decrease wear rate.

2.2 Effects of external environmental conditions

The development of HPPs aims to bring new solutions for mechanical engineering applications under more complicated, harsh environmental conditions e.g., with higher service temperature or corrosive liquids. To date, however, little effort has been made to understand wear behavior under those conditions. In this paper, the effects of external conditions such as high temperatures, lubricants and vibration will be particular reviewed.

2.2.1 High temperatures

Just a decade ago or so, thermosetting polymers were considered most as heat resistant, durable and dimensionally stable than common thermoplastics, such as polyamides. Recently, new thermoplastic polymers with increased strength by a factor of 2-2.5 and operating temperature higher than 100-150 °C than polyamides' operating temperature with enhanced water and chemical resistance and reduced flammability have been synthesized [96]. Progress in this field was so significant that, the new materials were termed as 'super thermoplasts' or 'super constructional thermoplastic polymers. They might be applied in extreme conditions as a polymer matrix for composites instead of traditional thermosetting phenolic and epoxy resins [3, 38]. Polymers namely polyetheretherketone (PEEK), polyphenylene sulphide (PPS), polyetherimide (PEI),, poly ether sulfone (PES), thermoplastic polyimide (TPI) are attributed to the group of heat resistant super thermoplastics for high-temperature applications [21]. Their molecular structure contains hard and heat resistant fragments along with simple ester, sulphide, amide and ester groups. Ether and sulphide groups play the role of joints that provide chain flexibility without reducing heat resistance. Polymers of this group are

characterized by a strong intermolecular interaction. This factor, coupled with “joints” provides a high modulus of elasticity with considerable tensile elongation and as a consequence, high shock resistance. Due to this fact, such super thermoplastics are distinguished by strength characteristics of 5-10 times higher, on average, than those of epoxy based thermosetting resins. Modulus of elasticity of heat resistant super thermoplastics is as high as 2.5-4 GPa with tensile strength in the range of 70-130 MPa. Most of such materials retain good physical and mechanical properties over a wide temperature range. The heat resistance of such polymers is not only due to its chemical structure, but also on phase state-particularly the ratio of crystalline and amorphous phase together with filler dispersity [21, 31]. For thermoplastics, having partially crystalline structure (PPS, PEEK), heat resistance is determined by the melting point of crystalline phase, which is higher than the glass transition temperature by 150-180 °C. As fillers initiate the formation of crystalline phase, heat resistance of PPS and PEEK-based composites are higher by 100-160 °C compared to neat polymers [73]. Friedrich et al. [2-4] reported that poly (p-phenylene) (PPP) is a suitable candidate for numerous engineering purposes as far as the temperature remains below 140 °C. However, sliding wear performance was not as great as the one found on neat PEEK, however, could be improved incorporating fillers in PPP matrix. Chang et al. [52] studied the influence of nano-filler addition on tribological properties of PEI and PEEK composites at both room and high temperate. They conclude that, though the addition of sub-micron particles does not seem to improve wear resistance at room temperate, however, was remarkably enhanced wear resistance at elevated temperatures were noticed. Zhang et al. [67] studied temperature dependences tribological behaviors of amorphous PEEK without any lubricant and conduced that

an increase in temperature at tribo-contact cause crystallization of amorphous PEEK which increases its rigidity and has a substantial effect during the sliding procedure. Chang et al. [54] investigated the wear characteristics of PBI as well as PEEK at elevated and room temperatures. According to their report, PEEK had greater wear resistance than PBI even at the higher temperature, in spite of the deterioration of its mechanical properties.

As mentioned in the introduction section, HPPs were developed with the intention to use them in harsh conditions where external environmental temperature or temperature rise at tribo-contact due to severe friction and wear plays a dominant role. Zhang [55] et al. carried out a detail temperature dependence tribological aspects of pure PEEK under dry sliding conditions. As shown in Fig. 2.8 [55], friction coefficient rises when the test temperature rises.

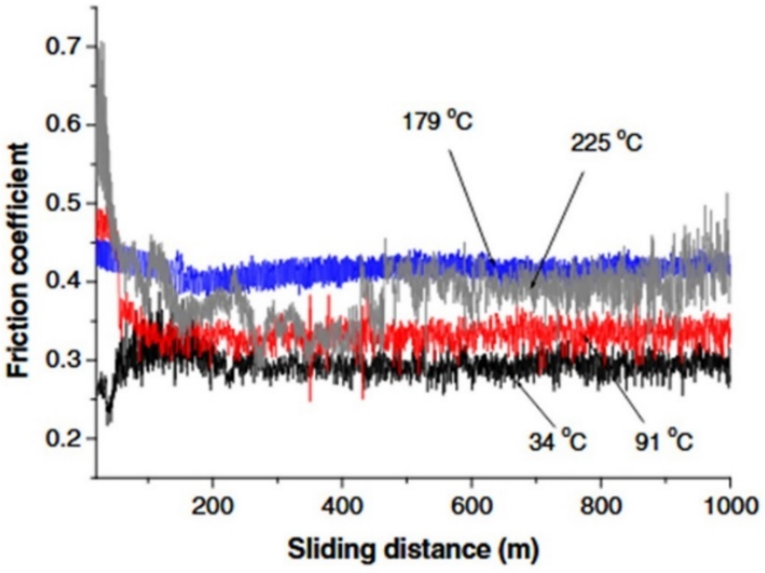

Fig. 2. 8. Coefficient of friction of PEEK with the increase of sliding distance at different temperatures [55].

However, one has to take to in consideration that, actual temperature in tribo-contact is much higher than that of environmental temperature due to the role of flash temperature that is being generated at tribo-contacts. As can be seen from Fig. 10, there is a transition in friction coefficient when temperature increase from 179 °C to 225 °C. This transition is also evident in the evolution of wear rate as depicted in Fig. 2.9, [55] at different environment (nominal) temperatures.

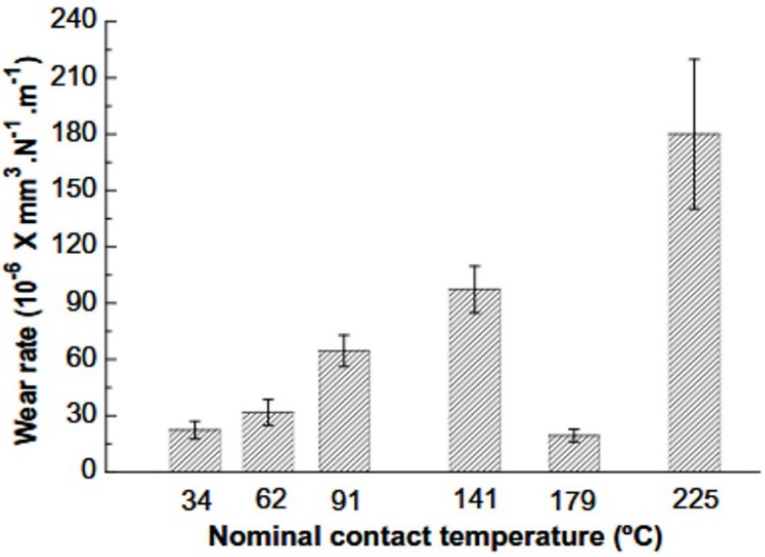

Fig. 2. 9. Wear rate of PEEK at different nominal contact temperatures during dry sliding against 100Cr6 steel ball [55].

The transition on both friction coefficient as well as wear rate at the certain temperature is because of the effect of two phenomena: (a) change in contact condition and (b) change in materials' micro-structure. Temperature increase defoliates the strength of polymers and softens it. As a result, the material became readily flow able and thus gave rise to stick-slip condition. In stick procedure, there is no comparative removal

between counter-body and polymer surface because of strong adhesive force. Therefore, the sliding surface exhibits a greater tangent deformation than that of sub-surface and material gathers in front of the sliding counterpart. The tangential stress is lesser than the critical stress compares to adhesive force and the contact region between mating surfaces rises with the time. When the exerted stress on polymer surface surpasses the critical stress [90-93], stick-slip step is started and continues till the reduction of stress below that critical level. Additionally, material pile-up results in strain hardening because of tangles of long molecules [36], encouraging the slip stage close to the material stack region. In addition to that, as confirmed by DMA analysis, temperature rise generally decreases the storage modulus of materials to some extent [93]. However, a rapid decrease in young's modulus takes place during transformation of polymers from glassy state to viscoelastic state. In addition, increased hysteresis loss due to an increase in temperature might be a vital factor accountable for the raised coefficient of friction [94]. As confirmed by SEM analysis of wear tracks, large sheet-like remains was detected on (or near) wear tracks and in related to wear mechanism, it could be defined as a 'transfer' mode, in which situation the strength of interfacial attachment in the sliding surfaces is greater than PEEK's cohesive strength [27]. Samyn et al. [56] demonstrated that global bulk temperature is vital for changeovers of friction, while a changeover of wear characteristics is controlled by the localized temperature. The polymer material might be transported to the mating surface gradually. Lastly, the gathered material on the mating surface detaches in the form of large pieces [56]. For investigating the influence of temperature on structural changes of polymers, Zhang et al. [35, 60, 65] carried out XRD and differential scanning calorimetry (DSC) analysis on samples before and after sliding

test. It was concluded that external temperature could affects amorphous/crystalline transition of PEEK when the temperature is comparable to materials' glass transition temperature (T_g). Before crystallization, both coefficient of friction and wear rate rises with the rise of temperature. Thermal properties of different polymers such as glass-transition temperature (T_g), melting temperature (T_m) and heat deflection temperature (HDT) together with their respective coefficient of friction (μ) has summarized in Table 2.1.

Table 2. 1: Thermal properties of different polymers as available in literature.

Polymers	**Coefficient of friction (μ)**	**Glass-transition temperature (T_g)**	**Melting temperature (T_m)**	**Heat deflection temperature (HDT)**
PET	0.33 [20]	60 [74]	252 [74]	62 [74]
PSU	0.37 [2]	85 [76]	-	174 [76]
PES	0.62 [76]	225 [76]	200 [76]	203 [76]
PVDF	0.24 [56]	-	170 [76]	260 [76]
PEI	0.1 [58]	230 [76]	190 [76]	210 [76]
PPS	0.43 [47]	83 [74]	285 [104]	108 [76]
PEEK	0.40 [1-3]	143 [1-3]	343 [1-3]	152 [76]
PPP	0.87 [98]	150 [89]	340 [3]	-
PBI	0.67 [98]	400 [54]	-	427 [94]
PTFE	0.1 [2]	27 [76]	325 [76]	90 [76]
PI	0.48 [32]	320 [67]	385 [76]	238 [76]
EP	0.53 [35]	132.5 [57]	-	-
PAR	-	190 [25]	-	174 [76]
PC	0.45 - 0.55 [76]	145-148 [67]	260-270 [67]	129 [76]
PET	0.141-0.245 [76]	80 [76]	250 [76]	66 [59]
PEK	0.29 [76]	165 [92]	-	>316 [22]
TPI	0.43 [32]	250 [78]	-	332 [23]

2.2.2 Lubrication

A decent number of publications are available in the literature regarding the tribological behaviour of HPPs sliding in both dry and wet conditions [5-8, 14-21, 71]. Gao et al [46] investigated wear and friction behaviour of epoxy polymer composites

using water as a lubricant. Based on their findings, it could be concluded that incorporation of short glass fibre (SGF) or short carbon fibre (SCF) in epoxy polymer is not beneficial whereas the incorporation of graphite lessens coefficient of friction without having any positive impact on wear rate. Yamamoto et al. [73] investigated the wear and friction behavior of PEEK and PPS under water lubricated conditions. They noted that, the hardness of PEEK decreased as a result of sliding in water, though it does not happen only by immersing in water. Thus, it implies that, water absorption in PEEK only takes place under the presence of external loading. With respect to that, the research taking consideration of lubrication on PEEK is less, as HPPs are most suitable for applications where the external addition of lubricant is not permissible. However, some applications of HPPs involve water or another liquid medium. Under such conditions, water might perform as a cooling agent and means that friction induced mechanical and thermal influences might be subdued in such an atmosphere. In fact, the temperature rise in an aqueous environment under different loadings is lesser than 10 °C and heat might be effectively dissolute from contact zones. As generally expected, the introduction of lubricant in tribo-contact will decrease the coefficient of friction and wear, does not always hold true in the case of HPPs. In reality, some HPPs exhibit enhance wear and friction in certain lubricant medium. Yamamoto et al. [73] investigated the effect of water as the lubricating medium in tribological behaviors of PEEK and PSS in both similar and dis-similar tribo-contact. As shown in Fig. 2.10, the effect of water in both cases is evident, as the coefficient of friction decrease in all cases. The hydrodynamic exhilarating of water film is very high and consequently, the water layer carried more load. Therefore, direct rubbing between tribo-contact is reduced which in turn decreases the coefficient of friction. Though

water as a lubricant has a positive effect on lowering the coefficient of friction, however, the scenario is completely opposite in the case of wear behavior as shown in Fig. 2.11. The authors [73] have investigated the effect of lubrication on friction and wear as 'bearing modulus (φ)' and claimed that glass fibers incorporated PEEK composite displayed meager wear performance in water lubricant compare to that of carbon fiber incorporated PEEK composite. In contrast, neat PPS exhibits better wear and friction behavior whereas incorporation of carbon or glass fibers declined the rate of wear as an expense of increased friction coefficient. Thus, not only the type of lubricant but also the nature of fillers in HPPs composite plays a synergies role towards overall wear and friction. Thus, carbon fiber incorporated PPS shows greater wear resistance in water lubricant than glass fiber incorporated PEEK namely 0.2 x 10^{-6} mm^3/Nm and 1 × 10^{-6} mm^3/Nm, respectively.

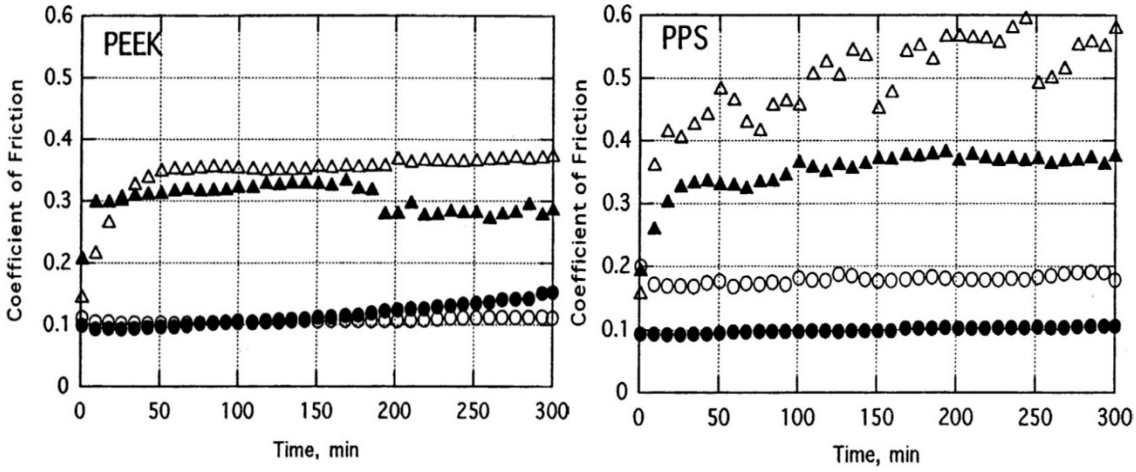

Fig. 2. 10. Effect of water as a lubricant on the coefficient of friction: polymer/polymer (Δ) dry; (▲) in water and steel/polymer (○) dry; (●) in water [73].

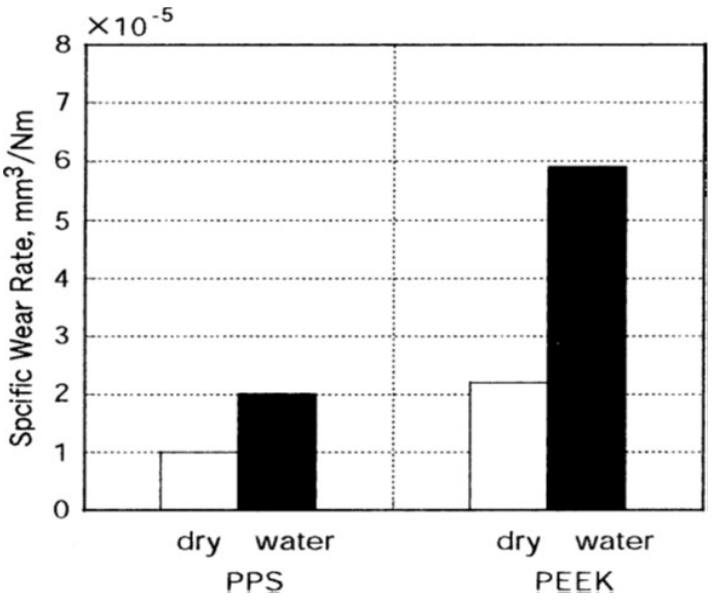

Fig. 2. 11. Effect of water lubricant on the wear rate of HPPs [73].

For all PEEK-based composites, specific wear rate at sliding speed beyond 2 m/s was lesser, that is about 10^{-8} mm^3/Nm compared to 10^{-6} mm^3/Nm at higher sliding speed. The sliding surfaces of PEEK composites experienced lesser damages compare to that of neat PEEK. As evident from Fig. 14, in both lubricated and unlubricated conditions, wear rate of PEEK is the couple of folds higher than that of PPS, under similar sliding conditions. The associated wear mechanisms were attributed to: (i) transfer layer formation, (ii) adsorption of water molecule and (iii) chemical bonding of transfer layer with the counter surface. In unlubricated conditions, pronounced transfer layer was noticed in the case of PPS compared to PEEK, which was further tarnished in water-lubricated conditions. The better ability to form a transfer layer in case of the PPS is the formation of chemical bonding between the transfer layer and steel counter surface. In contrast, the high wear rate of PEEK is due to lowering its mechanical strength at the sliding area under normal/tangential forces as a carbonyl group (-CO-)

of PEEK molecular structure get attacked by water molecules and contributing towards bulk plasticization [74].

The roughening of sliding surfaces as well as transmission of materials to steel counterpart were repressed by PEEK incorporated with fibres. In view of boundary lubricating circumstance, reduction in harshness of contact between sliding surfaces reduces specific wear rate. This was more pronounced at rubbing velocities of 2 and 4 m/s, where lubrication regime appeared to be hydrodynamic, as the value of subsequent bearing modulus (φ) ranges from 9×10^{-8} to 2×10^{-7} [73], where hydrodynamic lubrication film was thinnest. As long as hydrodynamic or mixed lubrication circumstances could be maintained, or the degree of direct contact was maintained insignificant, glass or carbon fibres were useful in dropping the amount of surface damage on PEEK composites. Neat PPS itself displayed better wear behaviour compared to neat PEEK and addition of incorporated particles does not offer any distinct improvement. PPS composites display greater specific wear rate than PEEK composites in hydrodynamic regime at rubbing velocity beyond 2 m/s with equivalent φ value being greater than 9×10^{-8}. Thus, with hydrodynamic lubrication of PEEK composites might be more encouraging than PPS composites. Though, PPS and PEEK are recognized as high hydrolysis as well as chemical resistant polymers [75-76], the higher wear rate of PEEK in water was assumed because of reduced mechanical strength due to water molecule absorption which interrupts its long molecular chain structure. Under lubricated condition, although the seeming contact area is relatively small compared to the dry condition, contact stresses is compatibly high and complexities might rise due to the generation of hydrodynamic films. With the purpose

of minimizing hydrodynamic influences, it is desirable to select the input variables so that 'wear scar diameter' [77-79] is lesser than corresponding critical values all the time, where wear effectively ceased. The capability of liquid lubricant to be engrossed by the polymer is controlled by the values of solubility variables of the fluid (δS) and polymer (δP). The closer δS is to δP, lower is the critical stress and propensity to crack is higher instead of crazing as reported for the case of polyamide 66 (δP = 28 $(MJm^{-3})^{1/2}$) in water (δS = 48.5 $(MJm^{-3})^{1/2}$). The similar tribological behaviour of different polymer and polymer composite under water lubricated condition was also reported by other researches. For example, Friedrich et al. [80] reported similar behaviour on PET, PI, PEEK and their composites, Wang et al [81] on PTFE based composites [82], Gao et al [19, 46] on EP and PEEK composite and Golchin et al [83] on PPS composite.

Another aspect of water lubricated condition is the inhabitation of TLs formation on the counterpart. Water runs through the surfaces of polymer composite and mating component and takes away wear debris. This cleaning process exposes the virgin surface of the polymer to counterpart uninterruptedly. This might be the cause for not showing eminent running-in stage in wear curves [84]. Thus, TLs which is generally noted in dry sliding, fails to generate in the presence of lubricants. Furthermore, the water may encourage to rise the chemical corrosion of steel counterpart and thus making the surface rougher compared to its initial state. The experiments showed that immersion of steel in water improves its wettability as well as accelerates wear of polymer [85, 86]. Besides, the interfacial amalgamation of the matrix and incorporated particles was deteriorated in water under higher load. The deteriorated interfaces might

perform as crack nucleator and accelerate the spread of fatigue crack on sub-surface. The cyclic stresses generating from the contact of the polymer composite with hard asperity of counterpart resulted layer peeling on the surface. The exfoliation on worn surface suggested that fatigue delamination took place at the time of friction procedure. Therefore, huge quantity of sheet like exfoliation gathered on the worn surface and caused a severe abrasive effect. Actually, both friction and contact temperature were significantly raised under pressure up to l4 MPa and furthest facilitate effortless plastic flow and accelerate cracking of the matrix, particularly in the interfacial area.

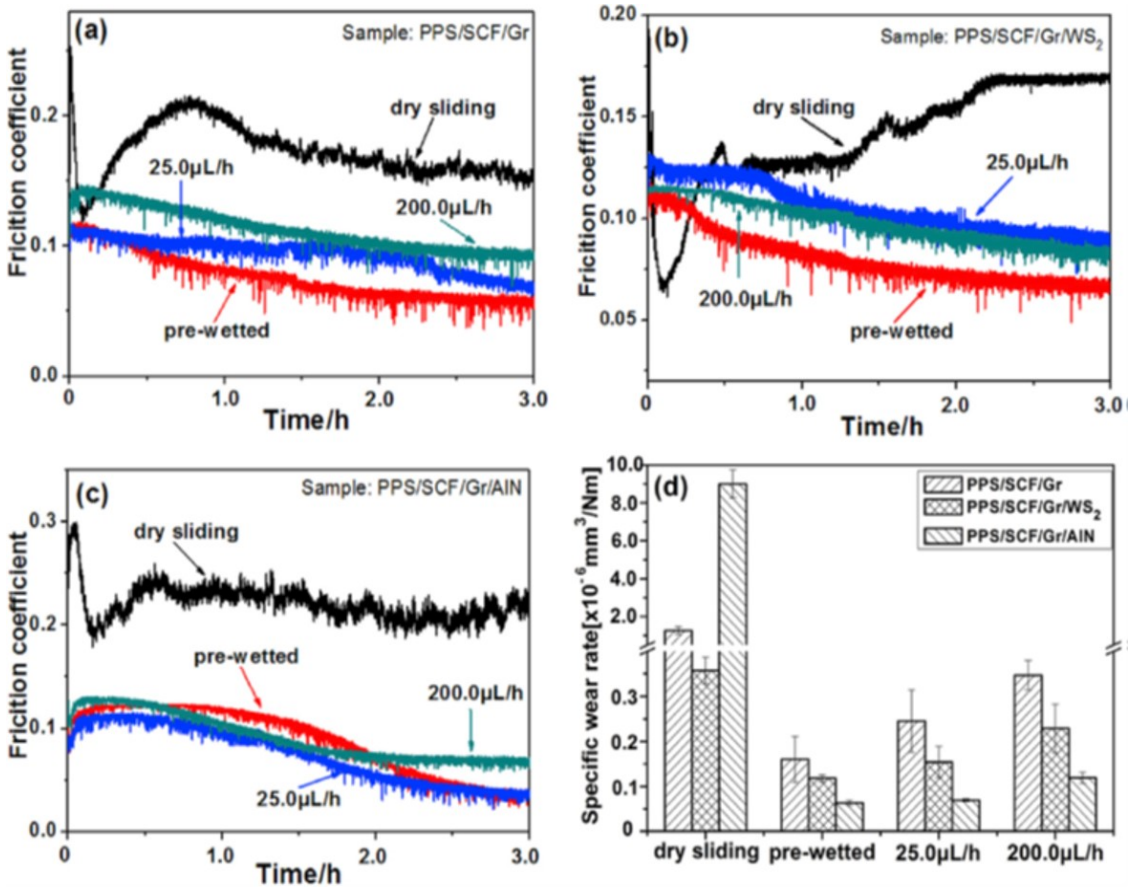

Fig. 2. 12. Effect of diesel as a lubricant on friction and wear on PPS based composites [84].

In addition to water lubricated condition, Zhang et al. [87] reported the tribological behaviour of EP composite under diesel lubricated condition as shown in Fig. 2.12. Unlike water lubricated condition, wear rate does not increase in diesel lubricant condition as diesel does not get absorbed by PPS composite and maintain boundary lubrication condition in the form of a thin fluid film which efficiently transmits the load and keep both friction coefficient as well as wear in low scale compared to dry conditions.

In view of above-mentioned discussion, the common lubrication mechanisms of HPPs sliding under counter surface is the formation of the transfer layer and for most of the cases, resembles as ‘mixed lubrication' effect due to dynamic nature of the tribo-contact. In addition to that, the synergic between the polymer and corresponding fillers play a vital role for the formation/retention of transfer layer during sliding. For instance, the nature and chemical affinity of the fillers used in the polymer composite also place an important role in the overall wear rate. As reported by Zhao et al. [88], PPS with Ag_2S shows better wear rate compared to other fillers during rubbing against steel counter surface. As PPS blended with Ag_2S slide against the steel counter surface, Fe from the counter surface reacts with S to form FeS and $FeSO_4$, due to higher chemical affinity. Formation of these compounds ensure chemical bonding with the associated transfer layer and counter surface; and act as a stable lubricating like film and thus reduce the wear rate, as confirmed by XPS investigation. This was quite evident, as PPS without any filler, shows much higher wear rate under similar experimental conditions, due to the absence of strong transfer layer.

2.3 Correlation between mechanical and tribological properties

Although there is no simple relationship between the basic mechanical properties and tribological performance, it is important for materials engineers and scientists to understand the dependence of the friction and wear behaviour on intrinsic material parameters such as the type of fillers and basic mechanical properties. Such an understanding is critical for industries to select and design new, high-performance polymeric materials. According to commercial manufacturers (Ensinger, Germany; Solvay Advanced Polymers, USA), HPPs, PEEK and PPP possess quite extraordinary mechanical properties such as strength and modules, as shown in Fig. 2.13 along with other commonly used polymers. Both modulus and strength are much higher than that of thermosetting polyimide (PI). Particularly in that case of compressive characteristics, the strength of PPP under compression surpasses by a factor of 5 with respect to other polymers (PEEK, PC, PPSU). Generally, it could be concluded that PPP might be assumed as a high-performance polymer. At room temperature, this material provides a significant possibility when other high performing thermosets and thermoplastics stretch to their mechanical properties' boundaries.

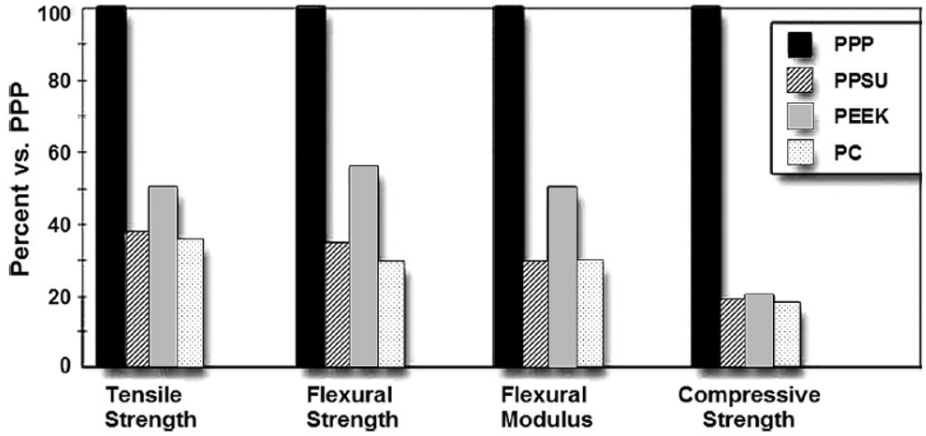

Fig. 2. 13. Ranking of different HPPs based on mechanical properties [3].

Based on literature survey, it seems that there is no direct relationship between the mechanical properties of materials and their corresponding tribological aspects. For example, Pei et al [1] pointed out that, among different HPPs, PPP poses highest elastic modulus and strength. However, when comparing their wear performance with PEEK and PBI under different '*pv*' sliding conditions, it was observed that, the worst wear resistance was given by PPP. Thus, care should be taken before correlating materials' wear behaviours based on their respective mechanical properties. In addition to that, materials that exhibits better room temperature tribological behaviour does not necessarily show the same at elevated temperature. This is because, different materials deformed differently at different temperature regium based on their inherent microstructure and polymeric chains. This is due to the integral nature of PPP, as confirmed by K. Friedrich et al. [28] in view of their amorphous nature through TGA-DSC analysis. PPP shows a broad temperature assisted swelling rather than a sharp melting point which is mostly true for all thermoplastics [101-103]. Therefore, when these materials are subjected to friction, generated heat at contact soften the amorphous polymer and came off at relatively ease in layer by layer (instead of fragmented particles) and results in higher wear rate.

In general, although the introduction of incorporating fillers in polymer causes discontinuity of material to some extent, their melting temperature and extent of crystallinity are mostly unchanged as reported by Friedrich et al. [34]. Therefore, the polymer matrix in the composite appears to vary slightly from the equivalent neat polymers in terms of their thermal behaviour. Incorporating fillers usually helps to increase the mechanical characteristics of the composites, for example, tensile

strength, hardness, elongation at break, and flexural modulus. The outcome of these parameters generally has a considerable effect on wear behaviours of composites. Therefore, materials having higher stiffness and hardness can effectually resist crack dissemination and deformation before breakage and hence, could experience significantly lesser specific wear rates. Thus, to include a different aspect of materials' mechanical and tribological factors on wear rate, an expression for lubricated circumstances was theoretically formulated from the perceptions of crack progression, damage build-up, and traditional mechanics as reported in detail by Lhymn et al. [89]. Accordingly, the rate of wear is inversely proportionate to the product of the elastic modulus (E), hardness (H), and elongation at break (ε) as shown in Eq. (2.7) [100-102]:

$$wear\ rate \propto \frac{1}{H.E.\varepsilon} \tag{2.7}$$

Recently, Hakami et al. [103] has investigated the influence of the various size of abrasive particles in the wear characteristics of different polymer samples. By comparing the effect of mechanical properties on wear rate subjected to different sized abrasive particles, it was observed that low particle size (125 μm) influence elongation at break and tensile strength more. In contrast, higher abrasive particle size (425 μm) cause larger penetration and results higher wear rate and chance of cutting material surface by these debris and overall debris formation enhances. This is also related to the surface roughness of mating parts. In case of higher surface roughness of the mating parts, initial 'running-in' phase exhibits high volume of wear as well as higher co-efficient of friction. Once the system has reached the 'steady-state' regime, both wear rate and coefficient of friction became plateau. Moreover, generated wear particles of polymers with lower hardness tend to clog abrasive's surface and increase

the real contact area, leading to an increase in wear rate [39]. In view of that, polymers' hardness and tear strength are dominant mechanical properties under such conditions. Identical outcomes were also presented by Chang et al. [42] for particle and fibre filler incorporated PEEK composites as shown in Fig. 2.14. As the content of nanoparticle ranges 5 - 20 wt. %, a higher linear relation to $1/H.E.\varepsilon$ was observed. In terms of the wear rate, the hybrid composites (where both fibre and particle incorporated) displayed a rising trend with the rise of ZrO_2 content in the range from 5 to 15 wt. % and additionally displayed a solid drop-off trend when the content of ZrO_2 was 20 wt. %, that is exceeding the critical incorporate content. A combination of differing types of filler shows different influences on mechanical properties as fibre type fillers could significantly enhance hardness and modulus. However, the tensile strain at break reduced significantly as the fibre was compounded which is counterbalanced by the presence of particle type fillers. Therefore, $H.E.\varepsilon$ might be controlled by varying the amounts of different fillers of hybrid composites towards optimization to achieve the highest possible values of $H.E.\varepsilon$ [16]. Additional research must be dedicated to find further details on how the mechanical characteristics influence the wear behaviours when a combination of different types of fillers are in use PPP, PBI, and other HPPs.

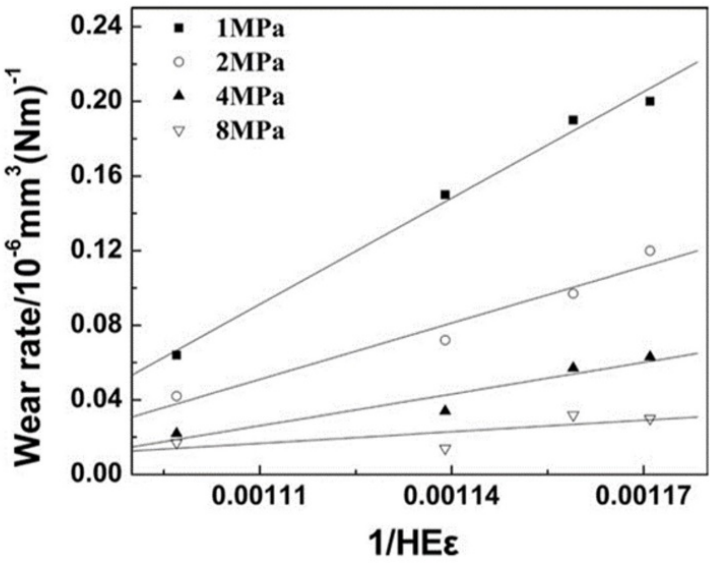

Fig. 2. 14. Influence of mechanical properties on the wear rate of the hybrid PEEK [16].

2.4. Summary

The present chapter discusses the aspects of tribological properties of HPPs and their composites. In summary, it could be mentioned that the application of polymer matrix composites in tribological fields is broad and growing in quest of increasing efficiency and lowering operating cost. The structural design of the materials highly depends on the engineering system where it should be used. With the intention of understanding the sliding wear mechanisms of HPPs and their composites, two factors should be taken into account: (i) materials and (ii) system parameters. In terms of materials, most of the times HPPs are incorporated with different types of micro/nano-fillers and their combinations. The fillers such as inorganic particles can improve the wear resistance either due to enhanced mechanical characteristics (such as hardness, modulus, and stiffness) or by forming durable and resilience transfer film layer between contact materials. However, the addition of fillers cause discontinuities in material and susceptible to generate hard wear-debris that act as the third body to enhance wear of

the system. In that respect, there is a critical filler content beyond which the addition of filler actually degrades the wear resistance of the materials. The critical filler content varies from materials to material, however roughly in the range of 5-15 vol. % as reported in literatures. A topographic smoothening and a probable rolling action because of the nano-particles are possible explanations for their improvement of the wear and friction performance. There is also a trend of using a mixture of particle and fibre type filler together to improve the performance of the materials. In that case, wear mechanism that took place is much more complex and required details investigation on that. In addition to materials' properties, wear and friction of HPPs and their composites are reasonably affected by number external factors such as, pressure, sliding speed, sliding time, nature of tribo-contact, frequency and amplitude of vibration, temperature, lubrication etc. Importantly, no linear relationship exists between friction coefficient and rate of wear. The above-mentioned discussion on various tribological aspects of HPPs and their composites can be used as a guide towards future design of different tribological and mechanical components with the development of new materials. In the last few years, the attention in polymers and polymer matrix composites for engineering fields, where lower friction and lower wear ought to be afforded, has grown up hastily. Additional encouraging impacts on the accomplishment of structural tribo-components should be anticipated from the advancement of functionally gradient materials applying various centrifugation methods and the addition of blended multi-type filler in the matrix. For designing future HPP composites, following factors should be considered: (i) compatibility of the fillers with the matrix, (ii) a blend of fiber and particulate type fillers, (iii) a positive

synergic of the fillers with counter surfaces. The main intention will be forming and maintaining effective TLs during the sliding.

In conclusion, despite numerous researches in this field as outlined above, a big research gap exists regarding overall performance of such composites in view of their structural changes that took place during the tribological process. In addition to that, fundamental concept of wear mechanisms is still unclear when the polymers are loaded with nano-fillers. Moreover, usage of such composites in water lubricated condition and high temperature applications is yet to sought after. Thus, the present research is required to create an in-depth understanding on the systemic investigation on overall characteristics of composites in harsh condition like elevated temperature exposure. In addition to that, particular role of TFLs on wear, friction and wear-mechanism and associated structural changes of the polymer structure, were also investigated not only qualitatively but also quantitively to focus their role on the wear process, which is very limited in currently available literatures. Further, The mainly studied of this project was on lubrication and temperature. The vibration and humidity were not the main focus of the current project. Nevertheless, the theory/understanding developed in the field has been helpful to explain the wear results, since vibration would inevitably during sliding process.

Chapter 3. Materials and experimental methodologies

3.1 Polymer matrix selection

Two different kinds of polymeric materials were explored in this work, that is, thermosetting polymer and thermoplastic polymer. A diglycidyl ether of bisphenol A (DGEBA) epoxy resin (Araldite-F, Ciba-Geigy, Australia) was cured by adding piperidine (Sigma-Aldrich, Australia), which was selected as a thermosetting polymer-matrix. In addition, the wear behaviour of three high-performance thermoplastic polymers, namely PPP (Solvay Adv. Polymers), PBI (PBI Performance Prod.) and PEEK (Victrex, UK) was particularly studied and compared in this work.

3.2 Reinforcements nanoparticles

Two different types of nano-filler were used as reinforced epoxy composites namely, rigid nano-silica (SiO_2) particles and soft carboxyl-terminated butadiene acrylonitrile copolymer (CTBN) particles, commonly known as nano-rubber. The average size of SiO_2 particle was 20 nm. The nano-rubber used to form the composite was CTBN with molecular weight (Mn) of 3800 and supplied at 25 wt. % concentration in bisphenol-A resin by Kaneka Corporation, Japan. The average size of nano-rubber particles was about 100 nm.

Inorganic titanium dioxide (TiO_2) (Kronos 2310) with an average diameter of 300 nm was used as a reinforced filler for PEEK matrix. The TiO_2 particles were in the rutile phase, which is the most stable one among different variants. Fig. 3.1 illustrate the shapes, size and distribution of nano-particles in matrix materials obtained by TEM and SEM.

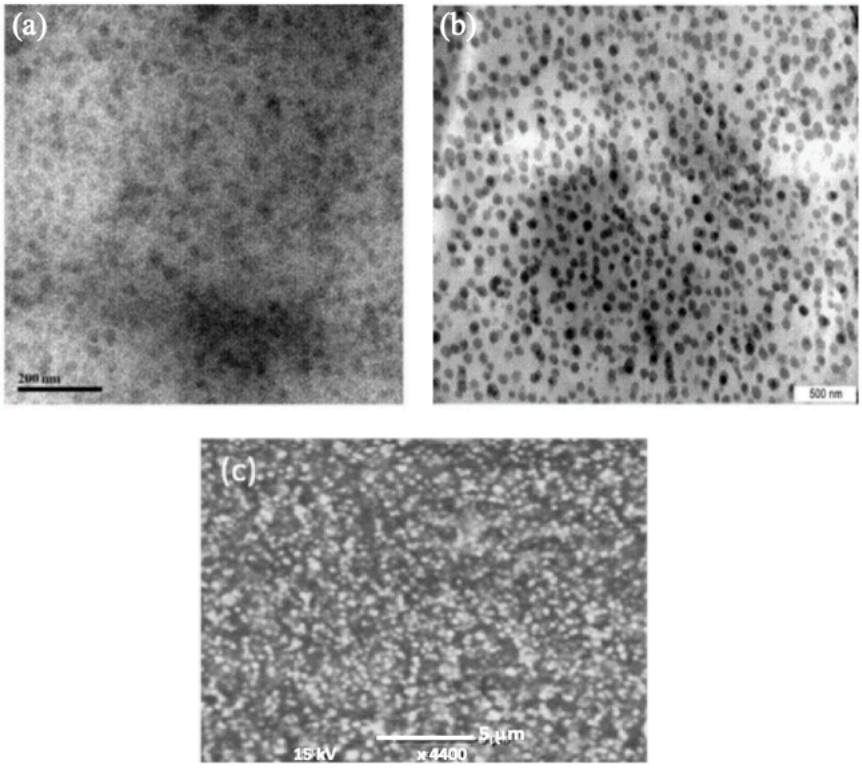

Fig. 3. 1. Distribution of nano-particles in polymer matrix: (a) 6 wt. % nano-silica, (b) 6 wt. % nano-rubber and (c) 15 wt. % TiO_2 .

It is important to note that, blending of agglomeration free nano-fillers in resin matrix is always a challenge and towards that, proper procedure was followed based on the information available in literature such as extended stirring follow up ultrasonication [17, 34-37]. In addition to that, recently developed novel nano-silica system (Nanopox XP) was used in present case (commercially procured), which is capable to accomplish uniform distribution of nanoparticles' fractions of up to 40 to 50 wt.% in resin matrix, as outlined in manufactures data sheet [35]. Nanopox XP products exist in the form of colloidal silica sols within a resin matrix and possess modified surfaces, characterized by spherically shaped silica nanoparticles with exceptionally narrow particle size distribution. The nanospheres, whose diameters measure about 15 to 50 nm, are

agglomerate-free and distributed within the resin matrix. The nanoparticles are synthesized chemically from an aqueous solution of sodium silicate. The OH groups found on the silica particles' surfaces get reacted with organosilanes. The organosilanes are selective to the bisphenol-A epoxy, leading to the formation of a hydrophobic organic surface coating [35].

3.3 Specimen preparation

3.3.1 Thermosetting epoxy composites

Epoxy resin was cured by adding piperidine with a ratio of 100:5 (epoxy/piperidine). Nano SiO_2 incorporated (40 wt. %) epoxy nanocomposite (Nanopox XP 22/0616) from Hanse-Chemie AG, Germany, was used as the master batch and epoxy matrix was then added in it in different rates to form the composies with given compositions as mentioned above. A relatively low viscosity epoxy nanocomposite was obtained via agglomerate-free colloidal dispersion of SiO_2 even with high nano-filler loading. Materials were primed by mixing plain DGEBA resin with requisite amounts of nano-SiO_2 or nano-rubber master batch and the precision was kept within 0.01%. Curing of the resin mix was done by adding the curing agent. The mixture was then poured into a preheated mold for curing at 120 °C for about 16-22 hrs. Post-curing for 2 hrs. at 100 °C was carried out to eliminate the residual stress introduced during the production process. Four different Nano SiO_2 loading was used to prepare the composites, namely 6, 8, 10 and 20 wt. %. In case of nano-rubber incorporated composites, two different content was used, namely 6 and 10 wt.%. Above mentioned processing parameters (temperature, duration and nano-filler loading) were selected primarily based on

information available in literature [21-37], resin supplier (such as curing time and temperature) and process optimization approaches.

3.3.2 Thermoplastic composites

PEEK and PEEK with different percentage of TiO_2 were prepared by a twin-screw extruder in Arburg all-rounder injection moulding machine with a length-to-diameter (L/D) and ratio of 33at around 400 °C for 4 hours. This particular temperature was selected for moulding based on process optimization and previous know-how [36-37]. The density of PEEK is about 1.3 g/cm^3 whereas TiO_2 is significantly denser, at about 3.9 g/cm^3. Different loading of TiO_2 was used to prepare the composite such as 5, 10 and 15 wt.%. The loading content was also selected based on information available in literature [21-37] and process-optimization. With increased reinforcement content in the composites, particle agglomeration and de-bonding of particles with the matrix is unavoidable, which deteriorate the properties of the composite.

3.4 Tribological testing methods

Wear tests were carried out via a pin-on-disk configuration by using a commercial tribometer (NANOVEA-MT/60/NI) as shown in Fig. 3.2 for a period of 2-24 hours under different pressure (*P*) and sliding speed (V). All polymer pin surfaces were polished against a rotating disk covered with polishing cloth with 0.1 μm alumina slurry and became flat with nominal surface roughness (Ra) of about 200 nm. All the test pins were polished similarly to avoid any experimental artefacts. Just before the tests, the samples were pre-heated at 50 °C for 3 hours to get rid of surface moistures. Dimensions of all specimens were 4 mm x 4 mm x 12 mm for pin-on-disk testing under

three different slide conditions: dry condition, water lubricated condition and at elevated temperatures.

A carbon steel disk (German standard 100Cr6) was used as counter body with hardness of about 1.3 GPa. The use of carbon steel disk was justified due to its high hardness, strength and stability of temperature during room and high temperature tests [36-37]. The internal diameter of the disk was 25 mm and external diameter of 42 mm with surface roughness (Ra) of about 220 nm, as measured by non-contact profilometer (STIL, France). The steel disk was also polished against polishing cloth with 0.1-micron alumina slurry. Specific wear rate was calculated by using equation (3.1) [35]:

$$W_s = \frac{\Delta m}{\rho \times F_N \times L} \left[\frac{mm^3}{N \times m}\right] \quad (3.1)$$

Where Δm was mass loss of specimens' during the test, ρ was density, F_N was applied normal force and L was total sliding distance. Each individual tests were triplicated under identical test conditions and average values were used for result analyses.

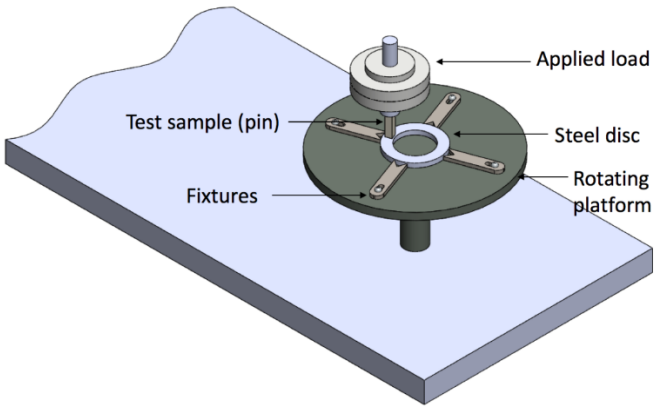

Fig. 3. 2. Schematic representation of tribometer apparatus.

3.5 Materials' characterization techniques

3.5.1 Scanning electron microscope (SEM)

To understand the wear mechanisms after the sliding tests, worn surfaces of both test coupons as well as steel counterbody were examined by Carl Zeiss field emission scanning electron microscope (FE-SEM). It is well known that, SEM is an important technique in the tribological field to study the morphology on interface/sub-surface of materials to understand the role of TFLs and wear debris formations in wear behaviour. After tribological tests, top part (worn surface) of the test coupons and a small section (5 cm) of the wear track from steel counter body were cut by a saw and placed in a standard SEM stub with double-sided carbon tape facing the worn surface/wear track up. In SEM, parameters like KV and current was optimized to achieve best images without any artefacts (sample charging, for example) and degradation of the surface. It was found that, 15 KV and 0.17 nA current provide the best images. The images were taken at different magnifications to get a representative view of the worn surfaces and during analysis, images of similar magnifications only was reported for comparison purpose.

3.5.2 Nanoindentation technique

A Hysitron nanoindentor (Hysitron Inc., USA) with a diamond Berkovich tip was used to carry out nano-indentation tests on the worn materials' surfaces to inspect the hardness of dilapidated surfaces with and without TFLs. The diamond Berkovich indenter was a three-sided pyramid with an inclination angle of 142.3°, a half angle of $\psi = 65.35°$, and with 150 nm tip radius [3]. The nano-indentation test parameters are

as follows: 3 mN of peak/maximum indentation load, 0.3 mN/s of loading/unloading rate and 5 s holding time at peak load. The selection of peak load and loading/unloading rate was based on the information available in literature [37]. Usually in the case of polymer/polymer composites, relatively low peak load and high loading/unloading time was used to characterize the TFLs to eliminate any effect of underlying based materials on it. 40 straight points of individual indentation tests were carried out along each wear track as shown in Fig. 3.3.

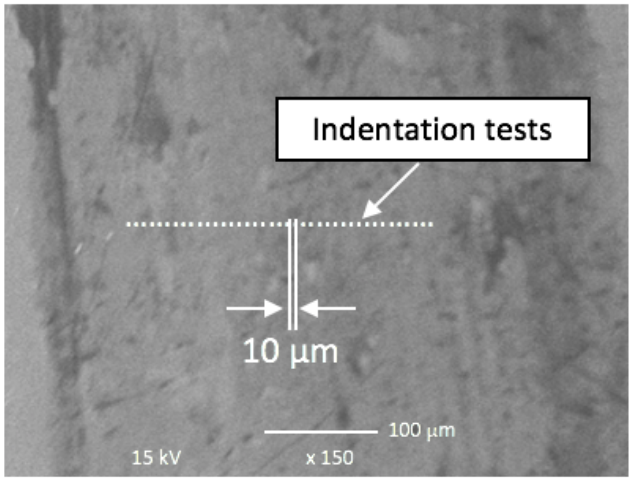

Fig. 3. 3. Schematic of the position of nano-indentation on wear tracks.

3.5.3 Fourier transformed infrared (FTIR) technique

The transmission or absorption of infrared radiation is measured using the FTIR technique considering the radiation's wavelength. Molecular elements and structures are identified by the IR absorption bands. The molecules undergo excitement at the sample surface into a more dynamic vibration state due to the absorbed infrared radiation. The molecular size and structure of the samples determine the wavelengths

that would be transmitted or absorbed. Therefore, the study investigated the changes in the structural patterns of the materials by applying the Fourier transform infrared technique (FTIR).

3.6 Mechanical characterisations

Mechanical properties of the samples were carried out by performing tensile tests on an Instron 5567 instrument at 5 mm/min crosshead speed according to ASTM D638-99 standard [29] by using type IV specimen. Each test was performed on at least five samples for each material composition under ambient temperature. Both longitudinal and lateral strains were monitored via clip-on extensometers against 50 mm and 25 mm gauge length, respectively. 0.2% offset strain was used for the definition of yield. Fracture tests were carried out according to ASTM D5045-99 standard. Sample thickness (B) and width (W) was 6 mm and 30 mm, respectively. A sharp crack between 0.45 W and 0.55 W was introduced by tapping a fresh razor blade at the notch tip. Equation (3.2) [29] was satisfied for valid plane strain toughness (K_{IC} or G_{IC}) measurements. At least four specimens were tested for each composition with a loading rate of 1 mm/min.

$$B, a, (W - a) \geq 2.5\,(K_{IC}/\sigma_y)^2 \tag{3.2}$$

K_{IC} was obtained according to equation (3.3) [31]:

$$K_{IC} = \frac{P}{B\sqrt{W}}\, f(a/W) \tag{3.3}$$

where P is applied load. B and W are thickness and width respectively. $f(a/W)$ is represent as a calibration function which depends on the cracks length ratio to the

width of the sample. Two methods were used to determine G_{IC}, which could be derived from the net fracture area and corresponding energy dissipation from the load-displacement curve or calculated by E, ν and K_{IC} via equation (3.4) [29].

$$G_{IC} = \frac{(1-\nu^2)}{E} K_{IC}^2 \quad (3.4)$$

Where ν is Poisson's ratio equal to 0.35. Good agreement was found between the two methods, so that G_{IC} values from equation (3.4) were reported in this work.

3.7 Data analysis and interpretation

As obvious from above-mentioned experimental details, a large volume of data-set was generated from tribological tests as well as associated physical and mechanical characterization of the materials. To ensure data accuracy and reproducibility, each of the individual tests were performed at least three times under identical test conditions. In the case of TFLs thickness measurements on wear tracks, 40 individual data point was obtained along the wear track to get a representative value of the TFLs thickness. During data analysis/interpretation, average values were used along with corresponding error bars. To analyse the wear mechanisms, SEM images were obtained at different magnification (from low to high) and similar magnified images of a given material was used for comparison purpose.

Chapter 4. Enhancement of mechanical and tribological behaviour of epoxy-based composites by nano-particles addition

4.1 Background information

Epoxy resin is brittle in nature and sensitive towards micro-cracks formation resulting in low impact toughness and fatigue resistance, although they may possess high strength, high elastic modulus, strong bond ability, and excellent chemical stability [109]. As a thermoset polymer, epoxy has 3D structure and their response in tribo-contacts is poor in general [110]. Toughening of epoxy is widely practiced. However, incorporation of soft and rigid nano-particles in it and its responses in tribo-contacts is yet to be fully explored [110-111]. Some of the factors that should be considered in reinforcing epoxy using nano-/micro sized reinforcements include wettability, retention of amorphous or crystalline structure, interface bonding, etc. [111-114]. There is a potential to better bonding and distinctive profile when the superior performance of the nano-/micro-filler strengthened elements is attributed to large interface area between polymer matrix and strengthening particles compared to natural polymer elements. However, it must be noted that tribological and mechanical properties do not have a simple one-to-one correlation [114-117]. The fracture and distortion of the polymers may occur with external force which facilitates the chain movement of its microstructure. Nonetheless, the presence of strengthening elements in polymer matrix or matrix rigidity can increase resistance to such movements. The concept applied in metal matrix reinforcement with carbide or inorganic oxide

particles is similar to that of strengthening the polymer matrix by incorporating hard particles [118]. However, incorporation of reinforcing particles (hard/soft) in polymer matrix does not always strengthen the matrix and sometime even exhibit detrimental nature [119-123]. In addition, formation of wear debris, in tribological applications, plays a significant role on overall material deformation. When polymers slide against metals, polymeric debris sometime forms continuous or discontinuous transfer film layers (TFLs), which plays a pivotal role on overall friction and wear response of the material. Up to now, quantitative characterization of TFLs is still limited though some insights has been achieved from qualitative way as reported in literature [37, 63].

The aim study of this work is to understand the effect of different kind of nano-filler reinforcement in epoxy polymer subjected to tribo-contacts in terms of mechanical and tribological properties and associated material deformation mechanism in terms of wear debris and transfer film layer formation.

4.2. Integration of nanoparticles with polymer matrix

In this chapter, pure epoxy has been used as matrix material. Two different types of nano-fillers, in different percentages, were used to form nanocomposites. The used nano-fillers are (i) rigid silica (SiO_2) particles and (ii) soft nano-rubber (CTBN). For SiO_2 reinforced composite, four different SiO_2 contents were used, namely 6 wt. %, 8 wt. %, 10 wt. % and 20 wt. %. Whereas, in the case of nano-rubber reinforced composite, two different nano-rubber contents were used, namely 6 wt. %, and 10 wt. %.

4.3 Results and discussion

4.3.1 Mechanical properties

The analyses of mechanical properties are very important in the context of understanding the tribological performance of nano-filler reinforced epoxy. The details of mechanical properties of epoxy and epoxy reinforced with nano-fillers are provided in Table 4.1.

Table 4. 1: Mechanical properties of nano-filler reinforced epoxy composites together with neat epoxy.

Materials	**Elastic modulus, E (GPa)**	**Strength, σ (MPa)**	**Fracture toughness**		**Density, ρ (g/cm^3)**
			K_{IC} (MPa $m^{1/2}$)	**G_{IC} ($kJ.m^{-2}$)**	
Neat epoxy	2.86 ± 0.08	42.1 ± 2.6	0.951 ± 0.029	0.277 ± 0.025	1.18 ± 0.02
Epoxy - 6 wt.% SiO_2	2.98 ± 0.10	43.1 ± 3.3	1.26 ± 0.04	0.465 ± 0.044	1.21 ± 0.05
Epoxy - 8 wt.% SiO_2	3.12 ± 0.15	42.7 ± 2.0	1.39 ± 0.07	0.546 ± 0.079	1.22 ± 0.09
Epoxy -10 wt.% SiO_2	3.14 ± 0.14	46.5 ± 1.1	1.57 ± 0.02	0.690 ± 0.050	1.29 ± 0.02
Epoxy - 20 wt.% SiO_2	3.48 ± 0.14	54.2 ± 4.3	2.11 ± 0.01	1.12 ± 0.05	1.30 ± 0.04
Epoxy - 6 wt.% CTBN	2.45 ± 0.02	39.5 ± 1.2	1.62 ± 0.03	0.946 ± 0.041	1.16 ± 0.08
Epoxy - 10 wt.% CTBN	2.30 ± 0.09	37.6 ± 0.8	2.25 ± 0.02	1.93 ± 0.10	1.15 ± 0.06

From Table 4.1 it is clear that with increasing nano-silica content in epoxy matrix, strength and stiffness generally increase. However, epoxy loses rigidity when rubber nano-filler was incorporated. The fracture toughness was seen to increase in both cases with higher nano-silica and nano-rubber contents. The rising G_{IC} value indicates that

higher reinforcing nano-filler raises the energy dissipation in the matrix in course of fracture propagation. Similar findings were also reported by Zhang et al. [124] as proportional increase in mechanical properties with corresponding nano-filler contents. This is obvious, since increasing reinforcements above a critical content the fillers could mostly ensures resistance to polymer chain movement and facilitates strength, stiffness and toughness. As mentioned in literature [29,63, 124], CTBN creates distinct boundaries with matrix interfaces and thus increases the toughness of the composite by a number of mechanisms such as activating cavitation, crack bridging and shear yielding of the matrix. In addition, the compatibility of nano-rubber and epoxy is well matched and resulted in significant increase in fracture energy. However, in order to toughen the epoxy with CTBN, the liquid polymer first forms a rubbery second phase which was dispersed throughout the epoxy matrix. After that, rubbery second phase (CTBN) became bonded with the matrix through the functional groups of the liquid polymer [124]. As the CTBN content increases, agglomeration became more prominent and thus detrition of the properties takes place as can be seen in Fig. 3.1 and Table 4.1. It shows both elastic modulus and strength decreases with increasing soft rubber content.

4.3.2 Friction and wear behaviour of epoxy-based composites

The wear tests were carried out at 5 MPa contact pressure and different sliding speeds (0.1, 0.2 m/s) at 24 hours sliding duration. All the tests were carried out in 'unlubricated' condition at room temperature, room humidity and pressure, as outlined in experimental conditions. Test parameters were selected based on the knowledge available in literature [20-37] and process optimization, to mimic the foreseen applications of such composite [5-17]. All the wear tests were repeated for at least

three times to ensure date accuracy and reproducibility under identical test conditions. Table 4.2 compares the tribological response data of nano-silica and nano-rubber reinforced epoxy composites. The specific wear rate for nano-silica reinforced epoxy reduced considerably, compared to the neat epoxy with both 0.1 m/s and 0.2 m/s sliding speed. With an increase in nano-sillica content, wear rate decreased progressively, and lowest wear rate was obtained in epoxy - 8 wt. % SiO_2 composite. With further raise in nano-silica contents, wear rate increased. In addition to lowest wear rate, maximum TFL thickness, TFL efficiency and coefficient of friction were also noticed in this particular case (epoxy - 8 wt. % SiO_2 composite) which can be attributed to positive interaction between the reinforcements and polymer matrix. The main reason of improved wear resistance of epoxy nanocomposites is due to its enhanced toughness (Table 4.1) up to critical reinforcement content. At higher nano-rubber content (Epoxy - 10 wt.% CTBN) the epoxy composite was so soft that, it just worn away without enough resistance against it.

Table 4. 2: Tribological response data for nano-silica and nano-rubber reinforced epoxy composite subjected to pin-on-disk sliding tests.

Materials	***'pv'* Factors**	**Tribological properties**		**Characteristics of TFLs on steel disk**	
		Specific wear rate ($\times 10^{-5}$ mm^3/Nm)	**Coefficient of Friction (μ)**	**Average Thickness h_f (nm)**	**TFL efficiency (λ)**
Net epoxy	5 MPa, 0.1 m/s	8.80 ± 0.55	0.49 ± 0.12	60.0	0.27
	5MPa, 0.2 m/s	8.64 ± 1.10	0.67 ± 0.09	46.03	0.21
Epoxy - 6 wt.% SiO_2	5 MPa, 0.1 m/s	7.07 ± 1.09	1.22 ± 0.22	343	1.56
	5MPa, 0.2 m/s	7.62 ± 1.02	0.99 ± 0.08	301	1.37
Epoxy - 8 wt.% SiO_2	5 MPa, 0.1 m/s	5.83 ± 1.29	1.63 ± 0.35	441	2.0
	5MPa, 0.2 m/s	5.66 ± 0.95	1.95 ±0.09	469	2.10
Epoxy - 10 wt.% SiO_2	5 MPa, 0.1 m/s	6.92 ± 1.09	1.38 ± 0.42	378	1.72
	5MPa, 0.2 m/s	7.81 ± 1.32	1.35 ± 0.13	356	1.66
Epoxy - 20 wt.% SiO_2	5 MPa, 0.1 m/s	8.05 ± 0.9	0.70 ± 0.25	284	1.29
	5MPa, 0.2 m/s	8.51 ± 0.88	0.99 ± 0.14	288	1.31
Epoxy - 6 wt.% CTBN	5 MPa, 0.1 m/s	7.92 ± 1.5	0.86 ± 0.23	285	1.29
	5MPa, 0.2 m/s	7.22 ± 0.85	0.97 ± 0.24	253	1.15
Epoxy - 10 wt.% CTBN	5 MPa, 0.1 m/s	8.41 ± 1.33	0.71 ± 0.22	198	0.90
	5MPa, 0.2 m/s	8.07 ± 1.28	0.81 ± 0.30	216	0.98

Graphical representation of the relationship between nano-filler content in epoxy with specific wear rate and coefficient of friction is shown in Figures 4.1 and 4.2. From the figures, it is clear that, specific wear rate reduced moderately at 8 wt. % nano-silica loading and 6 wt. % CTBN nano-rubber loading, which then sharply increase for higher content of nano-filler loading.

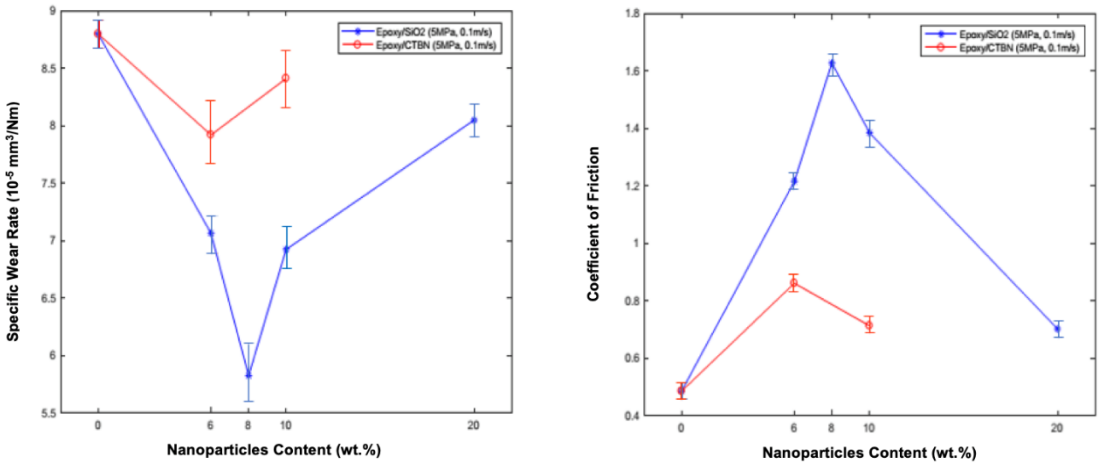

Fig. 4. 1: Specific wear rate and coefficient of friction for all materials subjected to pin-on-disk sliding test at 5 MPa normal load and 0.1 m/s sliding speed.

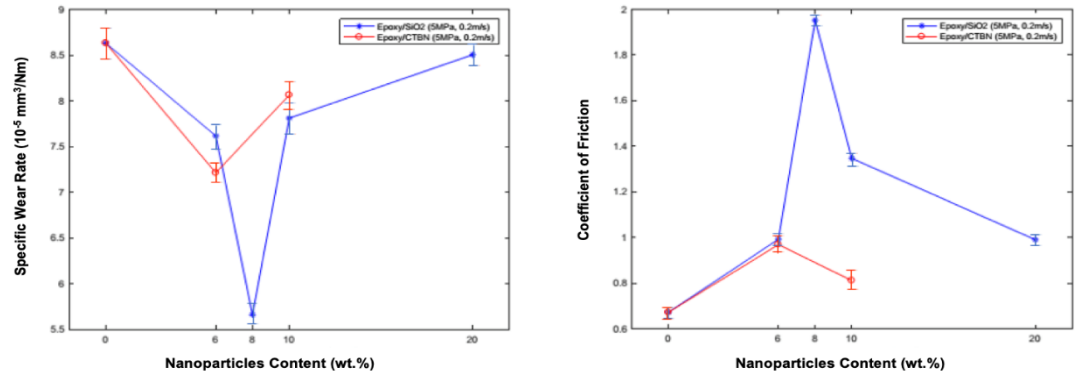

Fig. 4. 2: Specific wear rate and coefficient of friction for all materials subjected to pin-on-disk sliding test at 5 MPa normal load and 0.2 m/s sliding speed.

The positive effect of nano-filler loading in epoxy matrix in terms of specific wear rate is attributed to the formation of effective and thicker TFLs on steel counterpart. From the results (Figures 4.1 and 4.2) it is clear that reduction of specific wear rate, associated with an increase in coefficient of friction. To find out more about the role of TFLs formation on wear and coefficient of friction, TFLs thickness along the wear-

track on steel disk were measured with the help of nanoindentor as shown in Figures 4.3 and 4.4.

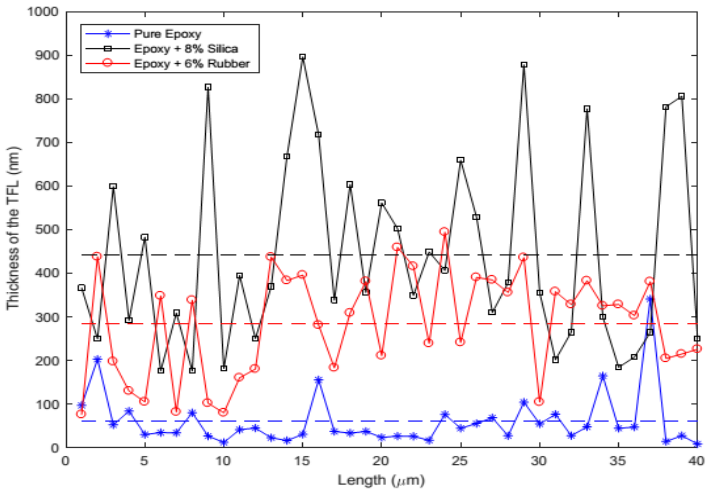

Fig. 4. 3: TFLs thickness distribution on wear-tracks on steel disk of neat epoxy, epoxy – 8 wt. % SiO_2 and epoxy - 6 wt. % CTBN composite subjected to pin-on-disk sliding test at 5 MPa normal load and 0.1 m/s sliding.

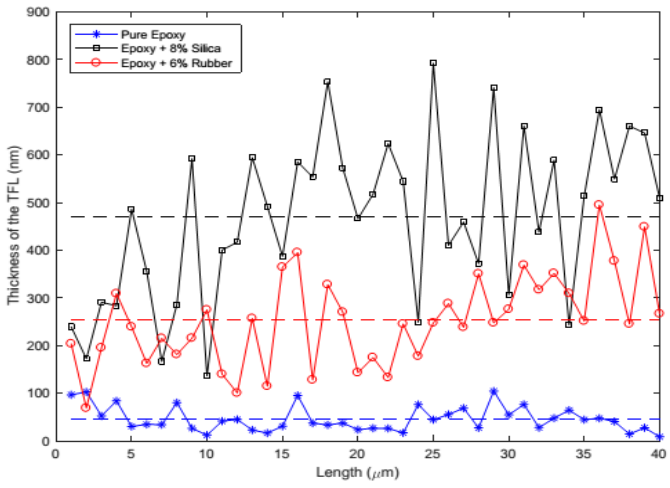

Fig. 4. 4: TFLs thickness distribution on wear-tracks on steel disk of neat epoxy, epoxy – 8 wt. % SiO_2 and epoxy - 6 wt. % CTBN composite subjected to pin-on-disk sliding test at 5 MPa normal load and 0.2 m/s sliding.

It is obvious that, in all cases, TFL formation is more pronounced in nano-filler reinforced composites compared to neat epoxy. With increasing rigidity due to the presence of nano-fillers in epoxy, transfer film layer thickness increased. And toughened epoxy showed higher TFL thickness regardless of variable '*pv*' factor (Table 4.2). The thicker TFLs also caused an increase in coefficient of friction compared to neat epoxy, due to higher adhesion between TFLs and polymeric specimens. The more effective formation of TFLs with nano-fillers can be explained by the allocation of nano-fillers. Though large agglomerations of nano-fillers are mostly avoided, there could be some regions where more entity of nano-fillers which are moderately closer to each other. This means that in those areas cluster-rich regions could be more frequently present. Due to stress concentration, weak bonding among nano-fillers could initiate matrix cracks during sliding wear process [29,63,124-125]. With time, this results in the formation and propagation of micro-cracks on the worn surface under cyclic loads during the sliding process. The wear debris then generated when these micro-cracks were associated with each other.

4.4 The effect of the addition of nanoparticles on tribological performance of epoxy-based composites

To get the insight of wear mechanisms, worn surfaces of the samples as well as wear tracks on steel counter face were further analyzed with the help of SEM as shown in Figures 4.5 and 4.6. It can be seen that, worn surfaces of pure epoxy (Fig. 4.5a, b, 4.6a, b) are rough with crumbling areas. Micro-sized wear debris have been separated from epoxy specimen, leaving asymmetrical craters. The texture of ploughed grooves were rough and scale-like protuberances were noticed along the sliding direction as well as some brittle cleavage fracture on the worn surface. As neat epoxy is somewhat brittle,

thus it also contains crack and break away from the surface and form brittle cleavage fracture due to shear stress. For neat epoxy, the dominant wear mechanism is adhesive wear and ploughing cutting. However, in case of nano-filler reinforced epoxy, continuous chunky layers of transfer films were observed on the steel counter faces (Fig. 4.5c-4.5f, 4.6c-4.6f), which effectively protect the specimens from the direct contact of steel counterpart. For composites packed with nano-fillers, the patterns of surface scratch altered considerably compared to neat epoxy; that is compact and smooth layers without noticeable cracks on steel counterpart and covers approximately the complete sliding contact area. Thus, for epoxy nanocomposites, the wear mechanisms changed to mild adhesive wear. However, with a further increase in reinforcement content, nano particles agglomeration became prominent and resulted in fatigue type wear with continues repetitive sliding actions. The overall material deformation is thus the actions of micro-ploughing. These could be a result of three-body abrasion wear induced by the hard wear debris trapped in the contact regions, which can be seen on the worn surfaces. Consequently, the lessening in wear rate of epoxy- 8 wt. % SiO_2 composite can be accredited to the development of the transfer film, which results in 'polymer-on-polymer' contact instead of 'polymer-on-steel' contacts. On the other hand, the real contact area can be increased between smooth, compacted worn surfaces covered with the transfer films. Consequently, coefficient of friction increases due to adhesive nature in the tribo-contacts. It is interesting to note that, complete TFLs formation takes place at relatively high nano-filler contents (8 wt. % nano-silica and 6 wt. % nano-rubber in present study), which may play a key role in determining the wear performance of nanocomposites in steady wear stage. During contact sliding, tribo-chemical reaction mechanism also takes place on the material

surface as a result of thermal (flash temperature) and mechanical (surface asperity deformation, shear stress) effects [119] and results in oxidation of the surface materials. The surface oxidation of epoxy and epoxy nanocomposites in tribo-contact was confirmed [29] by XPS analysis as the intensity of C–H (or C–C) peak decreased while that of C–O peak increased after the sliding wear. Mechanically induced reaction involves repeated action of the shear stress which led to polymeric chain scission in epoxy and its nano-composites [126].

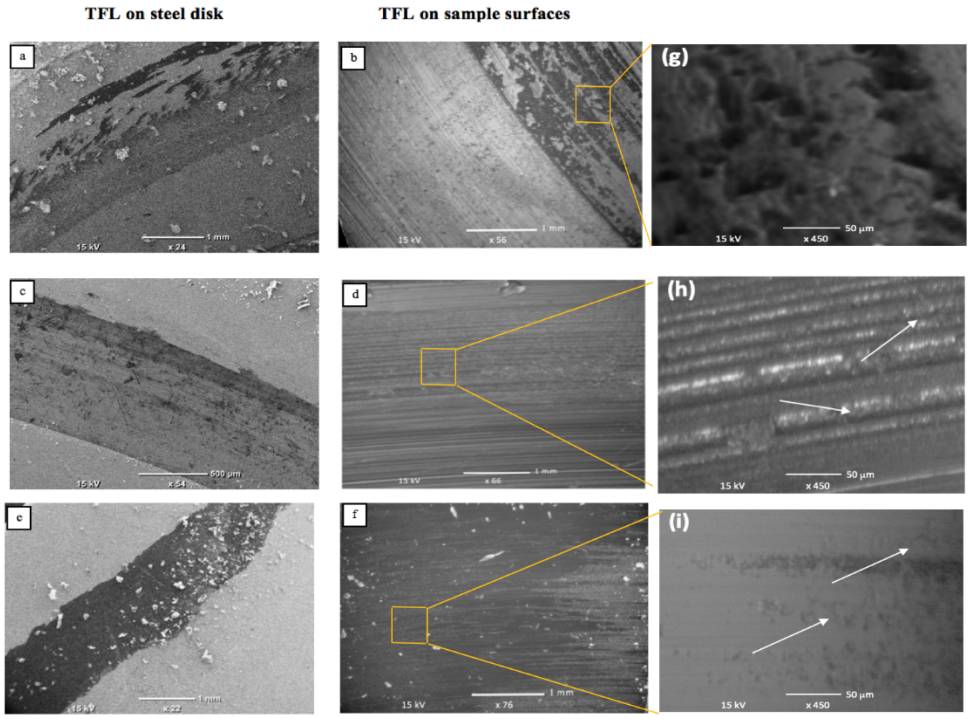

Fig. 4. 5: SEM images of wear tracks on steel counterpart and worn surfaces subjected to pin-on-disk test at 5 MPa normal load and 0.1 m/s sliding speed: (a) and (b) pure epoxy, (c) and (d) epoxy – 8 wt. % SiO_2, (e) and (f) epoxy – 6 wt. % CTBN. High-magnification of worn surfaces of (g) pure epoxy, (h) epoxy-8 wt. % and (i) epoxy-6 wt. %

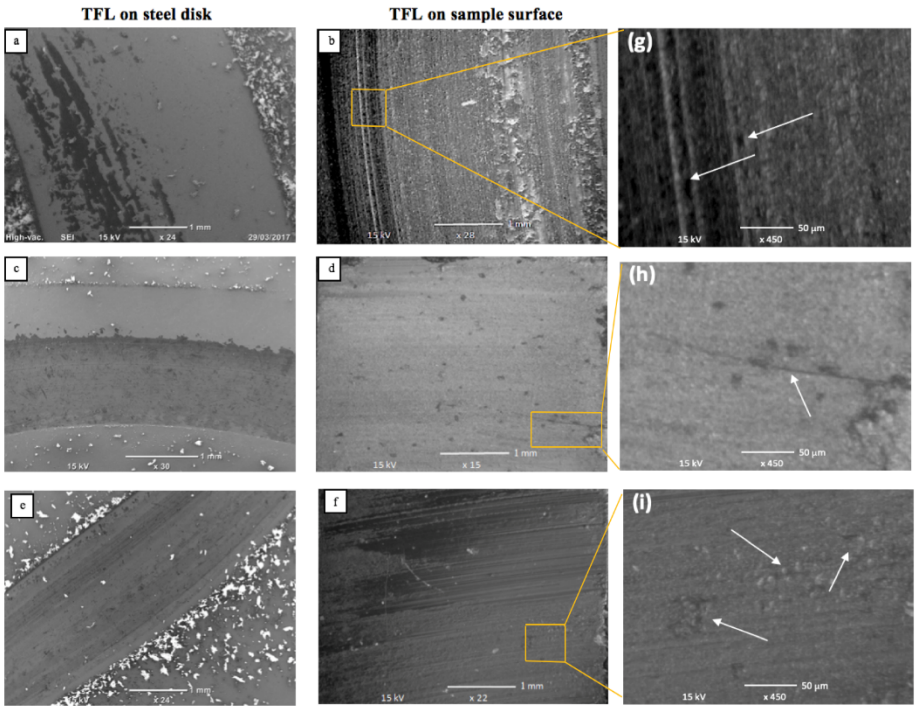

Fig. 4. 6: SEM images of wear tracks on steel counterpart and worn surfaces subjected to pin-on-disk test at 5 MPa normal load and 0.2 m/s sliding speed: (a) and (b) pure epoxy, (c) and (d) epoxy – 8 wt. % SiO_2, (e) and (f) epoxy – 6 wt. % CTBN. High-magnification of worn surfaces of (g) pure epoxy, (h) epoxy-8 wt. % and (i) epoxy-6 wt. %

It was also noticed during pin-on-disk tests that all the materials behaved in a brittle manner with visible cracks as shown in figs. (4.5 and 4.6). The average size of the wear debris of specimens was also observed during the tests and manually measured in SEM pictures. Fig. 4.7 shows the size of wear debris on the worn surface. Formation of smaller-scale debris is important to build-up of transfer film layers and these kinds of characteristics were found in case of epoxy – 8 wt. % SiO_2.

While the neat epoxy shows bigger sizes of lumps with random size of wear debris distribution, epoxy – 20 wt. % SiO_2 showed smoother wear debris with mostly uniform size distribution. This is attributed to the agglomeration of nano-silica particles as

shown in previous chapter (Fig. 3.1) along with '*pv'* factor that created the debris. It is interesting to note that, wear debris size increased for epoxy - 8 wt. % SiO_2 compared to epoxy – 20 wt. % SiO_2. However, in the case of nano-rubber reinforced composites, due to reduced stiffness of epoxy matrix, epoxy - 6 wt. % CTBN and epoxy – 10 wt. % CTBN shows similar wear debris size distribution. Size of wear debris could be inverse function of the nano-filler loading as reported by Zhang et al. [124]. It was also accredited to the raise of the density of nano-filler rich regions and was considered as a key toughening mechanism as a result of force dissipation in micrometer scale. In conclusion, it is worth mentioning the correlations among inter particle distance and the property profile of the nano-fillers [77-79]. In addition, shape and size of wear debris are very much related to the brittle and ductile nature of nano-fillers itself. This explains the more effectiveness of nano-silica fillers in epoxy matrix compared to nano-rubber. It is also possible that, smaller wear debris could provide more effective continuous transfer film layers, which ultimately reduce wear rate. Nevertheless, it is also interesting to note that improvement in wear resistance of pure epoxy was achieved by the nano-filler incorporation in it. Although there is no straightforward association between mechanical properties and tribological properties, it is meaningful to carry out some more methodical research to understand the correlation among the microstructure of nano-filler reinforced composites and the pattern of wear debris, as well as its role on overall wear mechanism. In general, improved wear resistance of epoxy nanocomposites can be attributed to the overall improved mechanical properties such as hardness and toughness of the composite in the presence of nano-filler reinforcement. However, it is important to note that, once the nano-filler content is

beyond the critical level, nano-particle agglomeration cause inferior results as the composite losses its effective load transfer capability.

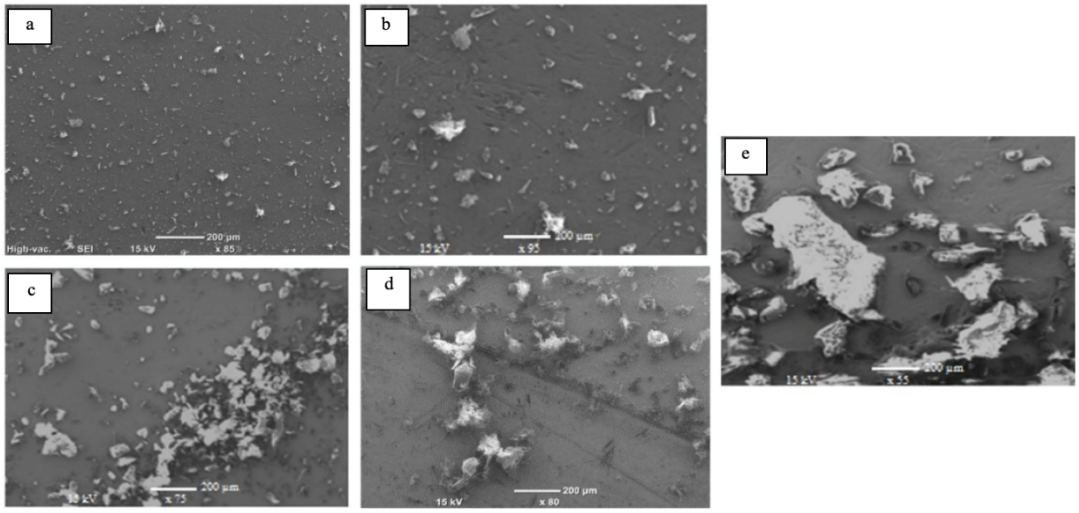

Fig. 4. 7: SEM images of wear debris arranged from smallest to largest sizes after pin-on-disk test subjected to 5 MPa normal load and 0.2 m/s sliding speed: (a) epoxy – 8 wt. % SiO_2, (b) epoxy – 20 wt. % SiO_2, (c) epoxy – 6 wt. % CTBN, (d) epoxy – 10 wt. % CTBN and (e) pure epoxy.

4.5. Summary

The pin-on-desk test has been used in investigating the wear characteristic of the nano-filler-reinforced epoxy. This was followed by a detailed investigation of the formation of the TFLs on wear tracks by carrying out nanoindentation and SEM tests. Generally, the tribological and toughness of neat epoxy are enhanced when incorporated with nano-particles (soft/hard). Furthermore, the stiffness and strength of the epoxy matrix will be improved through the addition of rigid nano-silica whereby studies indicate that 8 wt. % of rigid nano-silica demonstrated the best wear resistance outcome. On the other hand, detrimental effect on wear resistance was observed due to agglomeration of nano-fillers at a higher nano-silica loading. Addition of nano-rubber

in epoxy matrix improves the fracture toughness of epoxy compared to nano-silica; however, it demonstrated a lower wear percentage improvement on nano-rubber loading compared to neat epoxy. Hence, the correlation between the tribological and mechanical characteristics of the nanocomposites was not simple. The formation of wear debris showed dependency on nano-filler content loading in the composite.

The role of different kinds of nano- filler reinforced epoxy has been clarified in this chapter, it is one of the most preferred thermosetting polymers currently used in industrial applications. Further investigation on the role of the nano-particles in wear resistance will be illustrated in the next chapters by incorporating thermoplastic polymers under different sliding conditions.

Chapter 5. Enhancement of tribological behaviour of poly-ether-ether-ketone (PEEK) by addition of TiO_2 nano-particles

Various tribological applications have progressively used engineering polymers over the past decades. These tribological applications have pushed the research towards the development of high-performance polymers [33-35,127]. The characteristics obligatory for tribology associated applications include superior chemical, excellent cohesive strength, maintaining elevated service temperature, wear, and mechanical resistance. With these in agenda, poly ether-ether ketone (PEEK) is regarded as one of the most capable polymers for such applications due to its inherent semicrystalline thermoplastic nature with excellent mechanical and chemical resistance [128-129]. General polymers like PEEK can have their tribological and mechanical performance enhanced by incorporation of fillers in polymers in different states such as whiskers, fibers, particle or a combination of those. Considering the mechanical properties of PEEK as high-performance polymer is currently used as a sealing material in containers used for cooling water in nuclear power plants [31] and tribological features of PEEK in water is a significant concern. Most of the work available in literature focus on the tribological aspects of high-performance polymers under dry conditions with a few reports involve water lubricated conditions [19, 30,44,72,73,130]. Thus, there is a need for more investigation in this area concerning tribological dynamics in water-lubricated environments. Thus, the aim of this chapter

is to study the mechanical and tribological properties of PEEK strengthened with TiO_2 nano-particles at room temperature under dry and water lubricated sliding conditions. The characterization of the TFLs formed under various environments has been keenly checked, as well as their effect on the wear performance of polymeric specimens.

5.1 Materials and experiment

In this work, four samples were prepared, namely, pure PEEK, PEEK with 5% TiO_2, PEEK with 10% TiO_2 and PEEK with 15% TiO_2. All TiO_2 content was in weight percentage. As stated in literature, there is a tendency of particle agglomerations in the case of higher nano-filler loading; therefore, nano-fillers up to 15 wt.% was used n present case based on process optimization and previous investigations [35-37]. Tribological behaviour of all specimens were conducted by pin-on-disk testing under two different slide conditions: dry condition and water lubricated condition at room temperature. The period of each test was 24 hours under 5N normal load and 0.1 m/s sliding speed. After the sliding tests, worn surfaces of both test coupons as well as steel counterbody were examined by SEM. Nanoindentation used to investigate the hardness of tattered surfaces as well as to characterize TFL (as stated in Chapter 3). Fourier-transform infrared spectroscopy (FTIR) of the PEEK samples before and after pin-on-disk sliding test at dry and wet condition were recorded using an Agilent 4300 spectrometer at room temperature. Four scans were collected for each sample in the wavelength range between 4000 and 650 cm^{-1}.

5.2. Results and discussion

5.2.1 Mechanical characterization of PEEK composites

The analyses of mechanical properties are very important in the context of understanding the tribological performance of nano-particles reinforced PEEK composite. The details of mechanical properties of PEEK and PEEK reinforced with nano-particles are provided in Table 5.1. As can be seen from Table 5.1, PEEK + 5% TiO_2 has lowest strength, even lower than that of neat PEEK, among all the materials and relatively higher fracture toughness compared to other PEEK composite. This may be due to the breakage of polymeric chain structure of the composites, which overshadow the role of reinforcement. In other words, the content (%) of reinforcement is not enough to outcast the effect of disruption of polymeric microstructure due to the addition of reinforcements. This implies that this composite is subjected to more severe plastic deformation under the same loading condition. As the nano-particle loading increases, brittle fracture will be more prominent and most probably will facilitate larger chip type wear debris instead of continues type as foreseen in the case of PEEK + 5% TiO_2 composite. This hypothesis will be further validated with the help of wear debris morphology investigation as reported in later sections.

Table 5. 1: Mechanical properties of PEEK and PEEK composites.

Samples	**Elastic modulus, E (GPa)**	**Strength, σ (MPa)**	**Fracture toughness K_{IC} (MPa$\sqrt{m}$)**
Neat PEEK	3.7±0.05	93±1	6.09±0.42
PEEK+5%TiO_2	4.3±0.06	64±6	4.96±0.21
PEEK+10%TiO_2	5.0±0.10	80±4	4.21±0.14
PEEK+15%TiO_2	5.2±0.20	92±7	3.83±0.18

5.2.2 Physical characterization of PEEK composite

Fig. 5.1 shows SEM micrographs of PEEK incorporated with different amount of TiO_2 nano-particles and exhibit uniform distribution of nano-particles in polymer matrix. The tendency of nano-particle agglomeration is also evident particularly at higher of weight percentage of TiO_2. For example, the agglomeration size became about 1µm for PEEK incorporated with 15% TiO_2 nano-particles (Fig. 5.1(c)) compared to PEEK incorporated with 10% TiO_2 nano-particles (Fig. 5.1(b)) as confirmed from the SEM images. The measurements were carried out based on the SEM micrographs (Fig. 5.1) covering the whole area of the micrographs and average values were used for data interpretation.

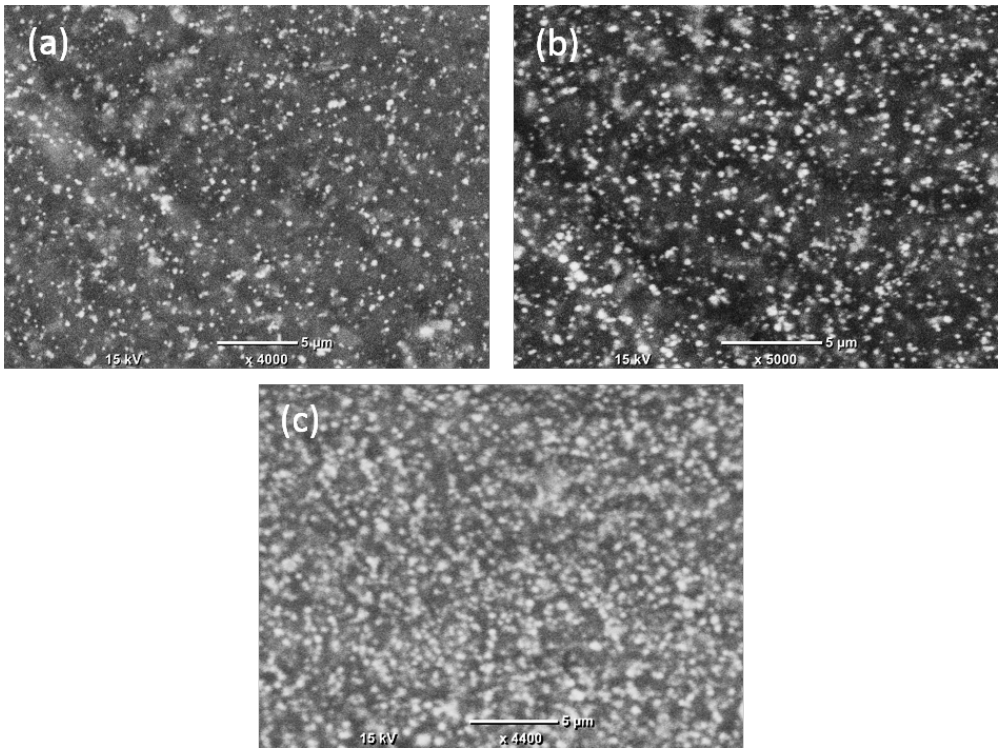

Fig. 5. 1: TiO_2 nano-particles distribution in PEEK matrix: (a) 5% TiO_2, (b) 10% TiO_2 and (c) 15% TiO_2.

5.3 Tribological behaviour of PEEK composites

5.3.1 Dry sliding condition

Wear-rate and coefficient of friction obtained from pin-on-disk wear test for different TiO_2 contained PEEK as well as for pure PEEK is shown in Fig. 5.2. Addition of up to 5% TiO_2 nano-particles in PEEK decrease wear-rate compared to pure PEEK, however beyond that, an increase in wear-rate was noticed. Thus, PEEK with 5% TiO_2 leads to highest wear resistance as well as coefficient of friction compared with other samples including pure PEEK. This information provides an insight about critical TiO_2 content in PEEK. Initially, coefficient of friction increases with the addition of 5% TiO_2 in PEEK compared to pure PEEK and beyond that (more than 5% TiO_2 addition) does not affect it significantly. This is due to the fact that, under dry condition, main lubrication of the TFL is mostly determined by the properties of amorphous PEEK polymer with negligible contribution from TiO_2 nanoparticles. A hypothesis was proposed by Zhang *et. al.* [65] that, tribological behaviour of PEEK is closely related to its viscoelastic behaviour, influence of interface temperature and strain rate of the PEEK surface layer involved in the friction process.

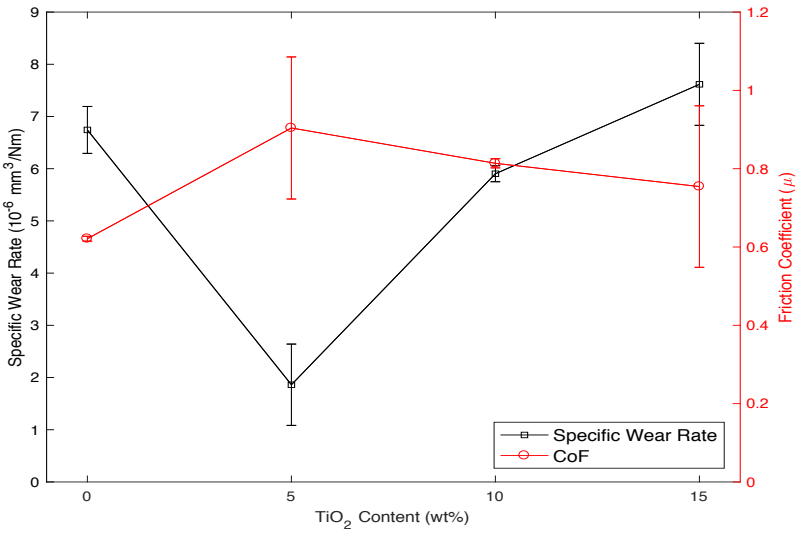

Fig. 5. 2: Specific wear-rate and corresponding coefficient of friction for different concentrations of TiO2 contained PEEK obtained from pin-on-disk test under dry condition.

In terms of wear resistance, adding TiO2 nanoparticles optimized the coefficient of friction, as an increase in coefficient of friction may occur associated with the decrease of specific wear rate. This can be explained by the formation of transfer film and adhesive wear will be predominant instead of abrasive wear. This hypothesis will be investigated further in subsequent sections in terms of transfer layer formation and their corresponding thickness in different test conditions. In addition, higher nano-particles content leads to agglomeration that could contradict load-transfer mechanism from matrix to reinforcement.

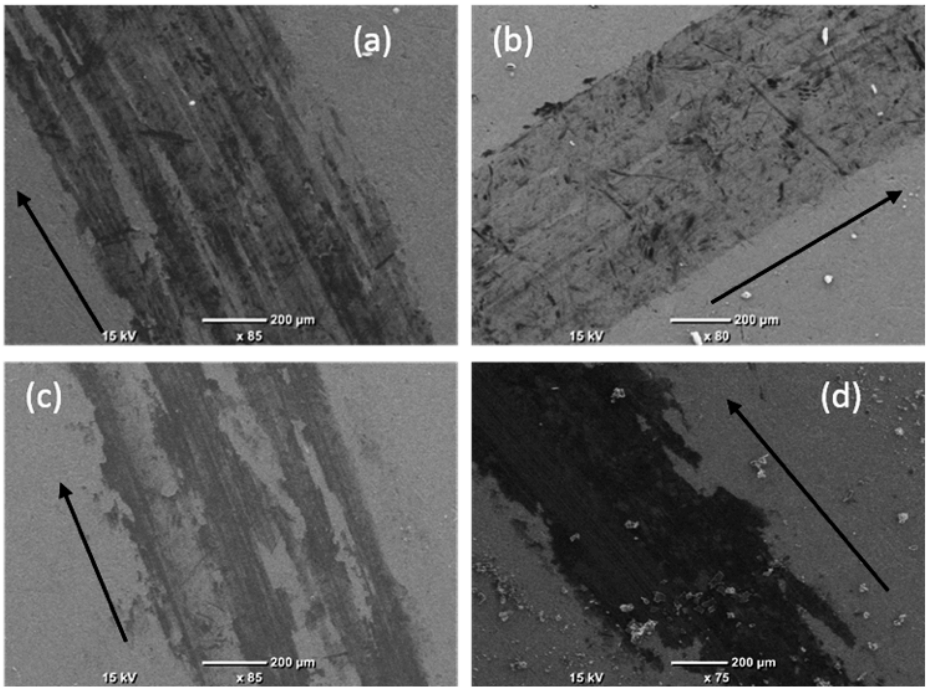

Fig. 5. 3: SEM micrographs of wear-track on steel disk sliding against pure PEEK/ PEEK- composite (dry-condition): (a) Pure PEEK, (b) PEEK+5%TiO_2, (c) PEEK+10%TiO_2 and (d) PEEK+15%TiO_2.

To investigate wear mechanisms, wear tracks on steel disk was investigated by SEM as shown in Fig. 5.3 and presence of plasticised polymer composite was evident. Sliding between materials results heat generation and cause the polymer surface to plasticize [71, 73]. This degradation diminishes load bearing capacity, which leads to easy detachment of polymer chips resulting severe wear [63]. In addition, higher nano-particles content leads to agglomeration that could contradict load-transfer from matrix to reinforcement. Further, accumulation of TiO_2 nano-particles has the capacity to weaken semi-crystalline structure of PEEK by interfering crystallite formation of macro-molecules as a result of heat generation in tribo-contact as mentioned in literature [31]. These facts are also supported by work of Zhong *et. al.* [128] where the

authors realized that higher nano-particles content dose not efficiently reduce wear rate due to the effect of nano-particles agglomeration.

To have an insight on different lubrication regime prevail in the present case, Stribeck type curve was plotted in terms of transfer film efficiency factor (λ) according to Chang et. al. [37] as shown in Fig. 5.4. As indicated in chapters 2 and 3, λ was defined as the ratio of the average thickness of the TFL to the surface roughness of the steel counterpart. Accordingly, a Stribeck type curve can be constructed to illustrate the different lubricant regime related to the film thickness, such as, (a) full TFL lubrication regime showing efficient form of lubricant, that is, the thickness of TFL is clearly larger than the surface roughness of the abrasive counterpart, (b) boundary lubrication regime results from abrasive scratching from the steel disk without TFL lubrication effect and (c) mixed lubrication regime is a mix between the full TFL lubrication regime and boundary lubrication regime.

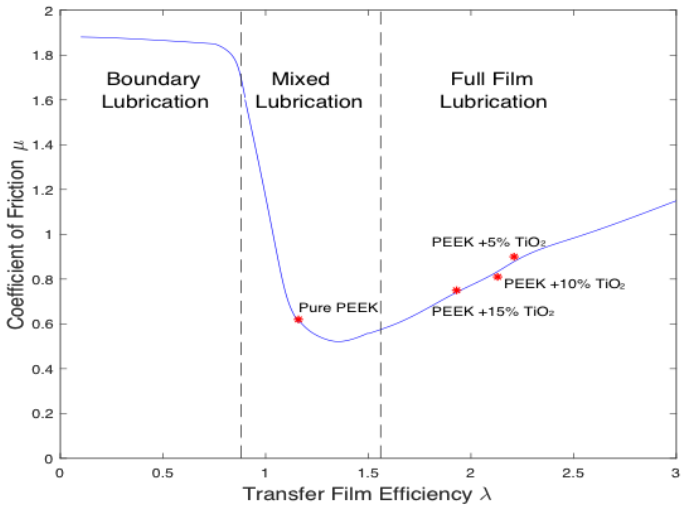

Fig. 5. 4. Stribeck type curve under dry condition for PEEK and PEEK composite.

The Stribeck type curve (Fig. 5.4) was originally developed to describe the lubrication regime in the presence of liquid/semi-solid/viscous lubricants. Though in present case, no lubricant was used, however, in tribo-contact the mating materials behave like semi-solid/viscous as reported in literature [37]. Thus, such curves give an essence of the kind of lubricating effect, as in tribo-contacts, materials exhibit plastic flows.

5.3.2 Water lubricated condition

Wear and friction behaviour investigated under water lubricated condition is shown in Fig. 5.5. In view of TiO_2 content in PEEK, wear-rate was almost unaffected which is opposite than that of dry condition tests. Compared to dry condition tests, water-lubricated conditions reduce the coefficient of friction values from 0.6 to 0.3 for pure PEEK, 0.9 to 0.1 for PEEK+5%TiO_2, 0.8 to 0.2 for PEEK+10%TiO_2, and 0.7 to 0.2 for PEEK+15%TiO_2. This is not only due to lubricant nature of water but also its coolant effect and thus friction-induced thermal and mechanical effects could be inhibited in aqueous environment [44]. It is also interesting to note that, increase of TiO_2 beyond 5% does not have any effect on wear behaviours of the composites as well as friction coefficient.

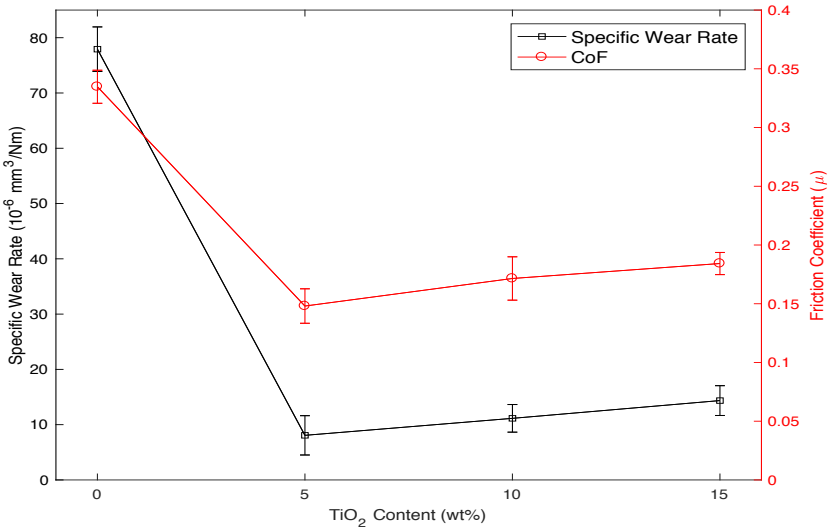

Fig. 5. 5. Specific wear-rate and corresponding coefficient of friction for different concentrations of TiO2 contained PEEK obtained from pin-on-disk test under water lubricant condition.

Fig. 5.6 shows SEM micrographs on wear-track of steel disk associated with water lubricant pin-on-disk test. In general, TFLs are less noticeable in all cases compared to dry condition tests. Nevertheless, the lower friction coefficient suggests the presence of aqueous lubricant film, although solid contact still occurred resulting in wear loss of polymer specimen. Thus, under water lubricated condition, mix lubrication condition could be considered.

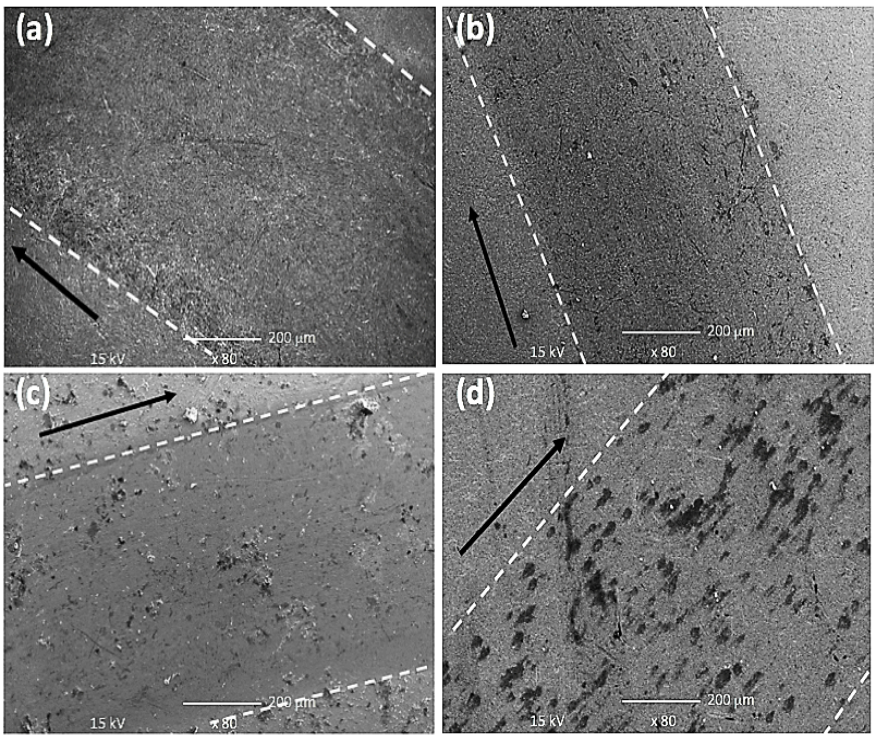

Fig. 5. 6. SEM micrographs on wear-track of steel disk under water lubricant conditions: (a) Pure PEEK, (b) PEEK+5%TiO_2, (c) PEEK+10%TiO_2 and (d) PEEK+15%TiO_2.

5.3.3 TFLs and wear debris formations

In both cases (dry and water lubrication conditions), addition of nano-particles in pure PEEK reduce specific wear-rate, though there is no general relationship between the trends in coefficient of friction and specific wear-rate. A lower friction coefficient signifies lesser shear force and lower contact temperature under same normal load and velocity. Therefore, the results express that nano-composites can be used in more severe loading conditions.

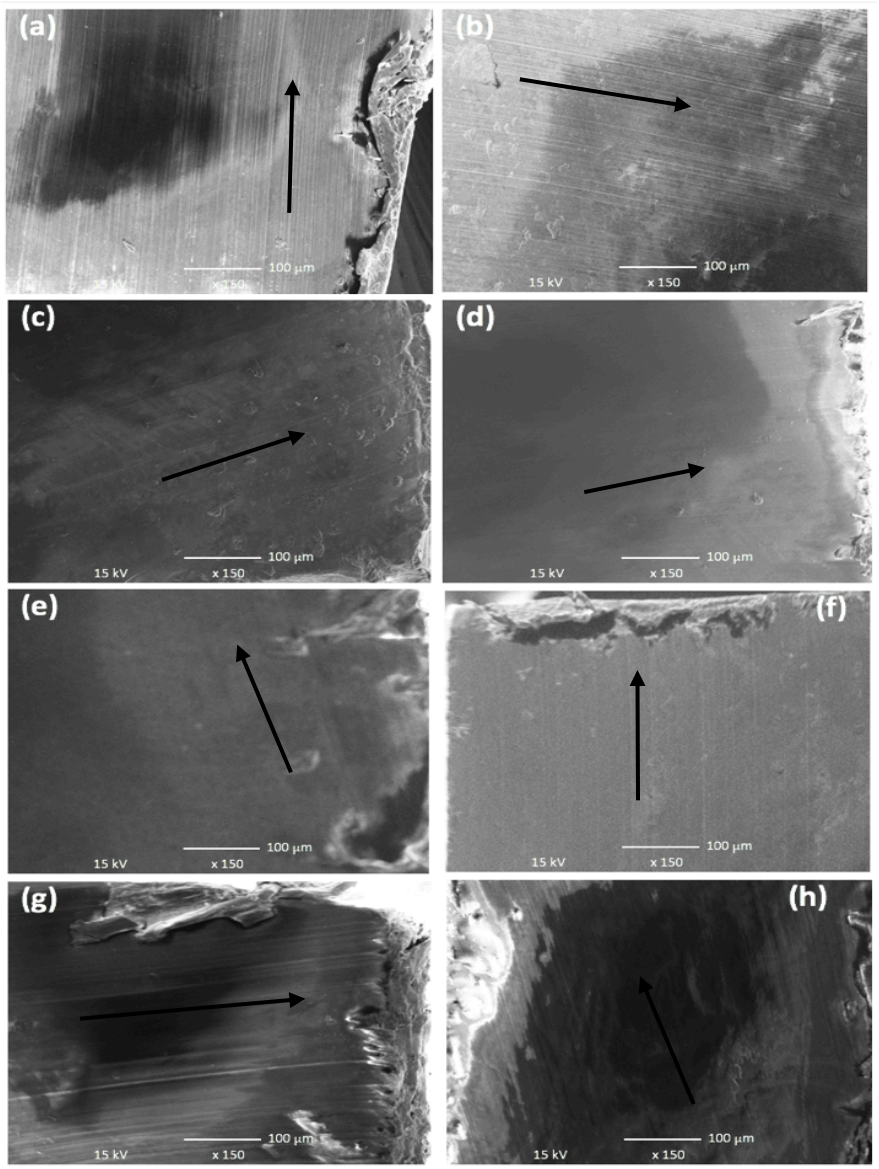

Fig. 5. 7. SEM micrographs on wear tracks in test coupons. Self-lubrication group: (a) Pure PEEK, (c) PEEK+5%TiO_2, (e) PEEK+10%TiO_2 and (g) PEEK+15%TiO_2. Water lubrication group: (b) Pure PEEK, (d) PEEK+5%TiO_2, (f) PEEK+10%TiO_2 and (h) PEEK+15%TiO_2.

As evident in Fig. 5.3, amount of debris has been increased with increasing TiO_2 content in PEEK. However, in case of water lubrication condition (Fig. 5.6), wear tracks are moderately smooth, indicating that the wear process was governed by placid scuffing mechanism [65]. Additionally, material removal occurred mostly by harsh

scratching due to the presence of stiff asperities on steel disk. In the case of pure PEEK, wear mechanism is dependent on polymer hardness and roughness of steel disk. At dry condition, high temperature generated by friction insists the polymer to undergo brittle-ductile transition and thus easier to forming effective TFLs. Such brittle-ductile transition is common in semi-crystalline PEEK microstructure, where long chemical chain among macro-molecules break down due to presence of heat generated by friction, in present case and cause brittle material to behave in soft ductile manner. The surface was covered by TFLs with grooves along sliding direction. However, throughout the wear process, changeover is evidenced by wear wreckage in appearance of layers instead of particulate wear debris. A comparison between worn surfaces of pins (PEEK/PEEK composites) could clarify more about the wear process. A collective comparison of wear-tracks on test coupons (PEEK/PEEK composites) is shown in Fig. 5.7. The devastation of wear under dry and water lubrication is clearly visible with the presence of grooves, abrasive wear marks, detached particles as well as plastic deformation and material pile up. The main reason for wear rate increase in water lubricated conditions is that, water molecules can be absorbed in the free volume of amorphous polymer phase through diffusion. This results in polymer softening and reduce the materials' strength [73]. In addition, absorbed water can also reduce the attractive forces between polymer macro-molecules chains and offer relatively easy material removal compared to dry condition tests [19]. Finally, the presence of water lubricant could hinder the formation of polymeric TFL on the steel couternface. Although the aqueous film may reduce friction, its load carry capacity is much lower than solid TFL, resulting in higher wear loss.

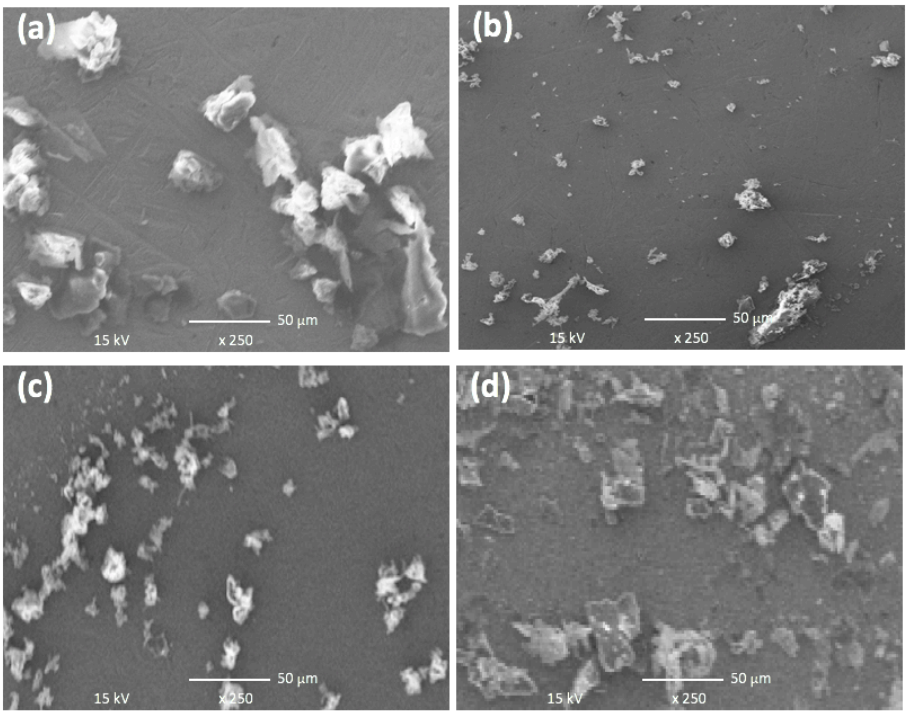

Fig. 5. 8. SEM micrographs of wear-debris formed during pin-on-disk sliding test (dry-condition): (a) Pure PEEK, (b) PEEK+5%TiO_2, (c) PEEK+10%TiO_2 and (d) PEEK+15%TiO_2.

Wear-debris formed during sliding tests were also examined, as shown in Figures 5.8 and 5.9 respectively for dry and water-lubricated sliding conditions. Formation of smaller debris is important to build-up efficient transfer film layers [4] and this particular characteristic was more prominent in the case of PEEK + 5 wt. % TiO_2 in both dry and water lubricated conditions (Fig. 5.8b and Fig. 5.9b). Overall, neat PEEK shows larger and fragmented debris, associated with relatively high wear loss. It is also interesting to note that, in dry sliding conditions, the debris are relatively more fragmented and smaller compared to water lubricated conditions. Large roll-over of

debris was also easily visible in water lubricated conditions (Fig. 5.9) and was absent in dry condition tests (Fig. 5.8).

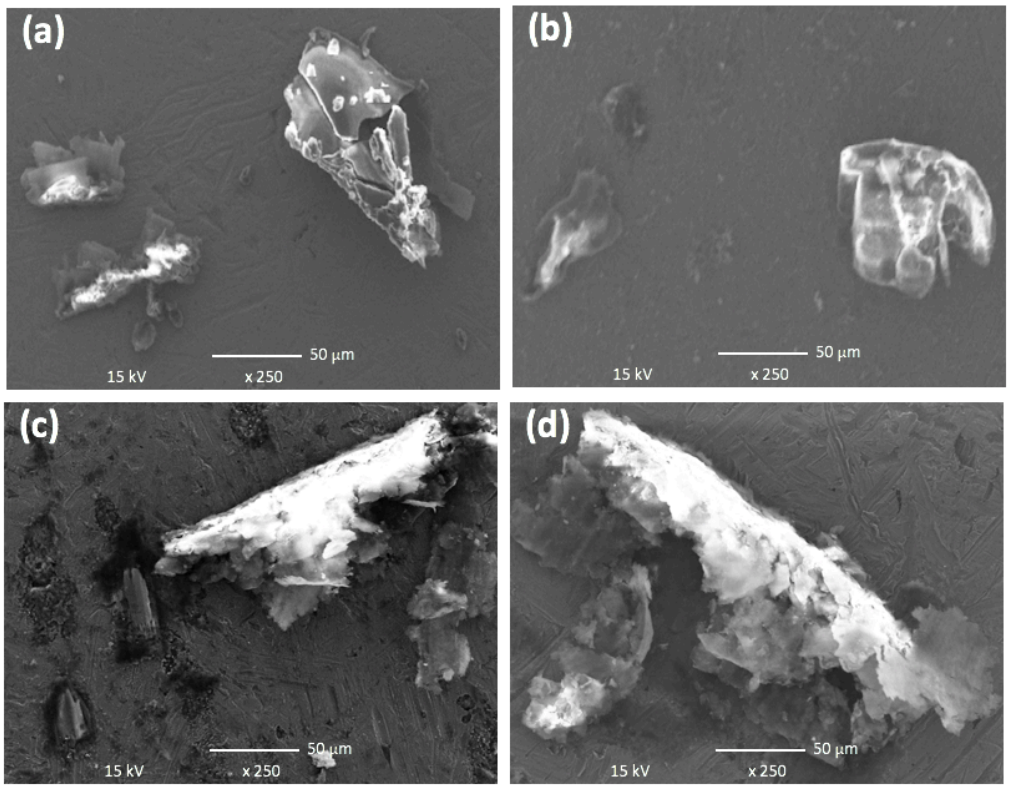

Fig. 5. 9. SEM micrographs of wear-debris formed during pin-on-disk sliding test (water lubricated condition): (a) Pure PEEK, (b) PEEK+5%TiO_2, (c) PEEK+10%TiO_2 and (d) PEEK+15%TiO_2.

Furthermore, as aforementioned, TFLs formation in water lubricated condition is not stable due to the presence of water and thus sliding occurs directly between polymer and steel disk. All the above-mentioned factors are responsible for the increase wear rate in water lubricated conditions, compared to dry condition pin-on-disk tests. SEM images only provides qualitative aspect of worn surfaces and general morphology of TFLs without any quantitative appraisal. In view of that, nanoindentation on TFLs in wear-tracks on steel disk as well as on test pin were carried out to address the

mechanical aspect of TFLs and corresponding characteristics as presented in following sections.

5.4 Characterization of TFLs by using nanoindentor

Nanoindentation technique has been proven to be useful for the evaluation of mechanical properties and deformation behaviour at nano/micro scale, particularly in thin films. Polymers tend to show significant creep under indentation load. Since indentation creep rate decreases with holding time under maximum load, effect of indentation can be minimized by adding nano-particles or by providing long enough holding time [131]. In the present work, characteristic of TFLs across the wear tracks were investigation with the help of nanoindentation as shown in (chapter 3) Fig. 3.3 with 10 µm interval.

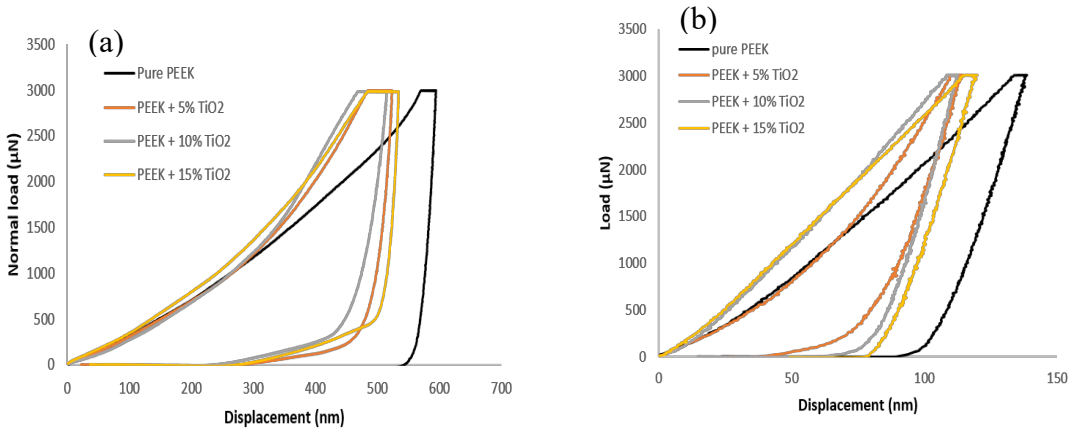

Fig. 5. 10. Representative load-displacement curves in the wear-track on steel disk after pin-on-disk test in dry (a) and water lubricated (b) condition.

Representative load-displacement curves in the wear tracks on steel disk under different test conditions are shown in Fig. 5.10. The presence of nano-particles in TFLs

is evident from the evolution of these load-displacement curves and for a given normal load, TFLs on PEEK deform more compared to TFLs on PEEK composites.

Table 5. 2 Comparison of tribological response of PEEK/ PEEK-TiO_2 nano-composite at different lubrication system.

Specimens	Type of lubricant	Characteristics of TFLs on steel disk			Tribological properties	
		Average hardness (GPa)	Average Thickness h_f (nm)	TFL efficiency (λ)	Specific wear rate ($\times 10^{-6}$ mm^3/Nm)	Friction Coefficient (μ)
PEEK	Dry	3.46	255.0	1.16	6.74	0.62
PEEK+5%TiO_2		1.37	486.4	2.21	1.86	0.90
PEEK+10%TiO_2		1.48	468.0	2.13	5.90	0.81
PEEK+15%TiO_2		1.63	423.9	1.93	7.61	0.75
PEEK	Water	10.54	36.5	0.17	77.9	0.33
PEEK+5%TiO_2		8.86	46.3	0.21	8.06	0.14
PEEK+10%TiO_2		12.03	8.7	0.04	11.14	0.17
PEEK+15%TiO_2		1.44	2.2	0.01	14.35	0.18

The hardness of TFLs on steel disks should be between the hardness levels of steel and polymer; however, hardness depends on the thickness of TFLs. During this nanoindention tests, stiffness of TFL, h_f (in equation 2.2) was assumed to be close to pure PEEK. In addition, dissimilarity of hardness of steel and pure PEEK is so large that small deviations can be ignored. Values of calculated hardness as well as transfer film characteristics and other tribological properties are summarized in Table 5.2. Apparently, hardness values confirm (in addition to SEM evidence) the presence of a polymeric TFLs on steel disk and momentous variations of hardness suggest that, the allocation of TFLs is not uniform to cover the whole wear-track. For illustration, hardness of composite H_c was almost as close as that of the steel, conversely, a thicker

TFLs correspond to lower values of H_c. It was noticed that, soft TFLs was pressed out, forming a 'pile-up' of material as plastic flow of polymeric TFLs was restrained by hard steel disk (Figures 5.3 and 5.6). Thus, wear process of polymer composite is undoubtedly reliant on the development of TFLs. PEEK contented with different amount of nano-particles are most effective to develop TFLs on steel disk, associated with lower wear-rate and a lower friction coefficient. To address the non-uniform distribution of TFLs, 40 individual straight point measurements were taken along wear- track as stated in experimental section as mentioned in Chapter 3.

As TFLs rigidity could significantly alter along wear-track due to non-uniformity, thickness of localized TFLs can be calculated from indentation test and then 'average thicknesses' could be utilized to measure wear properties but should not be considered as an overall property of equivalent TFLs. The use of average calculated thickness is one of the limitations of such technique in addition to indenter tip bluntness, pile-up and roughness of samples' surface. However, by considering the limitations of other techniques like surface profilometry and white light interferometry [4], this technique provides a practical quantitative way to explain the role of TFLs formed under different sliding conditions as explained by Chang *et. al.* [44]. Though, TFLs allocation was nonuniform and exaggerated by sliding conditions, the common trend is that, composites filled with nano-particles left thicker TFLs than the one without any reinforced particles. According to Tables 5.2, PEEK with 5% TiO_2 nano-particles has thickest TFLs, a best efficiency and lower hardness compared with other samples in both dry and water lubrication conditions. Pure PEEK, under water lubrication condition, was better than PEEK with 10% and 15% TiO_2 nano-particles in mechanical aspects; however, were worse in term of tribological properties. The formation of

thicker and thinner TFLs and their consecutive hardness value are also much more dependent on test environment (Table 5.2). Thickness of TFLs during dry lubrication is much higher than that of under water-lubrication. It is well known that, friction assisted heat soften the tip of pin in contact with counterbody (steel disk), therefore it will have more adhering film on steel counterbody and area of contact will increase to some extent. However, in case of water lubricated condition, friction heat dissipate, and retardation of softening will greatly reduce the formation of thicker TFLs and thus the hardness of TFLs will be higher and eventually represent polymer-polymer contact instead of steel-polymer/composite contact. This drastic change in friction mode facilitates abrasion type wear mechanism [37, 71] rather stick-slip mechanism [55].

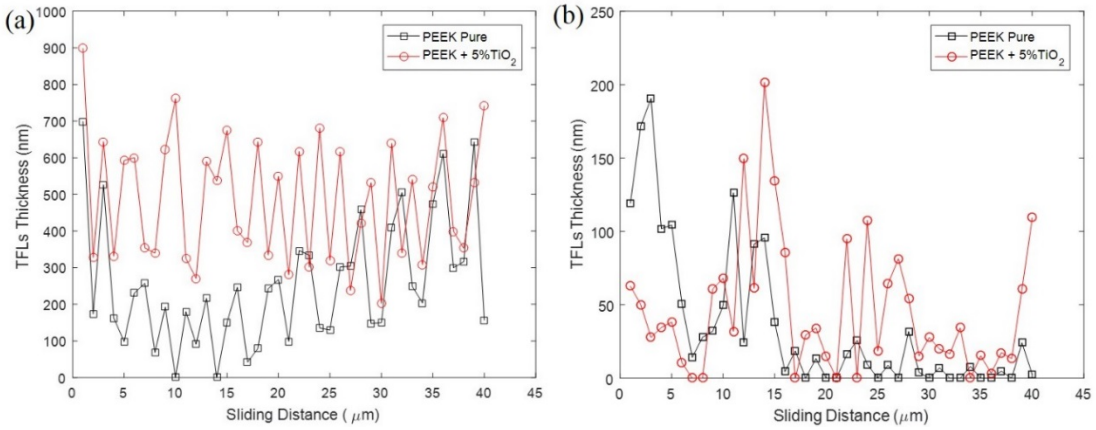

Fig. 5. 11. TFLs thickness distribution on wear-tracks in steel disk under (a) dry condition and (b) water lubrication condition.

Wear behaviour of modified polymers (PEEK incorporated with TiO_2 nano-particles) were mostly determined by the confiscation process of reinforcement [44]. During wear process, nano-particles not only resist the polymer chain movement [78] but sticks out from polymeric matrix and bear most of the load. Whilst steel disk is covered

with non-uniform TFLs, wear performance will be a combination of hard-on-hard contact, hard-on-soft contact and soft-on-soft contact. Consequently, these mechanisms will define the amount and uniformity of TFLs in real contact area. The graphs presented in Fig. 5.11 provided a comparison of TFL thickness along sliding distance between pure PEEK and PEEK with 5% TiO_2 nano-particles in it.

An irregular variation in resistance against indentation indicates that the indenter might have encountered nano-particles through the thickness while probing at various contact depths. In the case of uniform dispersion of nano-particles, theoretical hardness value will increase along with the absence of significant pile-ups, as macromolecular movement is restricted by nano-particles. The scattered data in present case illustrates confined relations of nanoindentation tip with nano-particles and surrounding polymer matrix, which might have been modified by the presence of nano-particles. A transfer film efficiency factor (λ) > 1, indicates that TFLs can efficiently cover the asperities of steel counterbody and thus, sliding occurred between TFL/polymer and is subjugated by adhesive/transfer wear mechanism. Above all, wear wreckage could be trapped and transferred back on damaged surface and lower wear-rate. Additionally, coefficient of friction will be relatively high, as strong adhesive force acts between TFLs and steel disk [37]. Fluctuation of friction coefficient is not surprising due to generation and regeneration of TFLs. In addition to that, characteristic of the hardness of worn PEEK surfaces (test coupons) was also carried out. Representative hardness evolution as a function of indentation load on those worn surfaces is shown in Fig. 5.12 as well as hardness of original PEEK surface (before any test) for comparison reason.

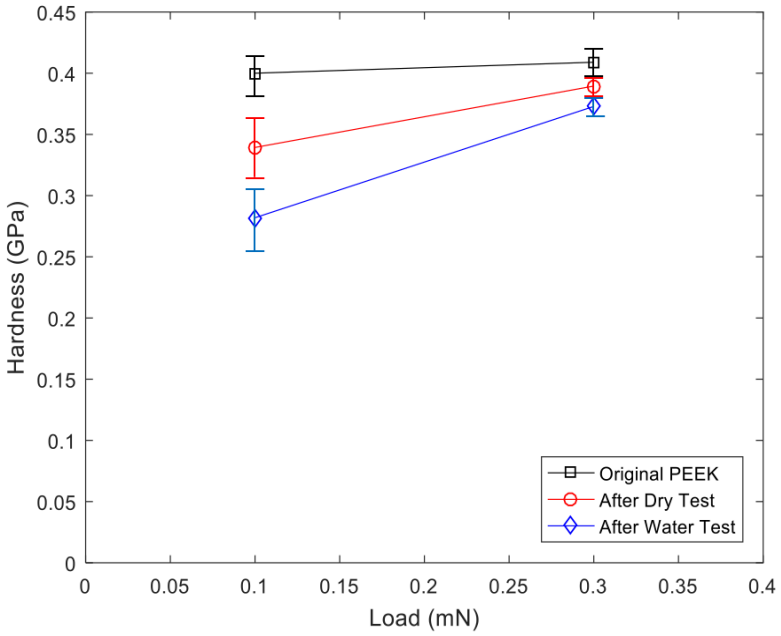

Fig. 5. 12. Hardness as a function of indentation load on worn PEEK wear-tracks after dry and wet test as well as original PEEK surface before any test.

As shown in Fig. 5.12, there is a decrease in hardness on worn wear-tracks of PEEK after pin-on-disk test in both dry and wet conditions, compared to original PEEK surfaces before any wear tests. By considering the original PEEK surface (before wear test), the worn surface become softer as a result of material degradation due to heat generation in dry condition and results in plasticize surfaces as mentioned in section 5.3.1. In the case of water lubricated conditions the result is worst. In addition to the lack of TFLs formation, swelling of polymers takes place due to water absorption and soften the surfaces.

To get the insight regarding structural changes on PEEK subjected to pin-on-disk sliding test, FTIR was carried out on PEEK samples. As shown in Fig. 5.13, the

spectrum of PEEK specimen at the initial state shows principal absorption peaks at 1648 cm^{-1} as well as 1590 cm^{-1} and 1486 cm^{-1}.

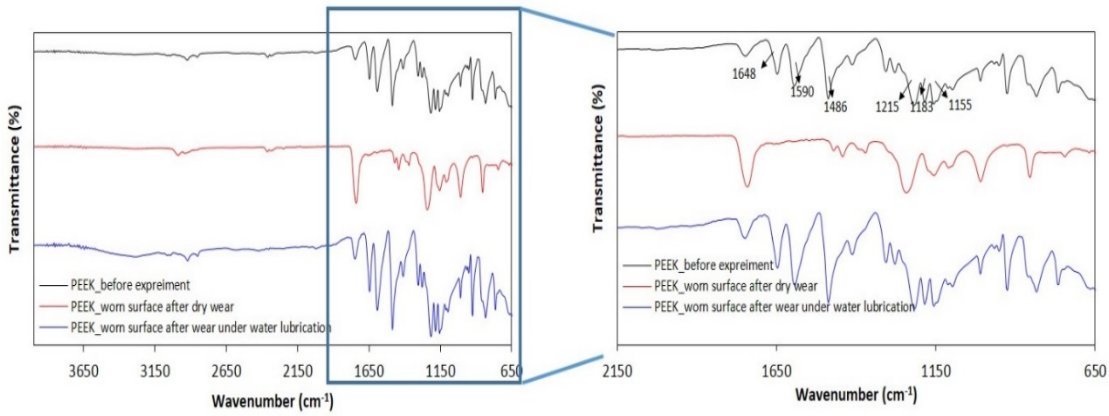

Fig. 5. 13. FTIR spectra of PEEK as its initial state as well as pin-on-disk sliding at dry and wet condirion.

These correspond to carbonyl stretch of the benzophenone segment and asymmetric stretch of diphenyl ether groups, respectively. In addition, the absorption bands at 1215 cm^{-1} and 1183 cm^{-1} as well as 1155 cm^{-1} are attributed to skeletal in-phase phenyl ring vibration and in-place vibration of aromatic hydrogens [132]. Above mentioned peaks disappear in the spectrum of PEEK worn surface after pin-on-disk sliding at dry condition, indicating that tribo-physical/chemical reactions occurred during the process as well molecular chain movement in the structure. It is proposed that when sliding takes place in the dry condition, the carbonyl carbon - phenyl molecule chain can be broken as a result of mechanical loading. Therefore, the carbonyl stretching, and asymmetric stretch of diphenyl ether are weakened. After pin-on-disk sliding test at wet condition, PEEK exhibit a peak broadening and increase in intensity as well as

a slight shift to lower frequencies which is attributed to the formation of hydrogen bonds between the carbonyl group of PEEK and the hydroxyl groups of water. In addition, the presence of water effectively alleviated the mechanical stress between the PEEK specimen and steel counterpart.

5.5. The role of nanoparticles on wear behaviour of PEEK composites

In general, rigid TiO_2 nanoparticle loaded PEEK will be stronger compared to neat PEEK. However, their deformation mechanism will be different under pin-on-disk sliding tests. With the increase content of nanoparticle loading, hardness and young's modulus will increase, however, due to formation of wear debris during pin-on-disk process material deformation scenarios will be more complicated as brittle fracture will play a vital role towards that. For PEEK + 5% TiO_2 composite, the wear debris is more likely generated by micro-ploughing or scratching due to plastic deformation and form continuous type wear debris. In general, increased volume content of nano-particles in composite increase the hardness which in turn reduces wear. However, higher amount of nanoparticle loaded consequent become more rigid and loses its toughness and prone to brittle fracture. This brittle fracture results in relatively larger chip type wear debris as well as accompanied surface crack followed by further pull-out of reinforcement particles from the matrix, resulting in the increased wear rate.

Based on aforementioned discussion, wear mechanism could be explained in view of PEEK and TiO_2 nano-particles interaction. Semicrystalline PEEK polymer forms crystallite structure and amorphous structure during its consolidation process.

However, during the formation of these crystallite structures, larger polymer chain packs themselves in ordered manner. Additionally, due to polymer chain entanglement, sometimes ordered packing of forming crystalline zone is retarded [19]. The formation details of this crystallite and amorphous region falls within thermodynamics of polymers and is beyond the scope of this paper. However, classically it is understandable that during the formation of ordered polymer structure in the presence of foreign particles in it involved space occupied by that particle within micro molecular crystallite region, distorts proper order and hence deformed zone is formed. This deformed zone insists additional chains to undergo amorphous phase transformation [19]. Therefore, an increase volume fraction of nano-particles cause increased possibility of amorphous zone formation. This explains the outcome from dry condition pin-on-disk tests with 10% and 15% TiO_2 containing PEEK exhibits lesser friction coefficient compared to the one with 5% TiO_2. On contrary, incorporation of nano-particles increase the hardness of TFLs in static test condition, that is during nano indentation, where nano-particles acted as chain movement retarder [78] and facilitate higher hardness value of TFLs. The whole process is shown schematically in Fig. 5.14.

During water lubrication, lower hardness of TFLs in the case of PEEK containing 5% nano-particles is attributed to the interference of nanoparticles within crystallite structure of PEEK. Additionally, TFLs thickness of 5% was higher compared to 10% and 15% nanoparticles contended PEEKs. Higher hardness and lower thickness of TFLs of 10% and 15% nanoparticles contended PEEK are subject to two factors: notably higher temperature dissipation in water and hydrophilic nature of TiO_2 nano-

particles and associated physico-chemical interaction with PEEK as shown schematically in Fig. 5.15.

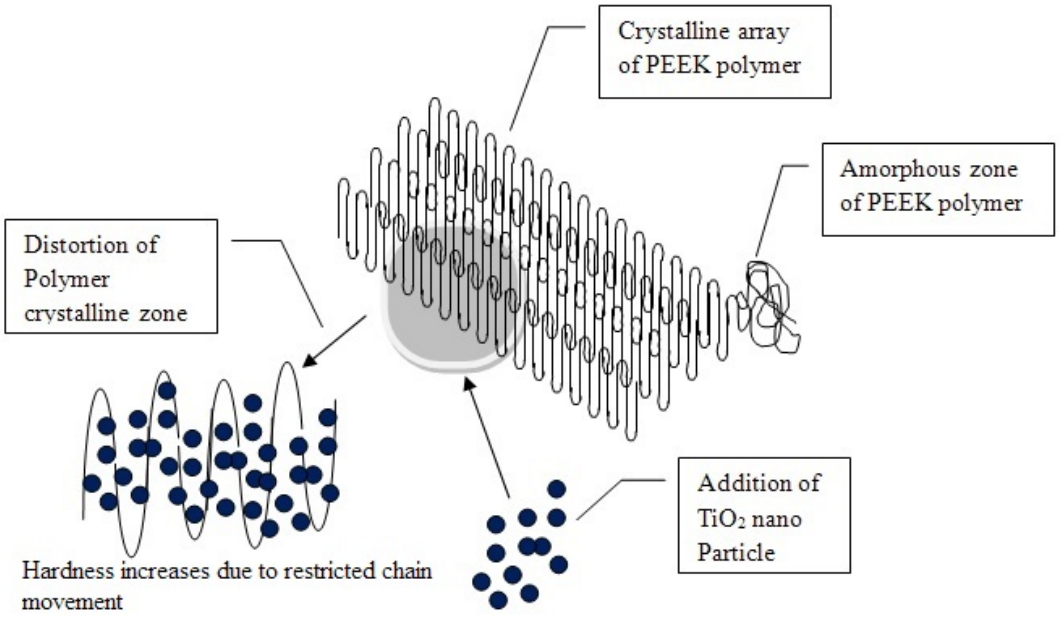

Fig. 5. 14. Schematic representation of nano-particles/PEEK interaction under normal load conditions.

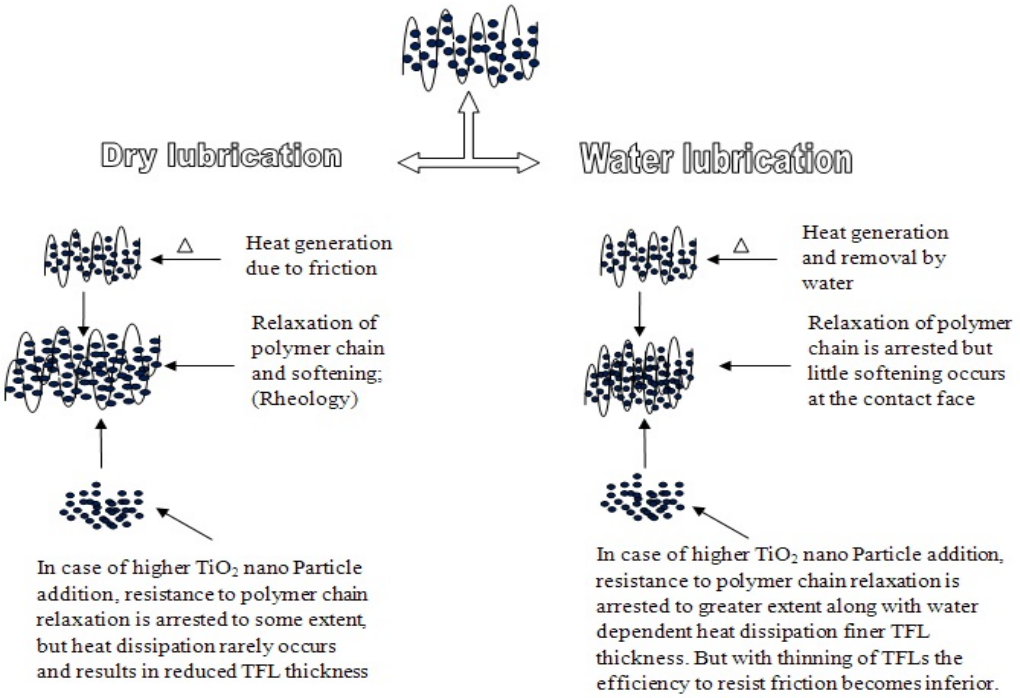

Fig. 5. 15. Interaction of nano-particles with PEEK during pin-on-disk test in dry and water lubrication condition.

This overall process, as described above, is the main reason behind inferior wear rate of PEEK and PEEK based composites in water lubricated condition, compared to dry conditions. As the rigidity of PEEK decreases when it is placed in water, it can't withstand the load in course of pin-on-disk test. On the top of that, nanoparticles in it also lose load-bearing capacity due the matrix relaxation which clearly explains the ineffectiveness of increased nanoparticles content in PEEK in water lubricated conditions. Moreover, formation of TFLs in aqueous conditions is more difficult as lubrication effect of water makes it more difficult for TFLs to attach on the surface [19]. The general agreement is that presence of water offer lubricating effect which reduces coefficient of friction and hinder stable TFLs formation which results higher wear rate compared to dry conditions test under identical test parameters. The prevailing wear mechanisms in such cases are mechanical micro-ploughing and abrasion.

5.6. Summary

Tribological characteristic of PEEK loaded with different amount of TiO_2 nano-particles has been investigated by pin-on-disk test. In addition, the characteristics of TFLs and related mechanical properties were investigated using nanoindentation. Both PEEK and PEEK-based composites improved wear resistance in dry condition compared to the water-lubricated condition, according to recent investigations and the analysis of results. Up to 5 wt. % nanoparticles content in PEEK yields best tribological property which is attributed to TFLs characteristics. Overall wear mechanisms are a mixture of abrasive and adhesive wear; and mixed lubrication (solid/solid and solid/water contact) prevails in aqueous media. Higher transfer layer

efficiency accounted for superior wear resistance at dry test conditions due to the results of brittle-ductile transition, which is absence in aqueous medium test as heat dissipated in water and resists such brittle-ductile transition.

Wear behaviour of PEEK and PEEK composite has been discussed in this chapter under dry and water lubricated conditions. The next chapter will focus on further investigation on these materials subjected to extreme temperature exposure during sliding wear.

Chapter 6. Tribological behaviour of HPPs and polymer composites at elevated temperature

One of the main focuses of the current work is to understand the tribological properties of three different high-performance polymers, namely polyparaphenylene (PPP), polybenzimidazole (PBI), polyetheretherketone (PEEK) and PEEK composites subjected to tribo-contacts at different temperature regimes. Towards that, an investigative approach of sliding wear behaviour was explored under a pin-on-disk experimental setup followed by a variety of materials characterization techniques to establish a relationship between the mechanical properties of these HPPs and their respective tribological performance.

6.1 Characteristics of HPPs

High-performance polymers (HPPs) are important engineering materials and have been continuously developed for different industrial applications due to their great strength concerning density and comprehensive integrity of their structures. HPPs and their composites are effectively applied in various areas such as bearings and seals, whereby they have demonstrated excellent tribological properties and during intensified applications under non-lubricated conditions [1, 2]. HPPs also hold potential for tribological applications at elevated temperatures. In practice, most polymers can't be used when service temperature approaches 120 °C, a situation that is encountered in many industrial applications. For example, water steam

environments and some combustion environments typically have operating temperatures that exceed 120 °C or even 150 °C. HPPs with high thermo-mechanical properties become the ideal candidates for such applications. For example, polyetheretherketone (PEEK) has a glass transition temperature of about 140 °C and a melting point of 343 °C [3,52]. Polyparaphenylene (PPP), with glass transition temperature at around 150 °C, is one of the stiffest and strongest unreinforced polymers at room temperature and is capable of matching the mechanical properties of many reinforced polymers [3, 37]. Along with its high strength, PPP is an admirable contender for weight-sensitive applications that require superior mechanical performance [52]. Polybenzimidazole (PBI) is thermoplastic in nature and shows high heat deflection up to 427 °C and retains its mechanical properties at temperatures above 205 °C, making it superior to any other unreinforced polymers [54]. Due to such exceptional mechanical and thermal properties, PPP and PBI can be used in many tribological applications as virgin materials, unlike PEEK, which often has to be used as a composite by incorporating several reinforcing particles such as TiO_2 [37]. Enhanced physical and mechanical properties of HPPs lead to the anticipation of decent tribological performance of HPPs over a broad range of temperatures. However, in reality, a direct positive correlation between the mechanical properties of such polymers (in general) and their respective tribological properties has yet to be achieved. The tribo-responses of HPPs subjected to elevated temperatures, as well as the associated wear mechanisms are not clear. During the wear process, mating materials get deformed and eventually, the physical removal of material will take place. The mechanisms of such physical material removal constitute a very complex thermo-mechanical process which is a function of number of parameters such as

interfacial physical/chemical reactions, the structure of the contended polymeric chains, the nature of the polymer (thermoplastic/thermoset), the functional group of the polymeric chain, tactility, the number of molecules and their corresponding weights, and the curing/setting behaviour [3, 4]. In particular, tribo-contact may result in the formation of transfer film layers (TFLs) on the counter face which eventually plays a key role in determining the overall tribological behaviour of both mating materials (as mentioned in chapter 2). Therefore, the characteristics of TFLs have been considered as a signature distinctiveness for particular polymers/fillers. To give it some semi-quantitative aspects, the TFL efficiency factor has been introduced, which takes into consideration the distribution of the TFL along a given wear track. This aspect of TFLs provides new insight regarding the deformation of materials in tribo-contacts [39-40, 90-91]. In view of that, it is important to have a clear idea regarding the intrinsic properties of HPPs for high temperature tribo-applications together with their tribological aspects.

6.2. Experimental results

6.2.1 Materials properties of HPPs

Commercially available HPPs, PEEK (Victrex, UK), PPP (Solvey Adv.) and PBI (Performance Prod., Celazole U60SD) were used in the present research. For comparison, PEEK composites reinforced with titanium dioxide (TiO_2) particles with diameters of approximately 300 nm were also prepared as stated in chapter 3. The TiO_2 particles were in the rutile phase, which is the most stable one among different variants [37]. Fig. 6.1 shows the representative scanning electron microscopy (SEM) images

of a polished PEEK composite (PEEK + 10 wt. % TiO_2) together with elemental mapping. As evident from Fig. 6.1, TiO_2 particles are well dispersed throughout the matrix. Three types of polymer composites were made: (i) PEEK reinforced with 5 wt. % TiO_2, (ii) PEEK reinforced with 10 wt. % TiO_2 and (iii) PEEK reinforced with 15 wt. % TiO_2. Some important physical and mechanical properties of the aforementioned materials are summarized in Table 6.1.

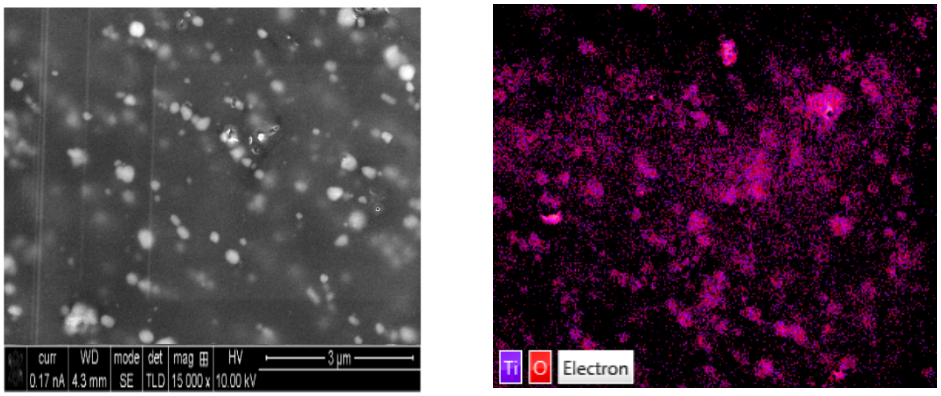

Fig. 6. 1. Representative SEM images of PEEK (PEEK + 10 wt. % TiO_2) composite (a) and corresponding elemental mapping (b).

As can be observed in Table 6.1, PPP has the highest elastic modulus as well as strength. Additionally, the hardness values of the polymers, based on load-displacement curves during nanoindentation as shown in Fig. 6.2, are 420 MPa, 710 MPa and 580 MPa for PEEK, PPP and PBI, respectively. Fig. 6.2 also indicates different elasto-plastic nature of the polymers, i.e., PBI and PEEK are predominately plastic (comparatively higher residual depth, [133]) whereas PPP is more elastic (comparatively lower residual depth).

Table 6. 1. Mechanical properties of HPPs investigated in this study [37,52].

Polymer	Modulus of elastic, E (GPa)		Strength, σ (MPa)		Strain at break, ε_B (%)	Impact energy a_{nI} (J/m)	Density, ρ (g/cm^3)
	Room temperature	170 °C	Room temperature	170 °C			
PEEK	3.55	0.38	100	39.42	34	54	1.3
PBI	5.86	5.4	159	132	3	28	1.3
PPP	8.3	1.88	207	-	5	43	1.2
PEEK+ 5%TiO_2	4.3	0.53	64	29.25	-	1.77	1.4
PEEK+ 10%TiO_2	5.0	0.693	80	32.14	-	2.09	1.6
PEEK+1 5%TiO2	5.2	0.519	92	32.99	-	2.86	1.7

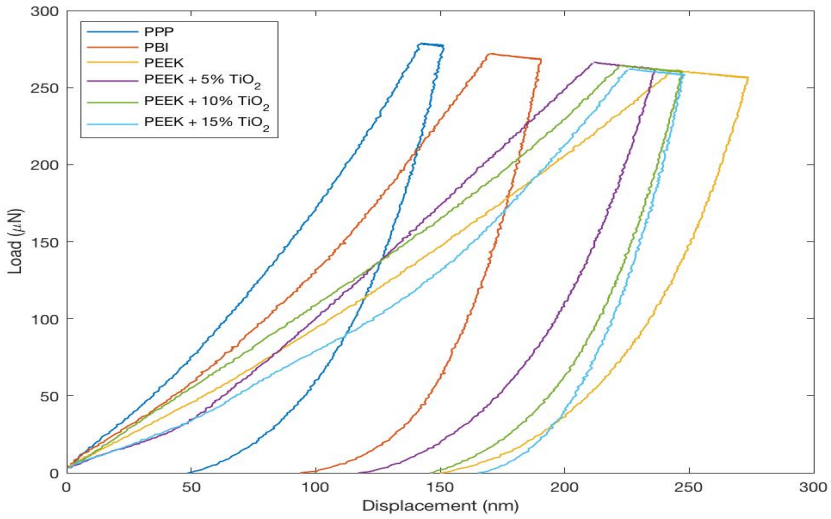

Fig. 6. 2. Load-displacement curves of various polymers during nanoindentation.

6.2.2 Evolution of coefficient of friction

The coefficients of friction of the polymers and polymer composites investigated in this study at different temperature regimes are shown in Fig. 6.3. It is noticed that the coefficients of friction for the PEEK composites, PBI and PPP sliding against the steel disks are reduced with an increase in temperature. However, for pure PEEK, the scenario is opposite, as the friction coefficient increases with test temperature. The friction coefficient depends on a number of factors such as the elastic/plastic nature of the materials involved in tribo-contact, the wear process, the development of TFLs, as well as a dependency on contact temperature [1-3, 37,52]. Nevertheless, in general, as materials' yield strength decrease, shear occurs relatively with ease. This tends to result in a lower tangential force, and thus friction coefficient, during the wear process.

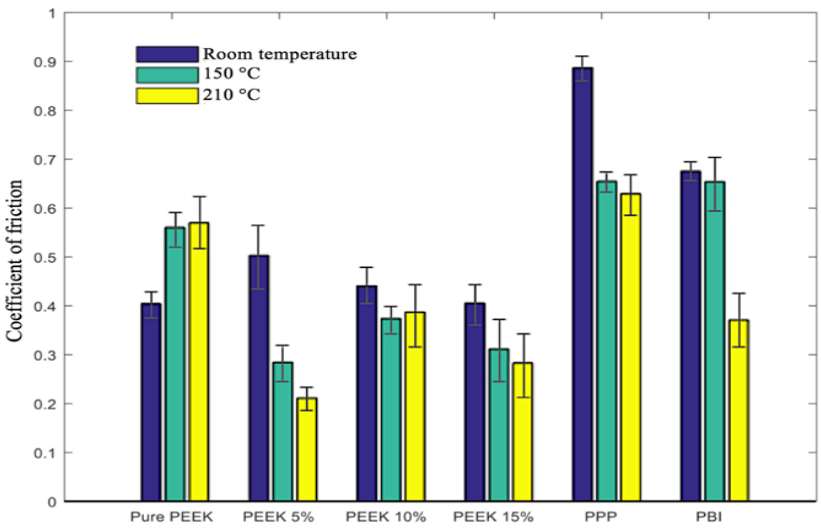

Fig. 6. 3. Coefficients of friction of the investigated HPPS during pin-on-disk tests against steel at different temperature regimes.

The dependence of room temperature friction coefficient in terms of the hardness of the associated materials is shown in Fig. 6.4. Apparently, it shows that the friction

coefficient increases with the hardness/yield strength of the materials. However, this may be indicative only and should be exercised with caution, as coefficient of friction also depends on surface morphology (i.e., roughness) of the mating parts. Thus, for the same material with same hardness, different surface conditions will lead to different friction coefficients. Similarly, the decreased yield strengths at elevated temperatures can explain the reduction of the coefficients of friction for materials such as PPP and PBI, as shown in Fig. 6.3. In the case of pure PEEK, the increase in the coefficient of friction at elevated temperatures could be attributed to the formation of TFLs due to material softening. This material shows more ductile behaviour at higher temperatures and results in more effective TFLs, which would promote adhesion and thus friction by changing from the initial contact of PEEK *vs.* steel to PEEK *vs.* TFL. This supposition will be verified further in detail in succeeding sections by investigating the morphology of worn surfaces after wear tests with the help of an SEM.

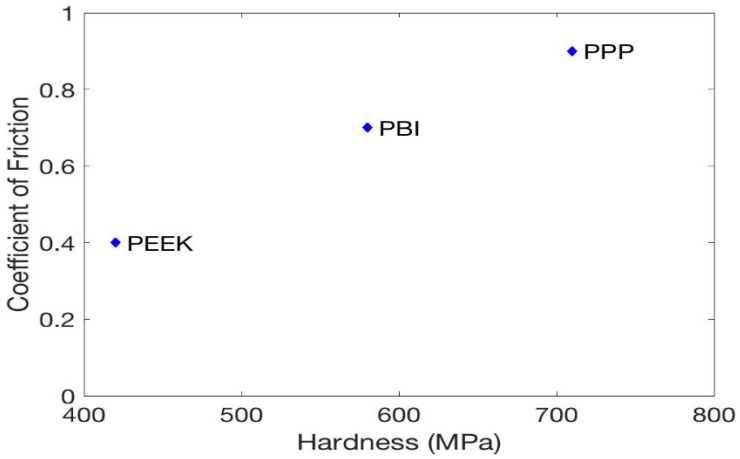

Fig. 6. 4. Dependence of room temperature friction coefficients on the hardness of materials.

6.2.3 Wear behaviour

The specific wear rate of the polymers and polymer composites at different temperature regimes are shown in Fig. 6.5. At first glance, it shows an exponential increase in wear as a function of test temperature for each type of material. PBI exhibits the highest wear resistance followed by pure PEEK and PPP at room temperature, which is consistent with the trend reported in literature [1, 3]. In general, the wear rate increases with temperature and a similar trend was also noticed in the present study. Nevertheless, in the case of PBI, the increase is very sharp whereas for PEEK and PPP, it is rather modest. Compared to pure PEEK, the PEEK composites did not show much advantage at high temperatures. However, this does not necessarily lead to the lower wear rate, due to the abrasive effect induced by the particles when they protrude through the TFLs. At elevated temperatures, the increased wear rate of PBI and PPP were consistent with the outcomes previously reported in literature [37], which could be attributed to the decrease in the materials' rigidity with the increase in temperature.

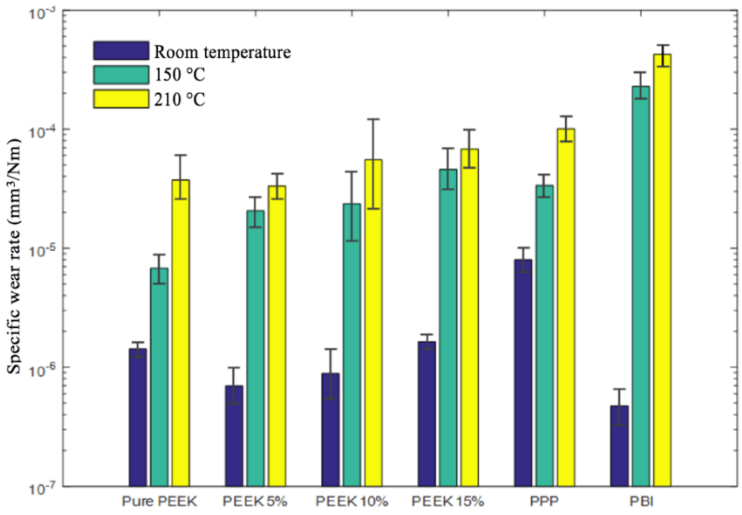

Fig. 6. 5. Specific wear rate of HPPs and their composites at different test temperatures.

Friedrich et al [3] confirmed the amorphous nature of PPP through extensive investigation with the TGA-DSC technique. PPP does not exhibit a sharp melting point but instead, shows swelling over a range of temperatures. This observation also holds true for other thermoplastics [3]. Consequently, under tribo-contact, these materials suffer from temperature assisted softening due to the generation of frictional heat and peel off at relatively ease in layer formation instead of fragmented particles. This results in a relatively higher wear rate. It is interesting to note that, at 150 °C temperature, the wear rate was almost four times higher for PBI compared to PPP. This observation is also true for the results obtained at 210 °C, where the wear rate of PPP was approximately three times lesser than that of PBI.

6.2.4 Structural changes of polymers/polymer composite during wear tests

Fourier transformed infrared (FTIR) investigation of the samples was carried out before and after the pin-on-disk tests to identify possible structural changes of the materials that might take place during the tests. FTIR spectra for pure PEEK and PEEK + 10% TiO_2 are shown in Fig. 6.6. As shown in Fig. 6.6a, the spectrum of PEEK after room temperature tests shows major absorption bands at different wavelengths such as at 1648 cm^{-1}, 1590 cm^{-1} and 1486 cm^{-1}. These specific peaks resemble medium stretching of cyanides and conjugate ketone, stretching of cyclic alkene and asymmetric nitro compounds, respectively. Together, the absorption peaks at 1215 cm^{-1}, 1183 cm^{-1} and 1155 cm^{-1} are similar in all conditions and correspond to characteristic strong in-phase vibration of vinyl ether, ester, and sulfonic hydrates [134-135].

The absorption peak at 1748 cm^{-1} before the wear test indicates a strong bond of carbonyl group of esters, vinyl and phenyl esters compounds in the polymer and

gradually relax with the increase in test temperature due to stretching of molecular chains of carbonyl and vinyl phenylester. In addition to that, there is a slight shift in peak position and increase in peak intensity at the higher wavelength region at elevated temperatures, indicating that structural changes of individual molecular chains were involved in the process of tribo-physical/chemical reaction especially at high temperature as PEEK became relatively more ductile (smeared over the surface). This claim is also supported by the study reported by Chang et al [54] who has investigated the ductility of PEEK at high temperatures by means of tensile fracture tests. Thus, it is expected to form larger size of wear debris as well as better uniformity in TFLs formation as described in section 6.3. In the case of PEEK + 10% TiO_2 (Fig. 6.6b), diminishing absorption peaks of about 1308 cm^{-1}, 1215 cm^{-1} and 1159 cm^{-1} were an indication of the strong presence of C-O which has a lower intensity at elevated temperatures [134]. Long absorption peaks of about 928 cm^{-1}, 834 cm^{-1} and 767 cm^{-1} were observed in all the conditions, which exhibits a strong presence of C-H, C-Cl, and C=C out of plane bending alkenes functional group and halo compounds in the polymer [134]. A higher peak intensity was noticed in the room temperature condition implying that the molecules were more involved in the process.

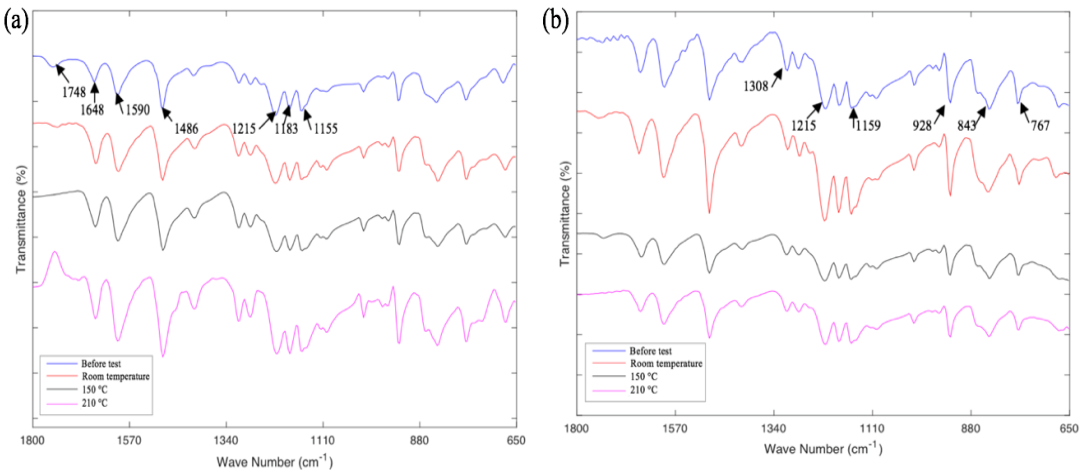

Fig. 6. 6. Comparison of FTIR spectra for (a) PEEK and (b) PEEK + 10% TiO_2 after wear testing at different temperature regimes.

In the case of PPP, there are more features in the FTIR spectra as shown in Fig. 6.7. For example, the absorption peak at 1744 cm^{-1}, which indicates strong stretching carbonyl group of esters, vinyl and phenyl esters, diminish and disappears gradually with the increase of test temperature due to breakage of molecular chains as well as asymmetric stretching of vinyl phenyl ester [135]. A diminishing absorption peak of about 1446 cm^{-1}, 1308 cm^{-1} and 1230 cm^{-1} are an indication of a strong presence of O-H, C-O and C-N groups. The sharp bands at about 1651 cm^{-1} were credited to C=N and C=C stretching vibration of imine/oxime and conjugate alkenes group, respectively. The interruption on the integrity of molecular chains i.e., breakage of the molecular chains, under all wear processes could lead to non-uniform TFLs. This could be further related to the nature of TFLs and wear debris formation, which will be presented in section 6.3.1.

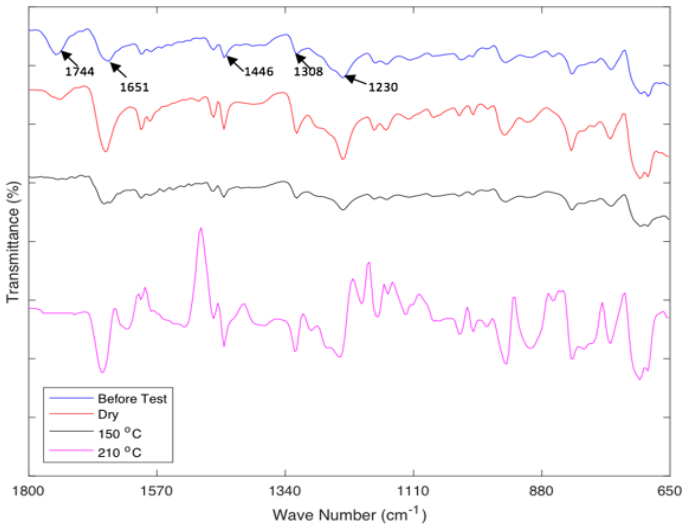

Fig. 6. 7. Comparison of FTIR spectra for PPP after wear tests at different temperature regimes.

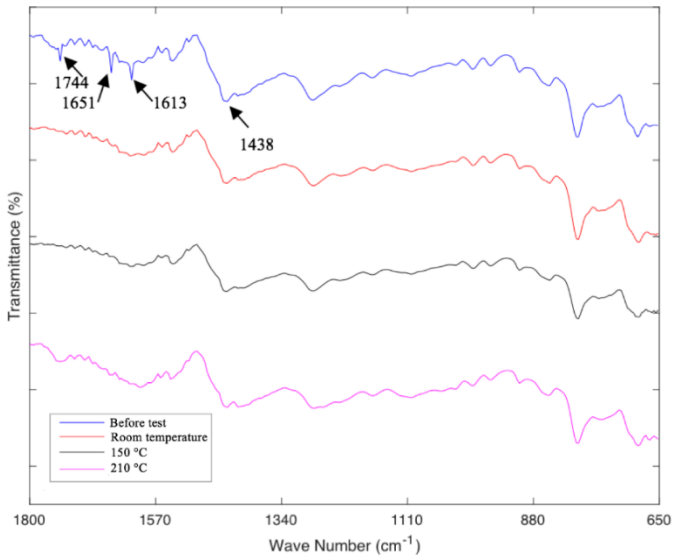

Fig. 6. 8. Comparison of FTIR spectra for PBI after wear tests at different temperature regimes.

Fig. 6.8 shows the FTIR spectra of PBI after pin-on-disk tests at different temperatures. The sharp bands at 1744 cm^{-1}, 1651 cm^{-1} and 1613 cm^{-1} were accredited to C=O and C=C stretching vibration of carbonyl, alkene group and strong stretching vibration of

α, β- unsaturated ketone [134]. These bands disappear/diminish after the wear tests, indicating the occurrence of interfacial tribo- reactions during the wear process in addition to breakage of molecular chains in the polymer structure. Mostly, carbonyl – carbon molecular chains broke down due to the mechanical loading and the subsequent sliding that took place during the process [135]. A major band, at about 1438 cm^{-1} after the room temperature test, shifted towards a lower wavelength after high temperature tests, which indicates breakage of O-H bonds of carboxylic and alcoholic groups.

Thus, the above FTIR investigation confirms that, in general, the structural alternation of polymer/polymer composites took place as a result of stretching or breakage of molecular chains of the structures. These structural changes also affect the formation of TFLs, which will be presented in the subsequent section (section 6.3). The stretching of molecular chains is more probable in the case of relatively ductile materials, like neat PEEK which facilitates towards smeared TFLs over the wear tracks. On the hand, the diminishing peaks more resemble breakage of molecular chains due to the brittleness of polymers like PPP and PBI at high temperatures and consequently, form particulate type wear debris with discontinuous TFLs.

6.3 Role of transfer film layers (TFLs) on friction and wear

6.3.1 SEM analysis

The importance of TFLs in tribo-contacts is well-documented in literatures [38, 63, 85,91]. In the present work, cross-sectional SEM analysis of the wear tracks on the steel counterpart was carried out to confirm and study the formation of the TFLs at different temperatures, as shown in Figure 6.9. It is clear that the TFL consists of the

wear debris from the polymeric specimen and may significantly changes the surface properties of the metal counterpart. For PEEK materials, the TFL formed at room temperature was not uniform, which filled the valleys of counterface with the thickness varied up to several hundreds of nanometers (Fig 6.9a). At the higher temperature, a rather continuous, uniform film could be formed by PEEK with 5 wt% TiO_2. (Fig 6.9b). In both cases, nanoparticles were noticed, though there was also a considerably higher amount of embedded TiO_2 particles at 210 ^oC. Therefore, with the increase of temperature, the polymeric wear debris in the contact region showed more viscos behaviour and could be smeared to form a continuous film. In this case, the rigid inorganic nanoparticles were more likely embedded into the softened TFLs, which in turn, reinforced the TFL and contribute to a thicker film due to the "spacer" effect [36]. On the other hand, the protruded TiO_2 particles may also reduce the adhesion between polymeric specimen and TFLs but tend to increase the wear rate by acting as the third-body abrasive mediums. The observation is consistent with the previously proposed suppositions in Sections 6.2.2 and 6.2.3. Although the high-resolution cross-sectional SEM images could provide detailed information for the localized TFLs, it is not adequate to describe the overall properties of TFLs which are normally discontinuous and non-uniform. Hence, the distribution of TFLs were further examined from SEM observations and nanoindentation tests across different length scales.

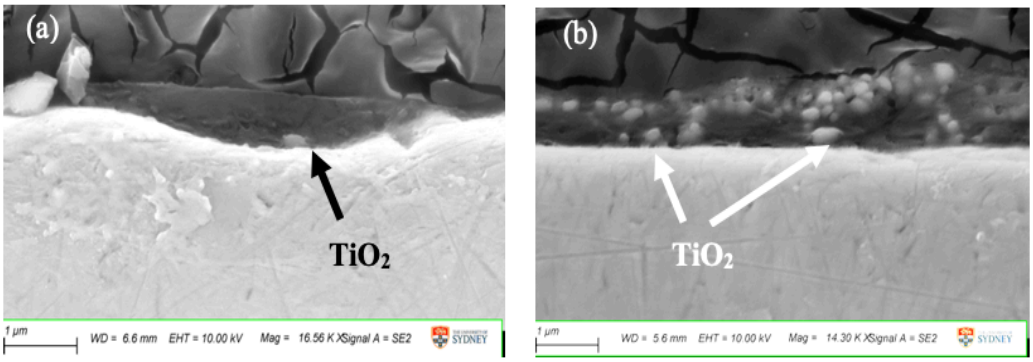

Fig. 6. 9. SEM Cross-sectional analysis of the TFLs formed by PEEK with 5 wt. % TiO_2 (a) at room temperature and (b) at 210 °C.

Figs. 6.10-6.15 systematically compare the TFLs on wear tracks and the corresponding worn surfaces of polymeric specimens. As shown in Figs. (6.9a-6.14a), the worn surfaces of pure PEEK are relatively smooth compared to the PEEK composites and other HPPs. It was also noticeable that the gradual increase in the test temperature, as well as localised temperature rises due to frictional heat, cumulatively thinned the TFLs for pure PEEK. The increase in wear rate with test temperature is mainly due to a loss of mechanical properties because of temperature-assisted softening. However, in the case of the PEEK composites, TFLs show less uniformity in appearance and the worn surface retain scratches at the middle of the pins (Fig. 6.10b-6.15b, 6.10c-6.15c and 6.10d-6.15d). There are also visible pit holes (black arrow) and directional scratch marks. This results in new counter-face formation because of abrasive wear at room temperature. Additionally, due to adhesive nature, breakage of the PEEK matrix occurs at the interface. Furthermore, the worn surface clearly shows ((Fig. 6.10b-6.15b, 6.10c-6.15c and 6.10d-6.15d) microgrooves that are parallel to the sliding direction which are probably caused by agglomerated wear debris that facilitates a three-body wear

mechanism. At elevated temperatures, the wear rate of the PEEK composites is clearly higher than at room temperature. Reinforced particle detachment was triggered due to lower resistance of the polymer matrix to hold TiO_2 particles due to temperature-assisted softening and results in smaller debris that was noticed on the worn surface.

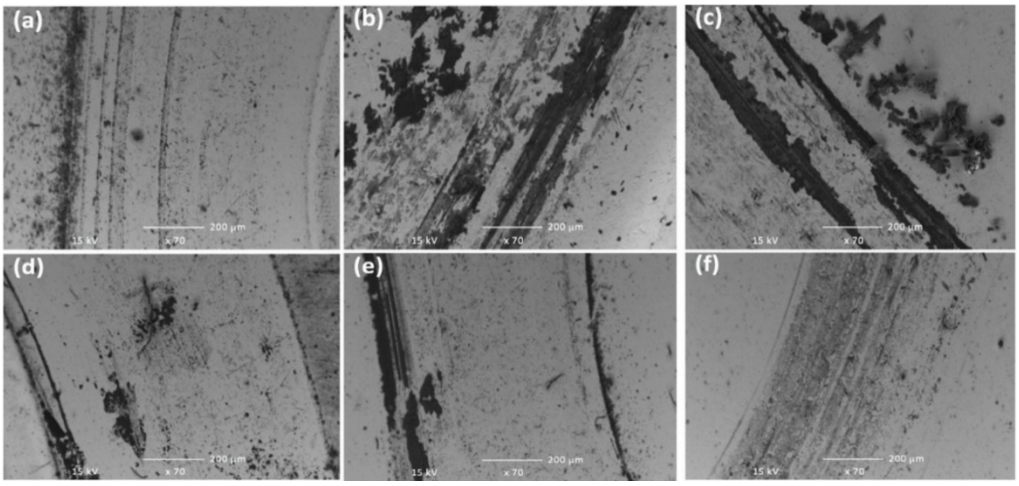

Fig. 6. 10. SEM images of TFLs on steel disk after wear test at room temperature: (a) Pure PEEK, (b) PEEK with 5% TiO_2, (c) PEEK with 10% TiO_2, (d) PEEK with 15% TiO_2, (e) PPP and (f) PBI.

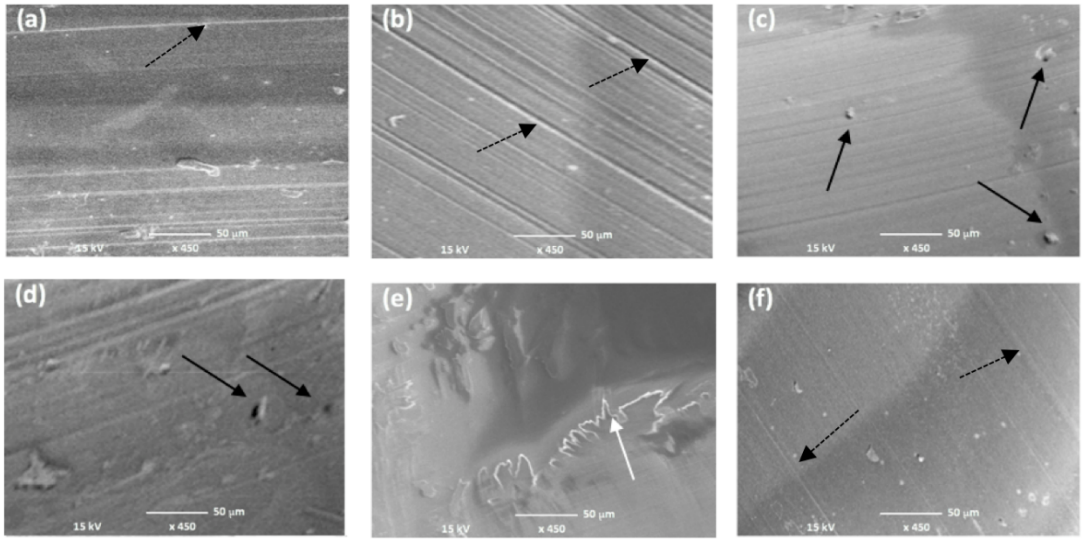

Fig. 6. 11. SEM images of worn polymer and polymer composites surfaces: (a) Pure PEEK, (b) PEEK with 5% TiO_2, (c) PEEK with 10% TiO_2, (d) PEEK with 15% TiO_2, (e) PPP and (f) PBI after wear test at room temperature.

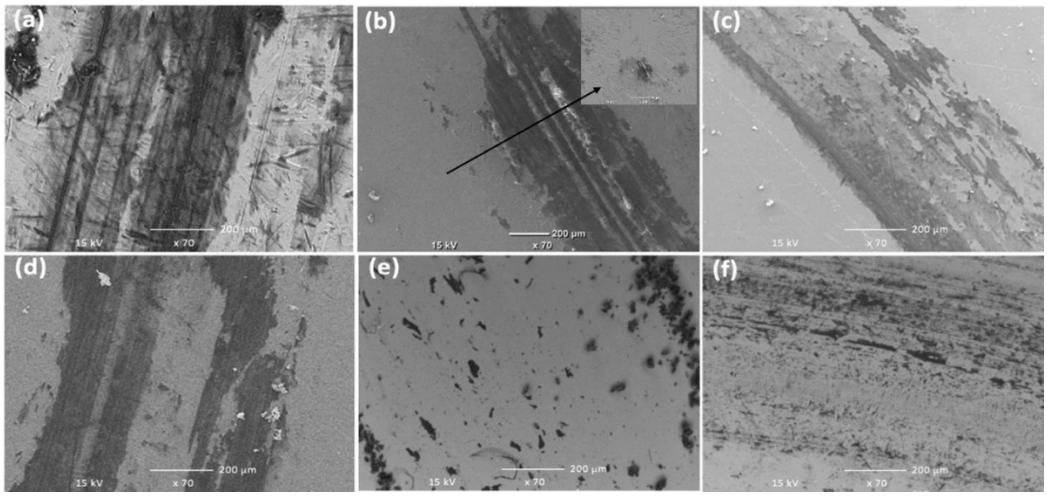

Fig. 6. 12. SEM images of wear-track (TFLs) on steel disk: (a) Pure PEEK, (b) PEEK with 5% TiO_2, (c) PEEK with 10% TiO_2, (d) PEEK with 15% TiO_2, (e) PPP and (f) PBI after wear test at 150 °C.

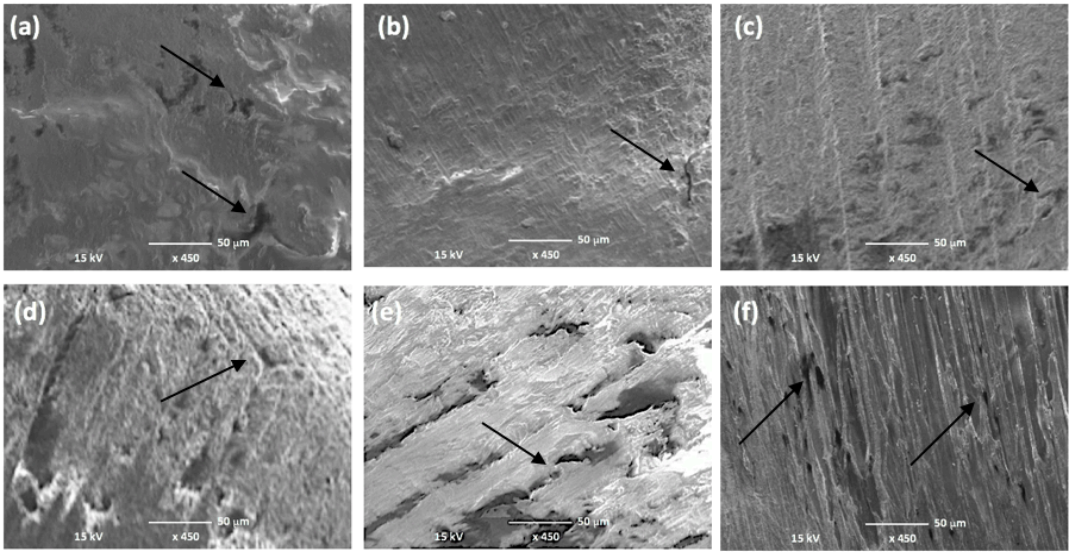

Fig. 6. 13. SEM images of worn polymer and polymer composites surfaces: (a) Pure PEEK, (b) PEEK with 5% TiO_2, (c) PEEK with 10% TiO_2, (d) PEEK with 15% TiO_2, (e) PPP and (f) PBI after wear test at 150 °C.

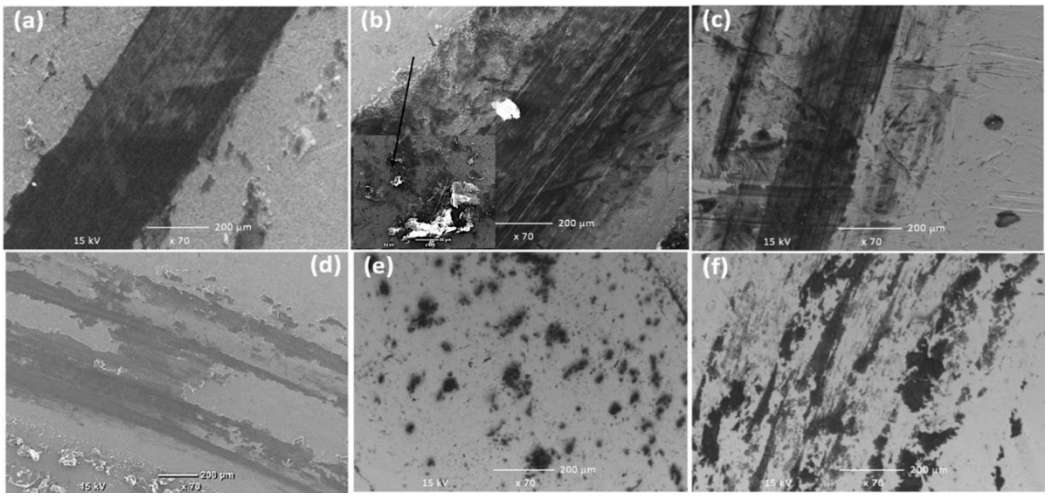

Fig. 6. 14. SEM images of wear-track (TFLs) on steel disk: (a) Pure PEEK, (b) PEEK with 5 % TiO_2, (c) PEEK with 10% TiO_2, (d) PEEK with 15% TiO_2, (e) PPP and (f) PBI after wear test at 210 °C.

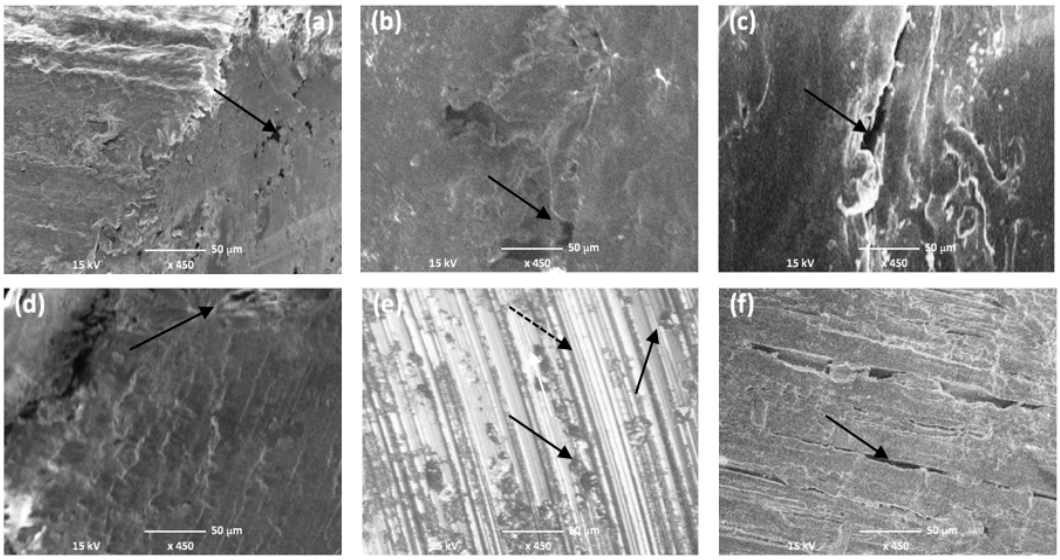

Fig. 6. 15. SEM images of worn polymer and polymer composites surfaces: (a) Pure PEEK, (b) PEEK with 5% TiO_2, (c) PEEK with 10% TiO_2, (d) PEEK with 15% TiO_2, (e) PPP and (f) PBI after wear test at 210 °C.

In the case of PPP (Fig. 6.10e-6.15e), the allocation of TFLs was not uniform and the worn surfaces contain pit holes (black arrow), crazing marks (white arrow) and exfoliated film ends (dashed black arrow). Thinner TFLs with a smoother worn surface can be explained by the room temperature rigidity of PBI.

Worn surface of pure PEEK after pin-on-disk testing at 210 °C temperature shows polymer film exfoliation, but this is absent in the PEEK composites. Rather, the worn surface shows severe material deformation without sharp directional scratch marks. PEEK showed more viscos and ductile, as 'smearing' on the surface is quite visible. After elevated temperature pin-on-disk tests, cracks were noticed on the PBI (Fig. 6.10f-6.15f) and PPP (Fig. 6.10e-6.15e) surfaces, which resemble that of brittle materials and thus, resulted in non-continuous TFLs as compared to PEEK. Nonetheless, TFLs and the worn surfaces of PPP and PBI showed moderate amount of material carryover and directional marks, respectively. Commonly during high temperature tests, a number of cracks appear on the PBI and PPP surfaces as they are very brittle and do not yield continuous TFLs like PEEK.

Fig. 6.16 shows an overview comparison of the wear debris formed on different materials at room temperature and at 210 °C. PPP generates small wear debris in both room and at high temperatures and PBI at high temperatures. Relatively larger (layer-shaped) wear debris may facilitate towards continuous TFLs and thus result in relatively lower wear rates, which particularly occurs for ductile polymers. As polymers get brittle, either due to semi-crystalline/amorphous structure or presence of

reinforcing particles, relatively smaller wear debris is more likely to be generated, resulting in a discontinuous film with higher wear losses which are in line with the findings reported in section 6.2.3 regarding wear behaviours of the investigated materials. The role of TFLs on friction and wear is also very complex. For example, in the case of pure PEEK, PPP and PBI, TFLs are mostly polymeric in nature which may act as a thin lubricating layer (semi-continuous in nature) in tribo-contacts. However, for PEEK composite, the scenario is more complex as the incorporation of nanoparticles may act as third bodies during the tests as these particles tend to detach during the sliding process and may even embed within the formed TFLs (as was discussed prior).

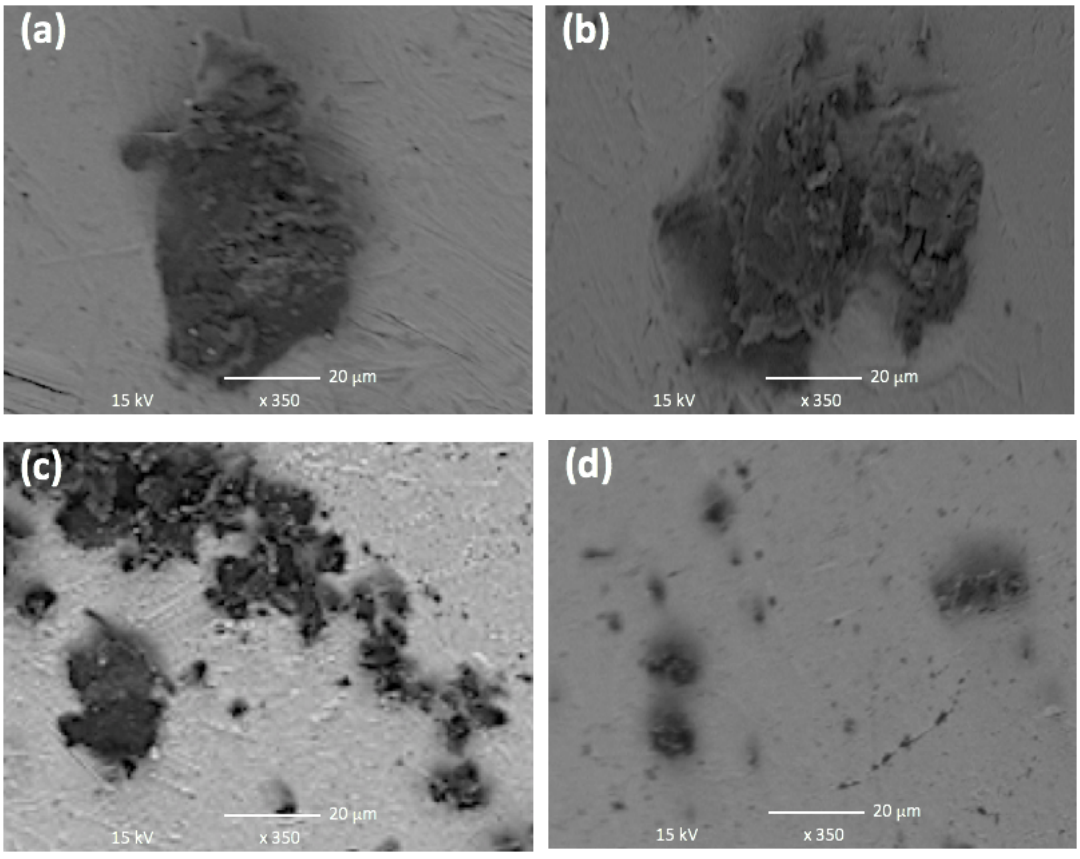

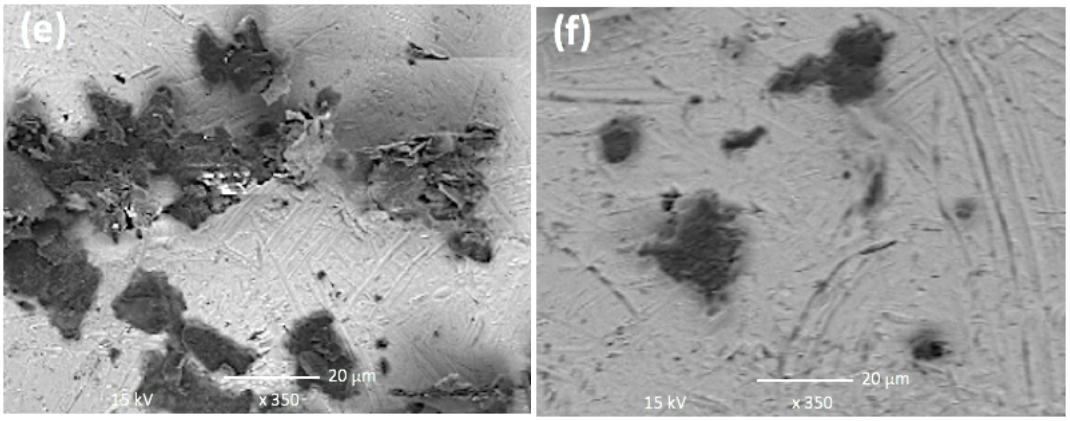

Fig. 6. 16. SEM images of wear-debris generated during wear tests at room temperature on (a) PEEK, (c) PPP and (e) PBI; and at 210 °C on (b) PEEK, (d) PPP and (f) PBI.

6.3.2 Characterization of TFLs by nanoindentations

SEM micrographs as presented above (Fig. 6.10 to Fig. 6.15) are a qualitative representation of the transfer layer that took place during the sliding wear tests. Transfer layer efficiency factor (λ), as described in chapter 2, is a quantitative way to express the role of TFLs on friction and wear, as elaborately reported by Chang et. al. [4]. Fig. 6.17 shows the distribution of TFLs along the wear track with the help of nanoindentation as described in previous communications [37]. As evident, PPP shows thinner and non-uniform TFLs whereas PEEK shows relatively thick and uniform TFLs. Those findings confirm the discussions in section 6.2.4 regarding severe damage of molecular chain at both room and high temperatures in the case of PPP. It is also noticed that the measured film thickness of PEEK composites filled 5% TiO_2 nanoparticles agreed with the SEM cross-sectional observation in Fig. 6.9. As PPP shows relatively less ductile or viscous behaviour, as was determined by nanoindentation (Fig. 6.2) and FTIR measurements (section 6.2.4 and Fig. 6.7), molecular chains are more likely to break rather than scratch in this case. The transfer layer efficiency factors (λ) of presently investigated polymer and polymer composites

were calculated according to ref. [37] and reported in Table 6.2. According to Tables 6.2, PEEK and PEEK composites show an increase in efficiency factor with the increase of test temperature. It is obvious that, friction-assisted heat caused softening of the mating surfaces and as a result, there was an increase in the amount of film that adhered on the counterbody due to, at least to a certain extent, increased material transfer and contact area. Compared to PEEK/PEEK composites, an opposite trend was observed for PPP and PBI (Table 6.2) where transfer layer efficiency factor decreases with the increase in test temperature. This was also reflected in the friction behaviour of PBI and PPP, as the materials exhibit somewhat lower friction coefficients with the increase in test temperature as compared to PEEK and the PEEK composites. As PEEK became relatively more ductile/less viscous, especially at higher temperatures, thicker and more uniform TFLs formed as compared to others (Fig. 6.14). In the case of PEEK composites, with the unique characteristics of nanoparticles as reinforcement, leads to an increase in efficiency and uniformity of TFLs at room temperature [36]. However, agglomeration of nanoparticles took place with increased volume fraction of nanoparticles which overthrow the benefits of nanoparticles as reinforcement in the case of PEEK with 10% TiO_2 and PEEK with 15% TiO_2. The breakages of molecular chain at high temperatures could also increase with increased volume of nanoparticles and make it worse in terms of non-uniformity in TFLs as well as ductility of PEEK.

Table 6. 2. Transfer layer efficiency factor (λ) after pin-on-disk test at different temperature regimes.

Sample	**At 23 °C**	**At 150 °C**	**At 210 °C**
Pure PEEK	0.45	0.97	1.01
PEEK + 5%TiO_2	0.62	0.87	0.91
PEEK + 10%TiO_2	0.59	0.77	0.88
PEEK + 15%TiO_2	0.33	0.49	0.54
PPP	0.41	0.18	0.17
PBI	0.78	0.73	0.72

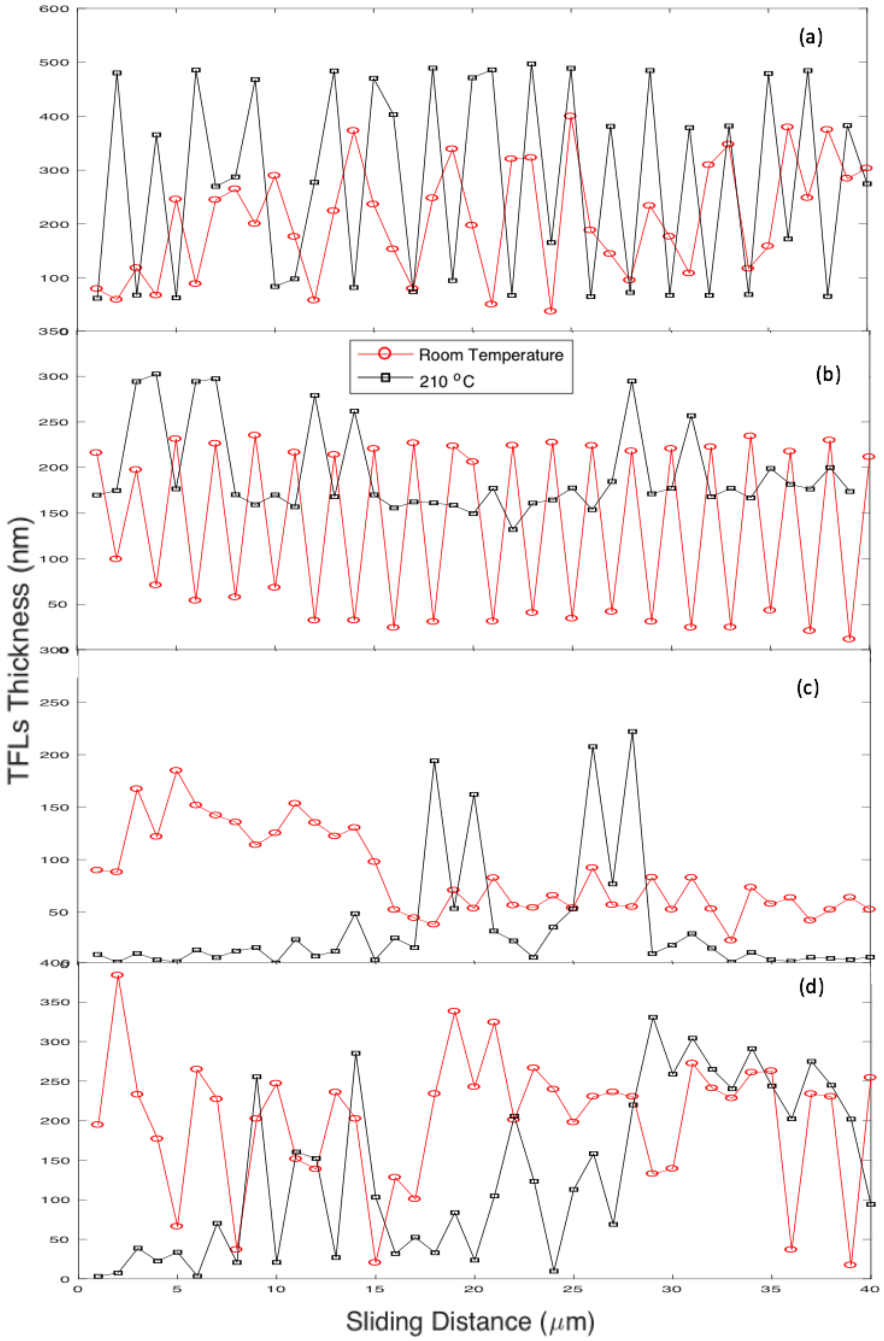

Fig. 6. 17. Distribution of TFLs on wear-tracks in counterbody after wear tests at room temperature and at 210 °C: (a) PEEK, (b) PEEK + 5% TiO_2 and (c) PPP (d) PBI.

6.4 Comparison between mechanical and tribological properties

As evident from the pin-on-disk tests, PBI exhibits the highest wear resistance at room temperature though PPP shows the highest mechanical properties such as highest yielding strength and young's modulus (Table 6.1). From the perspective of organic chemistry, there is little explanation towards the wear behaviour of these polymers unless the physical nature of their chemical structure and their wear response are taken into consideration at the same time. From the present research, it can be concluded that PPP does not show promising wear resistance even though it is mechanically sound compared to other polymers. The reason behind that is most probably it is relatively less viscous/ductile behaviour (Table 6.1 and Fig. 6.2) and the formation of thinner and non-uniform TFLs at room temperature. PBI which retains its rigidity at higher temperature (205 °C) also responded poorly during pin-on-disk test at 150 °C and at 210 °C. The most probable reason for such a behaviour is that PBI remains brittle at high temperatures, as mentioned in section 6.2.4 in light of molecular chain breakage by FTIR investigation. This result was in-line with the findings reported by Chang et al [54] as the authors have confirmed the brittle behaviour of PBI even under 210 °C by means of fracture tests. While PEEK has the relatively low mechanical properties among materials investigated in the present study, it achieved moderate wear resistance due to effective TFL formation. When thermoplastics like PEEK are subjected to elevated temperatures, they exhibit ductile behaviour and thus form durable TFLs, and therefore, resist wearing off. This evidence confirms the claim made in section 6.2.4 related to the stretching of molecular chains at high temperatures and is supported by tensile fracture tests reported in literature [54] as PEEK becomes purely ductile with an increase in temperature. However, in the case of PEEK

composites, the scenario is much more complex. The addition of reinforcing elements (nanoparticles in the present case) may cause breakage of molecular chains and the effect of that becomes more prominent at elevated temperature. Generally speaking, higher strength and modulus of materials are taken as an indication of favourable wear resistance. In particular, hardness is commonly considered for the selection of tribo-materials when the wear process is governed by the abrasive wear mechanism. However, there is no direct connection between mechanical properties of materials like strength and hardness with that of wear rate. Thus, wear is a system property instead of a material property. This remark is also valid in the current case, as the presently investigated PPP, which is the hardest among the materials investigated, had relatively poor wear resistance at high temperatures. At high temperatures, polymers are expected to lose some of their mechanical properties and thus, affect their wear resistance. To verify that, hardness measurements on worn wear tracks of test coupons, subjected to nanoindentation, are shown in Fig. 6.18.

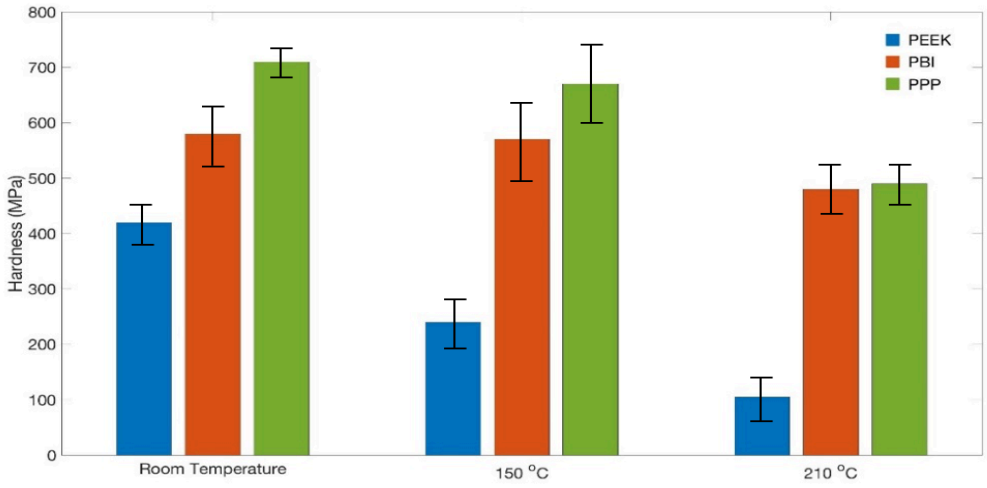

Fig. 6. 18. Hardness of the worn surfaces of the HPP test coupons after wear testing at different temperatures.

Fig. 6.18 clearly indicates that there is a decrease in hardness with an increase in test temperature after the wear test and confirms the aforementioned wear behaviours in these polymers at elevated temperatures. Despite their relative higher hardness, micro-cracks that formed on the PBI and PPP worn surfaces are aligned along the same wear sliding direction at elevated temperatures due to the brittleness of these materials and failed to provide uniform TFL films as compared to PEEK, thus accelerating their degradation. This explains their significantly increased wear rate at high temperatures.

Hence, the wear process under such conditions is governed by formation/re-formation of TFLs at the tribo-contact rather than the properties of the bulk materials. The proper selection of such HPPs will be considered, that is, not only their simple thermo-mechanical properties such as modulus, hardness or the critical temperatures, but also possible wear mechanisms that might overlook material degradation mechanisms involving TFLs. The latter is greatly affected by the brittle-ductile transition behaviour of polymeric materials, which is dependent on temperature.

6.5. Summary

In this chapter, wear and friction behaviours of HPPs and their composites were examined under pin-on-disk contact configuration at different temperature regimes. The formation of TFLs was systematically analysed and linked with overall tribological behaviour of HPPs and their composites. In general, formation and coverage of TFLs on steel counterpart is not uniform and it is temperature dependent. Among the materials investigated in present study, PEEK and PEEK composites

showed more effectiveness to develop resilient TFLs, even at elevated temperatures. Variations in coefficient of friction depend on the nature and form of TFLs, which was further governed by the retention/degradation of mechanical properties of investigated materials with test parameters. PBI shows better wear behaviour at room temperature, thanks to its mechanical properties. However, temperature sensitivity of PBI, particularly above their glass transition temperature, cause degradation of mechanical properties which make them relatively brittle and consequently failed to form effective TFLs. Though, there is no general correlation of mechanical properties of investigated materials with respective wear rate, the trend is that, higher the combination of hardness, rigidity and ductile of materials, better is the wear resistance, at least at room temperature. This observation was further supported by the structural changes of polymers/polymer composite, either due to nanoparticles incorporation or test parameters, which generate different TFLs that ultimately dictate overall wear mechanism of the system. FTIR investigation confirm structural changes of the materials subjected to high temperature tests. This structural change includes relaxation, deformation and breakage of polymeric chains, which gives rise to different TFLs distribution in the wear track.

Chapter 7. A simplified model of wear and friction behaviour of high-performance polymer/ polymer composites

In this Chapter, various wear models, to address the tribological behaviour of high-performance polymer and polymer composites were considered along with experimental validation. A number of factors that contribute in wear process were examined, including both materials' property and experimental variables. In addition to that, underlying wear mechanisms were taken into account towards wear modelling. In particular, the artificial neural network technique was adopted for wear analysis. The main objective of this work is to provide some useful insight in selecting materials for industrial applications. Towards that, the challenging issues involving the complex material removal mechanisms have also discussed in details.

7.1 Brief summary of existing wear models

There are many wear models available in literature that have been developed for qualitative wear analysis or quantitative wear prediction [136-138]. Most of the models aim to establish a relationship between wear and materials' intrinsic properties such as hardness and strength of materials [139]. In wear modelling, persistence material removal mechanism is the key factor that dictate the overall wear rate and should be taken into consideration. In addition, it should also be taken into account that, no single mechanism of material removal can be applied to all the wear situations. Wear rate of materials is not a basic material property and instead it is a response of the given system which material has to function. In practice, empirical equations to determine

the wear rate of materials were common in early days mainly due to its simplicity on nature and ability to construct a model by performing few experiments [140-143]. It is worthwhile indicating that the definition of specific wear rate is based on dimensionless analysis proposed by Rhee et al [144]. In their work, wear volume of a polymer-matrix composite can be presented in terms of applied load (F_N), speed of sliding (V) and also time of sliding (t) as represented in Eq. (7.1):

$$W = kF_N^a V^b t^c \tag{7.1}$$

where W is the loss of weight of the material being investigated; coefficient k, a, b and c are constants that are empirical in nature. These empirical coefficients can be experimentally derived where one of the three parameters (V, F or t) is variables and rest are fixed. The equation implies the constant k is a material property, which is independent of external variables such V, F and t. However, the main shortcoming of this approach is that, it totally ignores the synergy among variables, which is not the case in reality and other variables such as surface roughness, contact geometry etc. To address these, contact-mechanics-based approached introduced in early 1970's. One common example of such approach is the famous Archard's law [145, 146]. According to this law, volume loss of the material (w) in the tribo-contact due to wear is directly proportional to applied load (F_N) and distance travelled (s); however, inversely proportional to the hardness (H) of wearing material. This can be expressed according to Eq. (7.2) [145]:

$$w = k_1 \frac{F_N s}{H} \tag{7.2}$$

In Eq. (7.2), k_1 is proportional constant, which is non-dimensional in nature and commonly terms as 'wear coefficient'. It is important to note that, the surface layers'

hardness in tribo-contact is difficult to determine, as it fluctuate along the depth. Nevertheless, the ratio of K_1/H is often easier to use and termed as 'specific wear rate'. Specific wear rate is defined as volume loss of materials per unit meter (distance travelled) per unit load (applied load) [147]. Some typical values of such specific wear rate, as available in literature [147], is given in Table 7.1.

Table. 7. 1Specific wear rate of some common materials sliding against 'tool steel' under pin-on-disc configuration in the absence of external lubrication [147].

Material	**Wear rate (mm^3/Nm)**
Mild steel (on mild steel)	7×10^3
α/β brass	6×10^4
PTFE	2.5×10^5
Copper–beryllium	3.7×10^5
Hard tool steel	1.3×10^4
Ferritic stainless steel	1.7×10^5
Polythene	1.3×10^7
PMMA	7×10^6

The next generation of models representing the wear behaviour of materials are grounded on different failure mechanisms of materials and came in great numbers over the decades. This is due to the face that, wear resistance of any given material is a function of not only materials' intrinsic properties, rather it's a consequence of material's failure in contact under certain loadings. In this approach, the emphasis has been given to take consideration of values related to flow strength of material [145], fracture toughness (K_c) [14], fracture strain (ϵ_f) [149], fatigue properties [150] and brittle fracture properties [151] etc.

More recently, the advanced computing technology has been adopted in the field for wear modelling. For example, Sebani [152] et al has presented the modelling of wear rate based on Archard, ASTM, and neural network models. They have started with Archard models (Eq7.2) and used height reduction of the pin to calculate the pin wear according to Eq. (7.3) [19, 20]:

$$Pin\ Wear\ = \frac{\pi\, h}{6}\left[\frac{3\, d^2}{4} + \Delta h^2\right] \tag{7.3}$$

Where h is initial pin height, Δh is the height of material removed from the pin and can be found from Eq. (7.4) [128]:

$$\Delta h = \frac{\Delta m}{\rho.3.\pi.\left(\frac{d}{2}\right)^2} \tag{7.4}$$

where d is test coupon's diameter (mm), ρ is test coupon's density and Δm is mass loss of the test coupons during the test.

These above-mentioned methodologies considered empirical/semi-empirical, stress analysis, contact mechanics and computing approaches, respectively, which are still commonly used in the field of tribology. In general, there is no direct connection or simple agreement between the diverse models and equations to be found in the literature. According to Meng et al [143], there is a range of variables and mechanisms in existence that will be seen in different works. For example, Czichos et al [155] related the wear rate with hardness and yield stress of material on the basis of Archard model [145] on polymers in abrasive wear:

$$w = k_1 A_r s \tag{7.5}$$

Where w is wear volume, s is distance travelled during sliding and A_r is real contact area during sliding and taken as inversely proportional to hardness and k_1 is proportional constant. According to Chang et al [54], Eq. (7.5) can be simplified further based of the assumption that interfacial stress is governed by coefficient of friction and hardness is proportionally related to yield stress:

$$W_s \sim \frac{\mu}{\sigma^2} \tag{7.6}$$

Where W_s is specific wear rate, μ is coefficient of friction, and σ represent tensile yield stress. Accordingly, the wear data were analysed as functions of μ/σ^2.

In view of above-mentioned brief literature survey, it can be concluded that numbers of wear models that are available in literature existing in different forms. Many models are actually empirical or semi-empirical, based on wear data of certain polymers. Some of them are quite complex and difficulty to relate with physical phenomenon taking place in wear tracks. Up to now, wear data for representative high performance polymers (HPPs) such PBI and PPP are still scarce. In this respect, the objective of the present study attempts to model the wear behaviour HPPs using different approaches, by taking consideration of materials' properties as well as system properties.

7.2 Wear results for HPPs and their composites

In this chapter, tribological and mechanical properties of some HPPs like PEEK, PPP and PBI at room temperature as well as at 150 °C have been summarized in tabular form (Table 7.2). In addition, results from PEEK composites reinforced with different

percentage of inorganic titanium dioxide (TiO_2) were also presented and compared at different temperatures as stated in chapter 6.

Table. 7. 2. Tribological and mechanical properties of HPPs and their composite evaluated at room and elevated temperatures subjected to following sliding wear test conditions: 1 MPa normal load, 0.1 m/s sliding sped and 2 hours of duration.

Polymer	**E (GPa)**		**σ (MPa)**		**H (MPa)**		**ε (%)**	**K_{IC} (MPa$\sqrt{m}$)**	**W_s**		**μ**	
	RT	**170 (°C)**	**RT**	**170 (°C)**	**RT**	**170 (°C)**			**RT**	**150 (°C)**	**RT**	**150 (°C)**
PEEK	3.55	0.38	100	39.4	420	240	34	6.09	1.4	6.95	0.40	0.55
PEEK+5% TiO_2	4.3	0.53	64	29.3	422	218	1.77	4.96	0.63	21.6	0.50	0.28
PEEK+10 %TiO_2	5.0	0.69	80	32.1	448	225	2.09	4.21	0.89	26	0.43	0.37
PEEK+15 %TiO_2	5.2	0.52	92	33	520	222	2.86	3.83	2.56	45.2	0.40	0.31
PBI	5.86	5.41	159	132	580	656	3	3.85	0.53	164	0.67	0.64
PPP	8.3	1.88	207	188	710	670	5	2.9	6.16	34.5	0.87	0.65

After the wear tests, deformed surfaces of test coupons were examined by Carl Zeiss field emission scanning electron microscope (FE-SEM) to investigate the morphology

of the damages. In addition to that, steel counter body was also investigated to fulfil the same purpose. Some representative SEM images on that are shown in Figures 6.10-6.15 (in the previous chapter). Representative cross-section analysis of wear track in steel-counterpart has also shown in Fig. 6.9, which confirms the presence of transfer film layer (TFL). As evident in literature, such TFLs dictate the coefficient of friction in steady stage as well as wear between rubbing materials [37].

7.3 Wear modelling

7.3.1 Wear data analysis

As aforementioned, Equation 7.1 suggests the definition of the specific wear rate, *k*. With certain loading range, the value of *k* would be a constant, and independent of external variables such *V, F* and *t*. Thus, it can be considered as material property for material selection, and e.g. predicting the wear life of the material. However, when the loading condition becomes harsh i.e. with higher '*pv'* values, the wear rate may significantly increase with further increase '*pv'* and material won't be safe for the service. Thus, representation of wear rate in terms of '*pv*' factor shows a good representation of materials' tribological behaviour as shown in Fig. 7.1. To realize the effect of '*pv'* on wear rate of presently investigated materials, tribological tests were carried out under different combinations of pressure and velocity, namely: (a) 0.1 m/s and 1 MPa, (b) 0.5 m/s and 1 MPa, (c) 0.5 m/s and 2 MPa, (d) 0.5 m/s and 3 MPa and (e) 1 m/s and 2 MPa. As evidence from the figure (Fig. 7.1), at higher '*pv*' range (> 1 MPa m/s), wear rate of PPP and PEEK is sharply increase with further increase of '*pv'* values. However, the wear rate of PBI and PEEK composites remains almost

unchanged. The sharp increase of wear rate is normally attributed to degradation of the materials at higher contact temperatures occurring within higher '*pv*' range under specific conditions. In that respect, HPPs composites exhibits better wear resistance at higher '*pv*' range due to reinforcing effect of nanoparticles. PBI shows the highest wear resistance due to its inherent polymer microstructure. Regarding such data analysis it is very important to note that, in presence case only limited data points (6 points for each materials) were collected and plotted, due to time constraint to finalize the project. Thus, limitations and some uncertainties towards extrapolate the trend lines should be exercised with cautions, as wear rate and wear mechanics vary considerable with test parameters. Thus, present data set are only valid to predict the performance of the composites in the range of test conditions used in this work.

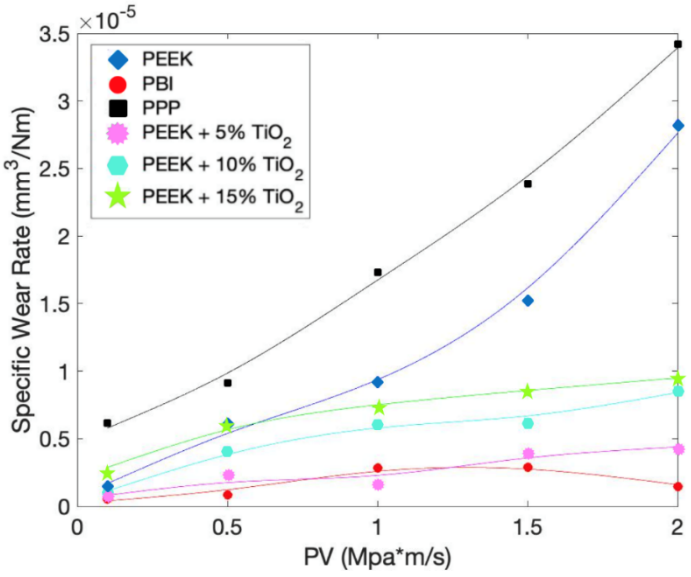

Fig. 7. 1. Variation of specific wear rate of presently investigated materials with respect to '*pv*' factor.

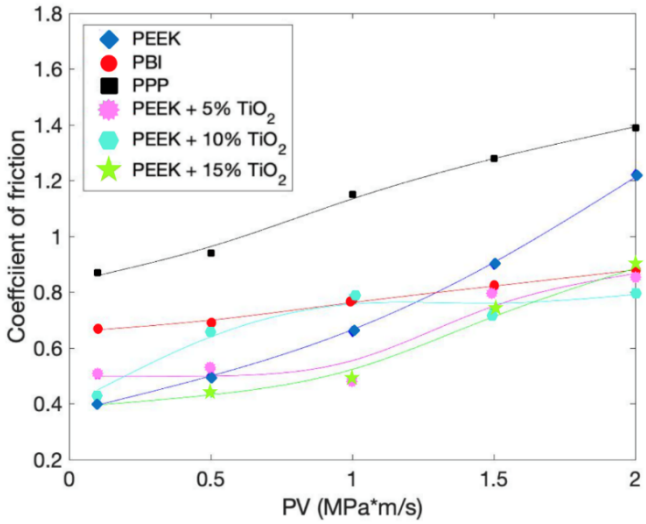

Fig. 7. 2. Evolution of coefficient of friction in terms of '*pv*' factors.

For comparison, the dependence of coefficient of friction on '*pv*' factor was also illustrated, as shown in Fig. 7.2. In lower end of the '*pv*' factor the coefficient of friction is almost constant; however increase with the increase of '*pv*' factor further. This is due to change in contact condition at the sliding interface, breakdown of TFLs as well as generation of frictional heat which is considerable in higher '*pv*' conditions. It is interesting to note, in the case of PEEK the coefficient of friction is lowest among all the materials at lower '*pv*' range, however, keep increasing with the increase of '*pv*' factor. This is a result of adhesive wear in that contact which is more prominent at higher '*pv*' rage due to degradation of materials due to both mechanical and thermal related phenomenon.

To analyse and compare wear data under different sliding conditions for wear modelling, it is important to use the data which is mostly independent of external variable. When it exceeds the '*pv'* limit, the materials' properties in contact region will

be significantly changes, associated with different wear mechanisms involved. This also somewhat indicates the complexity of wear modelling.

7.3.2 Correlation of the wear rate with basic mechanical properties.

Figures 6.9-6.15 also exhibit some important aspect regarding the persistence wear mechanisms that took place during the wear tests. The presence of abrasive marks and formation of wear debris confirm the existence of abrasive wear mechanics, whereas formation of TFL is the confirmation of adhesive wear. In addition to that, fragmentation of reinforcing particles were also evident. Details of experimental results and associated data analysis and discussion can be found in our previous communication (chapter 6).

Based on experimental results, as presented in section 7.2, it can be summarized that, in present case both abrasive and adhesive wear are dominant mechanisms and accordingly should be considered during the modelling of wear rate

7.3.2.1 Correlation between Hardness and Wear Rate

Hardness is the most commonly used material property for wear analysis. In fact, various wear modes have been proposed on the basis of hardness. For instance, it is a widely accepted assumption that abrasive wear took place due to the action of ploughing and cutting of relatively softer materials' surface. These actions took place in two forms: (1) deformation of material due to presence of harder asperities of counter surface and (2) deformation of material due to the exposed/detached hard particles, in the case of particle reinforced composite materials. As a first step to

understand the mechanism of abrasive wear, it is important to estimation the volume of wear that can generate wear particles. Let's assume a simplified contact model where the shape of the abrasive particle is conical in nature and the include angle is θ. The indentation depth made by that conical particle in the test material is d. This has been shown schematically in Fig. 7.3

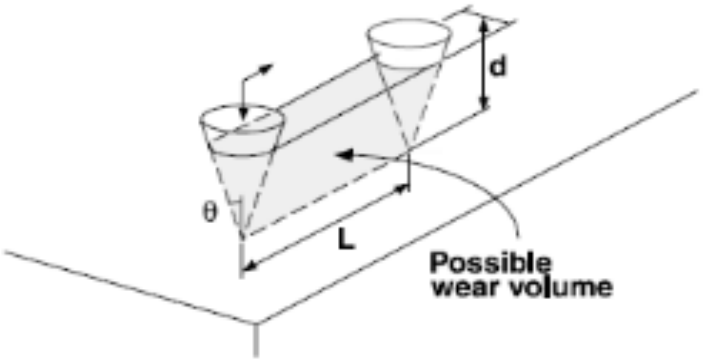

Fig. 7. 3. Schematic of simplified abrasive wear model [156].

According to above mentioned assumption, when this conical shaped particle ploughed through the material for a given sliding a distance (s), the possible wear volume $V_{abrasion}$, can be expressed as [156]:

$$V_{abrasion} = d^2 tan\theta \; s \tag{7.7}$$

On the assumption of Hertzian theory, contact pressure during plastic deformation is equal to that of the hardness H of relatively softer material and thus, real contact area of $\pi(d\tan\theta)^2/2$ can be stated as:

$$\frac{1}{2}\,\pi\,(d\,tan\theta)^2 = \frac{F_N}{H} \tag{7.8}$$

By equating Eq. 7.8 into Eq. 7.7, wear volume due to the action of abrasion can be expressed as:

$$V_{abrasion} = \frac{2}{\pi tan\theta}\frac{F_N s}{H} \tag{7.9}$$

The above Eq. (7.9) is the expression of ideal situation where wear volume generates due to the abrasive action of an abrasive particle that is grooving in relatively softer materials according to the model shown in Fig. 7.3. However, in reality the wedge may not grow from its starting size and thus does not contribute towards wear particle generation [157]. Thus, the volume of the grove is not equal to the volume of the abrasive. To accommodate such uncertainties, a coefficient has added in Eq. (7.9) as a modifier, which is known as abrasive coefficient $k_{abrasive}$ [156] and expressed as:

$$V_{abrasion} = k_{abrasive}\frac{F_N s}{H} \tag{7.10}$$

In the case of adhesive wear, asperities junctions between two mating parts deform, due to shear force and give rise to wear of materials. The real contact can be considered as the summation of equal sized *n* contact points. If a new contact point form as a result of deformation of former ones, the total contact points stay constant on course of sliding. If the contact area is circular in nature with radius *r*, then the possible volume of wear particles that are generated after sliding the distance of 2r is equal to the half of the volume of the sphere. Based on that, wear volume $w_{adhesive}$ for a total number of n contacts after sliding '*s*' distance can be expressed by Eq. (7.11):

$$w_{adhesive} = n\frac{2}{3}\pi r^3\frac{s}{2r} \tag{7.11}$$

As stated before, in plastic deformation zone, normal contact pressure is almost equal to the hardness of relatively softer material and thus, summation of total real contact area for n number of contact points $n\pi r^2$ is:

$$n\pi r^2 = \frac{F_N}{H} \tag{7.12}$$

Equating Eq. 7.12 into Eq. 7.11, possible wear volume $w_{adhesive}$ due to adhesion under the applied load load of F_N after travelling a sliding distance of s is expressed as [156]:

$$w_{adhesive} = \frac{1}{3}\frac{F_N s}{H} \tag{7.13}$$

According to Eq. (7.13), adhesive wear volume is also directly proportional to the normal load, real contact area and sliding distance; and inversely proportional to the hardness relatively softer material. In practice, number of different wear modes can operate individually or simultaneously during adhesive wear and there is no guaranty that wear particles size will simply correspond contact size. In addition, wear particles not necessarily generated from relatively softer material but also can come from counter body as well. To make the scenario more complex, generation of wear particles at each contact point varies and dictated by number of aspects such as microscopic shape of contact, microstructure of the material in contact region, surface contamination and imperfections as well as disturbances of the surroundings. To accommodate such uncertainties, a coefficient termed as $k_{adhesive}$ has included in Eq. 7.13 [151] and can be expressed as:

$$w_{adhesive} = k_{adhesive}\frac{F_N s}{H} \tag{7.14}$$

As both abrasion and adhesion took place simultaneously during the wear process and practically not possible to separate, effect of both abrasion and adhesion on wear can be expressed as:

$$V_{abrasion} + V_{adhesion} = (k_{abrasive} + k_{ahesion})\frac{F_N L}{H} \quad (7.15)$$

$$V_{ab+ad} = V_{abrasion} + V_{adhesion} = K^* \frac{F_N L}{H} \quad (7.16)$$

Where K^* is the wear coefficient. Based on above discussion it can be concluded that, hardness or yield strength of the material have most influence on wear of materials as theoretically predicted according to Eq. 7.16. The relationship between specific wear rate and such materials' properties of presently investigated materials are show in Fig. 7.4

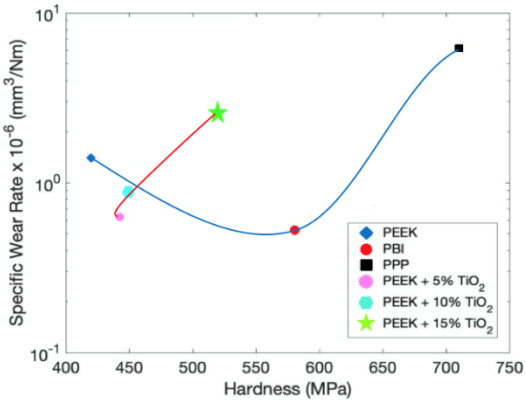

Fig. 7. 4. Variation of specific wear rate of presently investigated materials with respect to hardness.

As shown in the figure, wear rate decreases with the increase of hardness of neat polymers towards some extent and after that a further increase of hardness is associated with the increase of the wear rate. One possible reason is the decrease in toughness and ductility of material with the increase of hardness. In fact, some wear models

emphasized more the dependence of wear on the fracture energy of the polymer, e.g. in abrasive, which will be discussed in the following section.

7.3.2.2 Correlation between Fracture Toughness and Wear Rate

According to the well-known Ratner–Lancaster correlation [162-163], wear can be considered due to effect of elongation to break, i.e. the work to rupture determined by the product of stress and strain at rupture was used as damage criterion for the relationship. In this case, the fracture energy would play a key role in determining the wear rate of polymers. Thus, fracture toughness of materials are important properties to be considered in wear behaviour of materials as shown in Fig. 7.5.

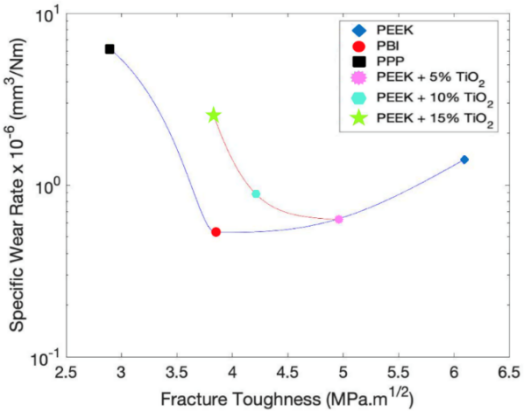

Fig. 7. 5. Effect of fracture toughness on specific wear rate of materials.

Similar to the results shown in section 7.3.1, PBI shows moderate fracture toughness which also contribute to their highest wear resistance. In contrast, though PEEK and PEEK composite shows highest fracture toughness, their wear resistance is moderate. However, the scenario is different for nano-particle reinforced HPP composites. Although the wear resistance of HPP composite can be improved with nanoparticles,

there is also a critical nano-particle content in HPPs, beyond which particle agglomeration took place and as a result increase the wear rate, which exactly happed in the case of 15 % TiO_2 loaded PEEK composite. Thus in present case 5 % TiO_2 addition in PEEK seems to provide the best wear resistance and thus, this is the critical particle content. Reinforcing particles in the polymer composites are ceramic in nature, thus prone to brittle fracture, though much harder compared to both polymeric matrix and steel counterpart. Assuming single particle contact by steel counterpart asperities, the actions can be mimicked as shown in Fig. 7.6. Therefore, fracture toughness greatly influences the wear rate materials, in particular the ones that are brittle in nature. In such cases, it is assumed that propagation of the lateral cracks towards the surface plays the vital role towards the generation of wear particles.

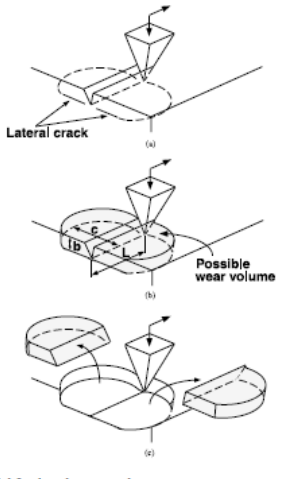

Fig. 7. 6. Abrasive wear model for brittle material [151].

7.2.2.3 Additional Remarks

Influence of mechanical properties such as hardness, fracture stress and ultimate strain on wear volume (V_{mech}) can be expressed according to Eq. (7.17):

$$V_{mech} = \frac{\mu}{H_T \sigma_T \varepsilon_T} \tag{7.17}$$

Where μ is coefficient of friction, σ is fracture stress, ε is ultimate strain and H is hardness of the materials. Figure 7.7 summarize the results based on equation 7.17. It is interesting to note that for pure polymers the equation well predicts the trend. However, for polymer nanocomposites, the wear loss is almost inversely proportional to friction coefficient. This can be explained by the formation of TFLs, which tend to increase friction but decrease wear.

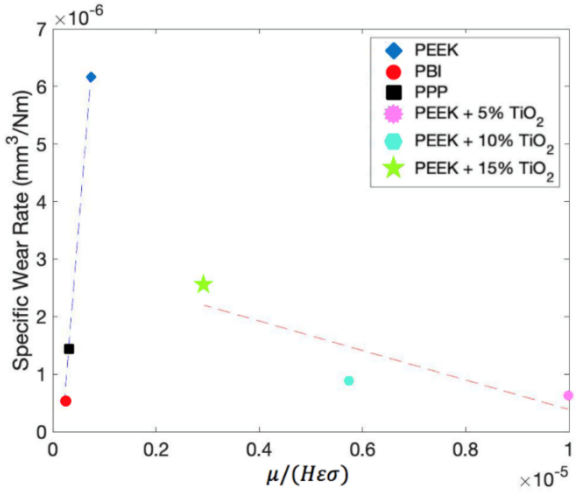

Fig. 7. 7. Variation of specific wear rate in terms of materials' properties that are most dominant to control the wear rate.

Finally, it is worthwhile addressing that mechanical properties of materials, as a whole, is temperature dependent. This is more prominent in the case of polymers and polymeric composites, as usually they are very sensitive to materials. The general temperature dependent equation for mechanical properties of materials is as follows:

$$A_T = A_0\left(1 - \frac{\Delta T}{T_0}\right) \tag{7.18}$$

Where, A_T is an arbitrary mechanical property at a given temperature T, A_0 is same arbitrary property at room temperature, T_0 is room temperature and ΔT is temperature

increase due to either friction or external test temperature or both. It is well known that the mechanical properties of materials are temperature dependent. Thus, when the material is exposed at a higher temperature than that of room temperature, their properties degrade as a function of temperature and expose time in that temperature. It is important to note that, in the case of pin-on-disk wear tests, temperature rise took place momentarily for a fraction of second at tribo-contact, which is known as flash temperature [17]. Thus for simplification purpose, mechanical properties degradation of material can be expressed in term of temperature dependent as shown in Eq. 7.18. This approximation (not taking consideration of time) will be close enough to model the friction and wear behaviour of materials as reported in the literature [147-151]. Hence, to predict wear rate using mechanical properties, it is necessary to determine the contact temperature. The latter can be used to estimate the actual mechanical properties for wear predication. Thus, equation 7.17 can be modified as:

$$V_{mech} = \frac{\mu}{H_0(1-\frac{\Delta T}{T_0})\sigma_0(1-\frac{\Delta T}{T_0})\varepsilon_0(1-\frac{\Delta T}{T_0})} \tag{7.19}$$

In practice, it remains challenging to calculate contact temperature or measure it experimentally, meaning that accurately predicting wear is difficult.

7.4. Modelling of coefficient of friction

As a rule of thumb, coefficient of friction increases with the increase of yield stress for pure materials. However, when the polymers are reinforce with nanoparticles, the scenario is much more complex as real contact area changes frequently with the change in wear mechanisms. Moreover, formation of transfer film layers (TFLs) change the initial polymer/polymer composite-to-metal contact to polymer/polymer composite-to- polymer/polymer composite contact. Thus the results do not show linear relationship, in general, due to the fracture of TFLs as shown in Fig. 7.8.

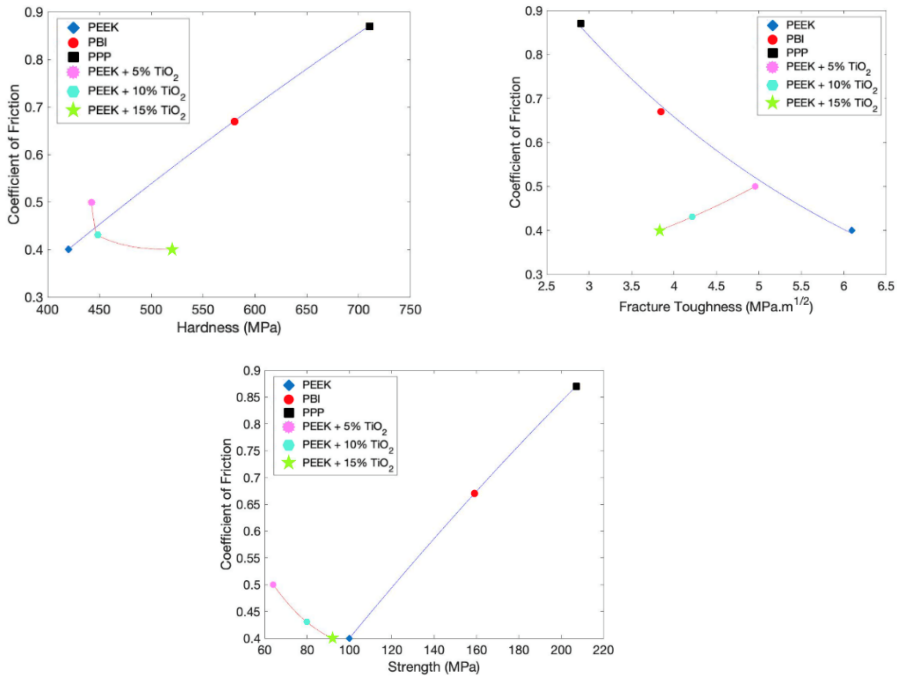

Fig. 7. 8. Variation of coefficient of friction in terms of (a) hardness, (b) fracture toughness and (c) strength.

The general trend is that, in all cases, PEEK shows the lowest co-efficient of friction. This is due to the fact that, PEEK can easily wear off layer-by-layer during the process and act as lubrication films (TFLs) between the contact which represent polymer-on-

polymer contact and thus keep the coefficient of friction in lowest level. The scenario can be represented schematically as shown in Fig. 7.8. Once the asperity is in contact with rigid surface, there is certain penetration depending on the hardness or yielding stress of materials; however, with the change in contact surface it changes accordingly. Thus real contact area (A_r) can be larger or smaller than predicted normal contact area (A_n). As the material become relatively ductile, real contacted area (A_r) will be larger than the normal contact area (A_n) (Fig. 7.9).

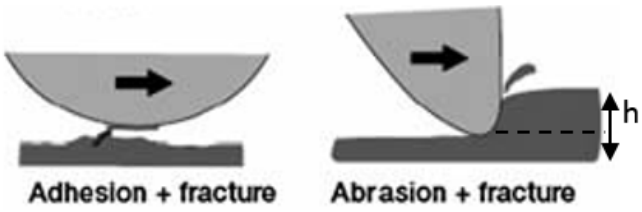

Fig. 7. 9. Schematic representation of effect of wear mechanism on coefficient of friction [151].

If the material shows relatively higher ductility, it push from the back and causes higher resistance force as well as more TFLs formation which in turn increase real contact area (adhesive) and results as higher coefficient of friction. In the case of relatively brittle materials, like epoxy which contain lots of cracks, real contact area (A_r) will be smaller than normal (A_r<A_n) contact area and reduces the friction coefficient. Therefore, harder materials are relatively rigid and brittle and does not fully contribute by yielding stress. In general, shear stress (τ) or yielding stress (σ) multiplied by the contact area will represent the friction force (F) and co-efficient of friction is obtained by dividing it with normal load (N) as shown in Eq. (7.20):

$$\mu = \frac{F}{N} \propto (\tau \; OR \; \sigma)(A_r) \tag{7.20}$$

Thus, yield stress of the material together with coefficient of friction is the dominant factors towards the wear rate which can be expressed according to Eq. 7.6 as stated in section 7.1.

Based on above discussion it can be summarized that, there is no simple relationship between mechanical properties of materials with wear rate. The general trend is that, higher hardness of materials reduce wear rate to some extent under some operating conditions and further increase of hardness actually decrease it as discussed above. On the other hand, coefficient of friction is significantly affected by the yielding behaviour of the materials as well as formation of TFLs due to wear debris generation. Thus an increase of hardness and strength generally increase the coefficient of friction of unreinforced materials. As the materials became reinforced with filers, abrasive wear is more likely to happen and thus give rise to non-linear behaviour.

As stated in section 7.3.1, limited data points were collected and plotted in this section, due to time constraint to finalize the project. Thus, any extrapolation of the trend lines should be exercised with cautions, as wear rate and wear mechanics vary considerable with test parameters. Thus, present data set are only valid to predict the performance of the composites in the range of test conditions used in this work.

7.5. Artificial neural network (ANN) in wear modelling

As evident from above mentioned discussion, there is no simple, universal relationship of mechanical properties of materials with wear rate and coefficient of friction. Normally, it became more and more difficult to establish a single equation for all different materials parameters, different wear conditions and different wear

mechanics. Thus, to get a correlation among experimental data and modelling, artificial neural networks as commonly known as ANNs is a popular tool to correlate the tribological behaviour of polymer composites with their respective materials' properties. This is a quantitative approach to solve experimental wear problems in oppose of traditional equation formulations [159-161]. In this work, ANN system was used to predict the experimental wear data of three different high-performance polymers (PEEK, PPP, and PBI) and PEEK composites under several environmental conditions such as dry condition, high temperature and different '*pv*' factors. ANN was inspired from biological nervous system and now used widely in solving various complex modelling problems in engineering fields. The ANN process involved a number of steps such as:

1. Acquiring data from experimental set-up.
2. Training the procedures and parameters of the ANN.
3. Evaluate the performance of trained network.
4. Application of trained ANNs towards modelling/simulation.

As suggested in literature, the accuracy of the prediction with the help of ANN will be better with the increase training datasets as well as optimizing of network construction. Thus, a large data set is a pre-requisite that has been obtained by a number of tribological experiments as stated earlier in this section. In present work, we have used Bayesian regularization [160] (BR) to train the algorithm. The ANN system has been applied to a total dataset of 60 tribological results. This included six inputs, 25 neurons in the hidden layer and 1 output. Accordingly, neurons in that layer were optimized from the experimental dataset based on random

technique to avoid any discrepancy and the process was repeated 20 times independently.

7.5.1 ANN prediction of wear rate

In the present work, the coefficient of determination has been used to evaluate the ANNs quality, which was identified by Eq. (7.21):

$$R = 1 - \frac{\sum_{i=1}^{M}(O(P^{(i)}) - O^{(i)})^2}{\sum_{i=1}^{M}(O^{(i)} - O)^2} \quad (7.21)$$

where $O_{P(^{i})}$ is the ith predicted property characteristic, O(i) is the ith measured value, O is the mean value of O(i), and M is the number of test data. Thus, larger database (R) means better prediction relatively with smaller data. In this work, ANN to predict the wear results of pure and composite materials under room and high temperature (150 °C) as well as under different pressure and velocity '*pv*'. The inputs data of ANN are: (i) Coefficient of friction and (ii) one of materials mechanical properties (hardness, yielding stress, fracture tautness, elongation at break and modulus of elastic) and the output was predictive wear rate. ANN was applied for both neat and composite materials and the results as presented below.

7.5.1.1 ANN prediction of wear rate on neat polymers

The ANN predictive wear rate on neat polymers as well as polymer composites under various experimental inputs are shown in Fig. 7.10-7.13.

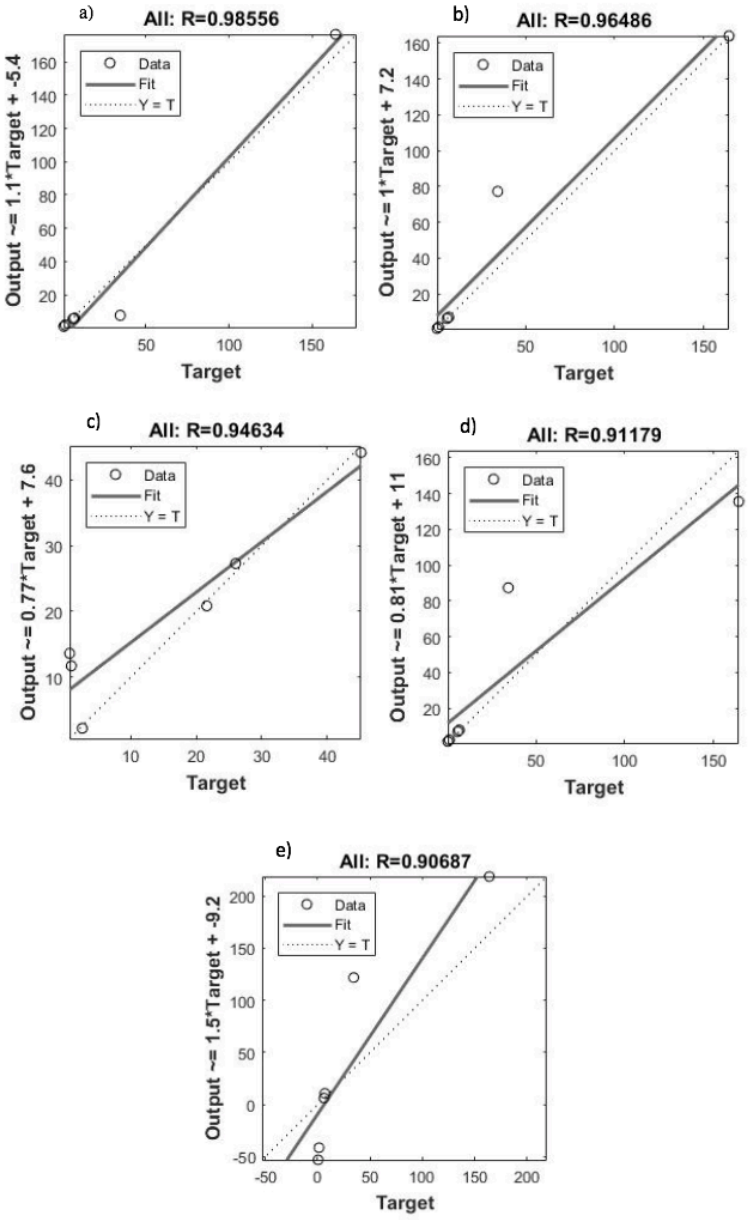

Fig. 7. 10. Comparison of ANN predictive wear rate on neat polymers under unlubricated and high temperature conditions (150 °C), with friction coefficient and different material parameters: (a) hardness, (b) yielding stress, (c) fracture toughness, (d) elongation at break and (e) elastic modulus as the input variables.

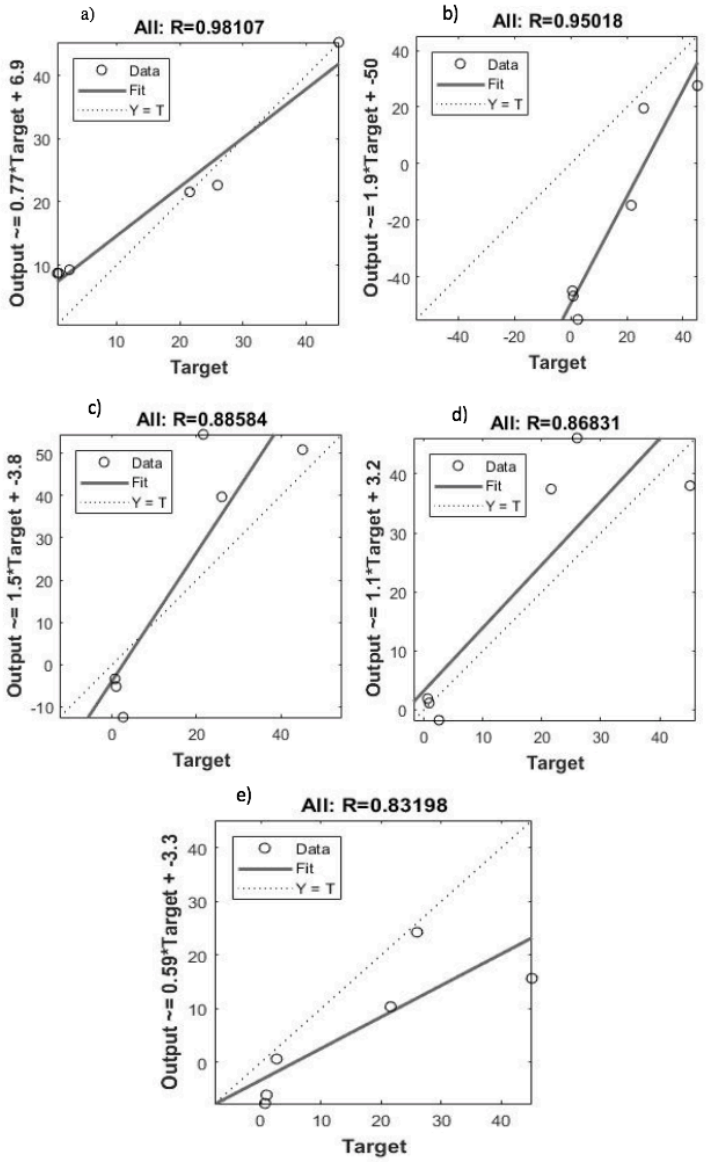

Fig. 7. 11. Comparison of ANN predictive wear rate on polymer composites under unlubricated and high temperature conditions (150 °C), with friction coefficient and different material parameters: (a) hardness, (b) yielding stress, (c) fracture toughness, (d) elongation at break and (e) elastic modulus as the input variables.

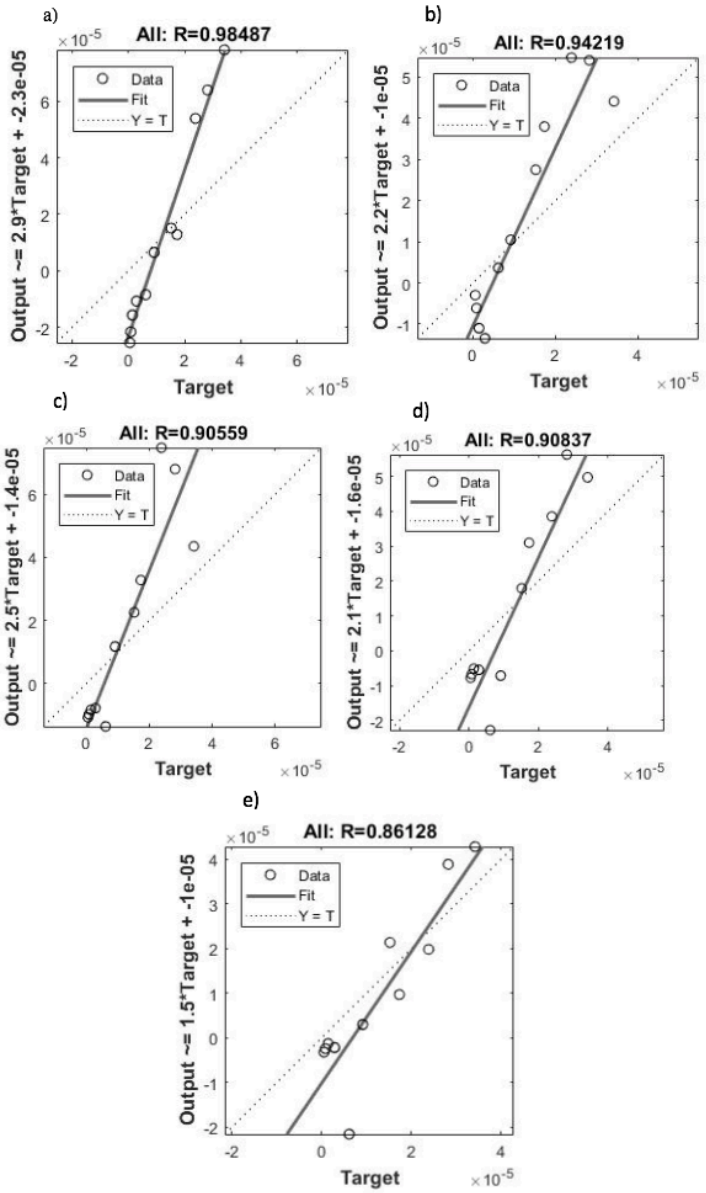

Fig. 7. 12. Comparison of ANN predictive wear rate on neat polymers under different '*pv*', with friction coefficient and different material parameters: (a) hardness, (b) yielding stress, (c) fracture toughness, (d) elongation at break and (e) elastic modulus as the input variables.

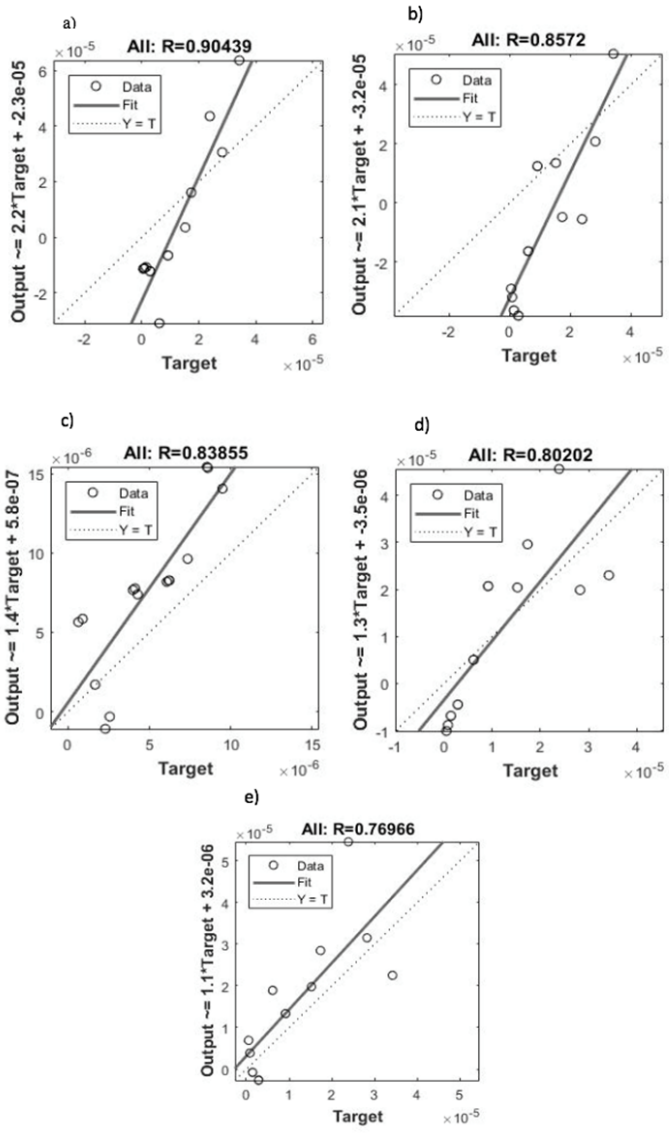

Fig. 7. 13. Comparison of ANN predictive wear rate on polymer composites at different '*pv*' under unlubricated and high temperature conditions (150 °C) with friction coefficient and different material parameters, i.e. (a) hardness, (b) yielding stress, (c) fracture toughness, (d) elongation at break and (e) elastic modulus as the input variables.

As evident from the above figures, hardness and yield stress of materials have most effective influence on the reliability (higher R) compared with other materials' properties. Thus, hardness and yield stress are the most important properties to be considered to select materials for tribological applications. The results also indicated

that, neat polymers show better results under all materials parameters compared with composite materials, which contradict the experimental findings. The reason behind that is still not clear and require further investigation, which was out of the scope of present project. Based on the above-mentioned findings, we can be concluded that "Importance analysis by ANN attempts to investigate the possible correlation between some simple mechanical properties of materials measure parameters (e.g. hardness and yield strength) to more complex properties (e.g. wear), which will be of additional help to materials research for mechanistic understanding." [160]

7.6. Summary

In this study, a simplified wear model was developed based on material's properties and material removal mechanisms process. The material properties used was modulus of elasticity, Poisson's ratio, hardness and strength. Deformation and material removal factors were also incorporated into the model. Subsequently, wear rate was calculated theoretically using the proposed model and verified with experimental results.

Chapter 8. Conclusion and future work

In present research, a systematic approach was utilized to study the tribological performance of thermoplastic and thermosetting polymers subjected to various sliding conditions. Additionally, the study sought to improve the polymer properties by incorporating nano-particles of different elements in neat polymer matrix. A summary of the findings and conclusion of the research were detailed below together with the key recommendations for further studies. The key points from the study are as follows:

- It was realized that, tribological and mechanical properties improved when nano-fillers such as soft nano-rubber (CBTN) and rigid nano-silica (SiO_2) were added into epoxy matrix. Essentially, nano-rubber inclusion improve the fracture toughness of the epoxy matrix but did not significantly contribute towards wear resistance capability of epoxy composite. However, upon addition, nano-silica not only helped to enhance the strength and stiffness of the epoxy composite, but also contribute in achieving the best wear resistance at nominal composition of 8 wt. % nano-silica loading. This was due to better reinforcement dispersion and continuous transfer film layer formation which eventually control the overall friction and wear mechanism. Ductility and brittleness of the nano-fillers themselves greatly influence the size and shape of wear debris.
- The study also examined the changes in the tribological characteristics of PEEK polymer with varying quantities of TiO_2 nano-particles in it. As confirmed by experimental findings, tribological performance and wear-resistance properties of PEEK and PEEK composites significantly improved in

dry conditions compared to wet conditions due to nano-filler addition. The optimum tribological property of PEEK occurred at 5 wt. % content of nanoparticles, at least for room temperature tribological aspects. Overall wear mechanisms are a mixture of abrasive and adhesive wear; and mixed lubrication (solid/solid and solid/water contact) prevails in aqueous media. This enhancement in tribological properties are attributed to the effective formation and retention transfer layer by brittle-ductile transition of associated materials. Notably, aqueous medium did not exhibit the brittle-ductile transition as the generated heat dissipated in water and hence, prevent the transition.

- In addition, an investigation was conducted at various temperatures to assess the performance of three thermoplastic polymers including PBI, PPP, and PEEK and their composites. The findings showed that, PEEK and PEEK composites have higher capability to develop resilient TFLs, even at high temperatures. It was observed that at room temperature, PBI demonstrated higher wear-resistance ability which was attributed to its mechanical properties. However, at higher temperatures above the glass transition temperature, PBI exhibited brittleness caused by failure to effectively formation of TFLs as well as degradation of its mechanical properties. Though, there is no general correlation of mechanical properties of investigated materials with respective wear rate, the trend is that, higher the combination of hardness, rigidity and ductile of materials, better is the wear resistance, at least at room temperature.

- Development of TFLs is controlled by the uniform nano-particles distribution within the polymer matrix. With the increase of nano-filler content, there is a high possibility of particles agglomeration and thus, effectiveness of nano-filler addition is suspended.
- Based on experimental data and concepts of material removal mechanism and material properties were used to develop a simplified wear model. Some of the material properties that were considered to develop the model include: strength, hardness, elasticity modulus as well as material removal factors and deformation mechanics. Thereafter, proposed model was used to determine the theoretical rate of wear which was then compared to the values from experimental findings. Based on the obtained results, it was realized that the developed model accurately predicted the rate of wear when different external parameters such as temperature, sliding velocity, and normal loads were considered. A conclusion was made that wear rate prediction capability improved when a system approach was incorporated in the developed model.

There is still sufficient space for future growths of such HPPs and their composites as pointed out hereafter:

- Most of the works reported in the literature regarding the tribological aspect of HPPs focused on the different type of fibre incorporated HPPs composite with few reports on particles incorporated HPPs. Wear mechanisms of particle type filler incorporated composites differ than that of fibre incorporated composites. Moreover, the recent trend is to use the combination of particle and fibre type reinforce in the same material, which makes the scenario more complex. In that

respect, a more fundamental investigation is foreseen in terms of their interaction and overall effect on friction and wear behaviours of such materials.

- Effect of vibration, both natural and system generated, is another under-research area in this field. Vibration may change the contact mode in mating material and accelerate /decelerate friction and wear accordingly. Proper care should be taken in that respect, as most of the time is has been overlooked.

- There is some contradiction regarding high-temperature tribological aspect of HPPs and their composite, as some authors reported that incorporation of particles does not necessarily increase the wear performance of HPPs composite particularly in high temperature. In addition to that, consideration will be taken regarding the cost of nano-filler incorporation in HPPs and their relative weighted advantages.

- The newly developed model provides useful information related to wear rate prediction of HPPs. The current structure of the model encapsulates materials property as well as material removal mechanisms towards overall wear rate of the materials. However, deformation of material took place in two distinct steps: (1) Initial deformation as the point when the normal load is applied against the counterbody which is both elastic and plastic in nature and (2) subsequent deformation of material on course of sliding process which is mostly plastic. In the current model the initial deformation during loading was overlook with the assumption that, it should be much smaller in magnitude

compared to deformation that took place on course of sliding. So, for model improvement, there is a need to theoretically/experimentally define that initial deformation and include the present model, which was beyond the scope of present work. Therefore, this study recommends a further investigation to find out the relationship between initial loading and corresponding deformation of material which may be defined through a relationship with the help of contact mechanics or experimental or both.

Bibliography

[1] X. Pei, K. Friedrich, Sliding wear properties of PEEK, PBI and PPP, Wear (2012) 274-275.

[2] K. Friedrich, H. J. Sue, P. Liu, A. A. Majid, Scratch resistance of high-performance polymers, Tribo. Int. 44 (2011) 1032-1046.

[3] K. Friedrich, T. Burkhart, A. Al Majid, F. Haupert, Poly-para-phenylene-copolymer (PPP): a high-strength polymer with interesting mechanical and tribological properties, Int. J. Pol. Mat. 59 (2010) 680–692.

[4] K. Friedrich, L. Chang, F. Haupert, Current and future applications of polymer composites in the field of tribology, in: L. Nikolais, M. Meo, E. Miletta (Eds.), Composite Materials (2011) Springer, New York, USA.

[5] Y. Yamaguchi, Tribology of plastic materials: their characteristics and applications to sliding components, Amsterdam (Elsevier) 1990.

[6] D. Tabor, Friction and wear – developments over the last 50 years, Pro. Int. Con. Tribo. - Friction, Lubrication and Wear, London, Ins. Mech. Eng. (1987) 157-172.

[7] J. C. Anderson, The wear and friction of commercial polymers and composites. In: Friction and wear and polymer composites, K. Friedrich (ed.), Composite materials series, vol. 1. Amsterdam, Elsevier 1986, pp. 329-362.

[8] B. H. Stuart, Tribological studies of poly (ether ether ketone) blends, Tribo. Int. 31(11) (1998) 647-651.

[9] K. A. Laux, C. J. Schwartz, Influence of linear reciprocating and multi-directional sliding on PEEK wear performance and transfer film formation, Wear 301 (2013) 727-734.

[10] W. Wieleba, The statistical correlation of the coefficient of friction and wear rate of PTFE composites with steel couterface roughness and hardness, Wear 252 (2002) 719-729.

[11] S. E. Franklin, A. Kraker, Investigation of counterface surface topography effects on the wear and transfer behaviour of a POM-20% PTFE composite, Wear 255 (2003) 766-773.

[12] M. L. Cannaday, A. A Polycarpou, Tribology of unfilled and filled polymeric surfaces in refrigerant environment for compressor applications, Tribo. Lett. 19 (2005) 249-262.

[13] E. E. Nunez, A. A. Polycarpou, The effect of surface roughness on the transfer of polymer films under unlubricated testing conditions, Wear 326 (2015) 74-83.

[14] H. Hunke, N. Soin, T. Shah, E. Kramer, K. Witan, E. Siores, Influence of plasma pre-treatment of Polytetrafluoroethylene (PTFE) micropowders on the mechanical and tribological performance of polyethersulfone (PESU)-PTFE composites, Wear 328-329 (2015) 480-487.

[15] H. Hunke, N. Soin, A. Gebhard, T. Shah, E. Kramer, K. Witan, A. A. Narasimulua, E. Siores, Plasma modified polytetrafluoroethylene (PTFE) lubrication of α-olefin-copolymer impact-modified Polyamide 66, Wear 338-339 (2015) 122-132.

[16] A. K. Basak, A. Pramanik, M. N. Islam, Failure mechanisms of nanoparticle reinforced metal matrix composite, Adv. Mat. Res. 774 (2013) 548-551.

[17] L. Chang, K. Friedrich, G. Zhang, New insights into wear behaviour of high performance polymers, 14th world congress in mechanism and machine science, Taipei, Taiwan, 25-30 October 2015.

[18] S. Bahadur, The development of transfer layers and their role in polymer tribology, Wear 245 (2000) 92–99.

[19] C. Gao, G. Zhang, T. Wang, Q. Wang, Enhancing the tribological performance of PEEK exposed to water-lubrication by filling goethite (α-FeOOH) nanoparticles, Roy. Soc. Chem. Adv. 6 (2016) 51247-51256.

[20] S. Bahadur, C. J. Schwartz, The influence of nanoparticle fillers in polymer matrices on the formation and stability of transfer film during wear, Tribology of polymeric nanocomposites, K. Friedrich and A. K. Schlarb, eds., Elsevier, New York, (2008) 548–34.

[21] S. Bahadur, C. Sunkara, Effect of transfer film structure, composition and bonding on the tribological behavior of polyphenylene sulfide filled with nano particles of TiO_2, ZnO, CuO and SiC, Wear 258 (2005) 1411-1421.

[22] N. G. Demas, J. Zhang, A. A. Polycarpou, J. Economy, Tribological characterization of aromatic thermosetting copolyester-PTFE blends in air conditioning compressor environment, Tribol. Lett. 29 (2008) 253-258.

[23] J. Zhang, N. G. Demas, A. A. Polycarpou, J. Economy, A new family of low wear low coefficient of friction polymer blends based on polytetrafluoroethylene and aromatic thermosetting polyester, Pol. Adv. Technol. 19 (2008) 1105-1112.

[24] T. Sheiretov, W. Van Glabbeek, C. Cusano, Evaluation of the tribological properties of polyimide and poly(amide-imide) polymers in a refrigerant environment, Tribo. Trans. 38 (1995) 914-922.

[25] T. C. Ovaert, S. Ramachandra, The effect of counterface topography on polymer transfer and wear, Int. J. Mach. Tools Manuf. 35 (1991) 311-316.

[26] T. C. Ovaert, H. S. Cheng, Counterface topographical effects on the wear of polyetheretherketone and polyetheretherketone-carbon fibre composite, Wear 150 (1991) 275-287.

[27] Z. Rasheva, G. Zhang, T. Burkhart, A correlation between the tribological and mechanical properties of short carbon fibres reinforced PEEK materials with different fibre orientations, Tribo. Int. 43 (2010) 1430-1437.

[28] K. Friedrich, J. Flöck, K. Váradi, Z. Néder, Experimental and numerical evaluation of the mechanical properties of compacted wear debris layers formed between composite and steel surfaces in sliding contact, Wear 251 (2001) 1202–1212.

[29] ASM Handbook Volume 8: Mechanical Testing and Evaluation, Ed. H. Kuhn and D. Medlin (2000), ASM International, ISBN: 978-0-87170-389-7.

[30] Nuclear reactor abeyance seal system relies on Victrex PEEK (News article), Sealing technology, 2013 (9) (2013) 16-17.

[31] M. Z. Rong, W. H. Ruan, Nanoparticles/Polymer Composites: Fabrication and Mechanical Properties. In: J. Karger-Kocsis Kocsis, S. Fakirov editors. Nano- and Micro Mechanics of Polymer Blends and Composites, Munich: Hanser Publishers 2009, p. 93-140.

[32] K. Friedrich, Polymer composites for tribological applications, Advanced Industrial and Engineering Polymer Research, 1 (1) (2018) 3-39.

[33] G. Zhang, B. Wetzel, Q. Wang, Tribological behaviour of PEEK-based materials under mixed and boundary lubrication conditions, Tribo. Int. 88 (2015) 153–161.

[34] K. Friedrich, Z. Zhang, A. K. Schlar, Effects of various fillers on the sliding wear of polymer composites, Compo. Sci. Technol. 65 (2005) 2329–2343.

[35] J. Zhang, L. Chang, S. Deng, L. Ye, Z. Zhang, Some insights into effects of nano particles on sliding wear performance of epoxy nano composites, Wear 304 (2013) 138–143.

[36] L. Chang, K. Friedrich, Enhancement effect of nanoparticles on the sliding wear of short fibre-reinforced polymer composites: A critical discussion of wear mechanisms, Tribol. Int. 43 (2010) 2355–2364.

[37] L. Chang, K. Friedrich, L. Ye, Study on the transfer film layer in sliding contact between polymer composites and steel disks using nanoindentation, J. Tribol. 136 (2014) 1-12.

[38] K. Tanaka, Transfer of semicrystalline polymers sliding against a smooth steel surface, Wear 75 (1982) 183–199.

[39] M. G. Jacko, P. H. S. Tsang, S. K. Rhee, Wear debris compaction and friction film formation of polymer composites, Wear 133 (1989) 23–38.

[40] P. S. M. Dougherty, R. Pudjoprawoto, C. F. Higgs, An investigation of the wear mechanism leading to self-replenishing transfer films, Wear 272 (2011) 122-132.

[41] N. S. M. El-Tayeb, I. M. Mostafa, The effect of laminate orientations on friction and wear mechanisms of glass reinforced polyester composite, Wear 195 (1996) 186-191.

[42] L. Chang, Z. Zhang, C. Breidt, K. Friedrich, Tribological properties of epoxy nanocomposites: I. Enhancement of the wear resistance by nano-TiO_2 particles, Wear 258 (2005) 141–148.

[43] L. Chang, Z. Zhang, Tribological properties of epoxy nanocomposites: II. A combinative effect of short fibre with nano-TiO_2, Wear 206 (2006) 869–878.

[44] A. Abdelbary, Wear of polymer on wet condition, In Wear of Polymers and Composites, A. Abdelbary, ed., Woodhead Publishing, Elsevier (2015) 95-112.

[45] Q. Wang, Q. Xue, H. Liu, W. Shen, J. Xu, The effect of particle size of nanometer ZrO_2 on the tribological behaviour of PEEK, Wear 209 (1-2) (1997) 316–321.

[46] C. Gao, G. Guo, F. Zhao, T. Wang, B. Jim, B. Wetzel, G. Zhang and Q. Wang, Tribological behaviours of epoxy composites under water lubrication conditions, Tribol. Int. 95 (2016) 333–341.

[47] Q. Wang, Q. Xue, W. Shen, J. Zhang, The friction and wear properties of nanometer ZrO_2-filled polyetheretherketone, J. App. Pol. Sci. 69 (1998) 135-141.

[48] X. Shao, W. Liu, Q. Xue, The tribological behaviour of micrometer and nanometer TiO_2 particle-filled poly (phthalazine ether sulfone ketone) composites, J. App. Pol. Sci. 92 (2004) 906-914.

[49] Q. Wang, Q. Xue, W. Shen, The friction and wear properties of nanometre SiO_2 filled polyetheretherketone, Tribol. Int. 17(30) (1997) 193-197.

[50] V. E. Bakhareva, I. V. Gorynin, A. V. Anisimov, I. V. Lishevitch, I. V. Nikitina, Heat resistant antifriction carbon plastics with super thermoplastic polymer matrix, Inorg. Mat.: App. Res. 6 (6) (2015) 595-601.

[51] S. W. Zhang, State-of-the-art of polymer tribology, Tribo. Int. 31 (1998) (1-3) 49-60.

[52] L. Chang, Z. Zhang, L. Yec, K. Friedricha, Tribological properties of high temperature resistant polymer composites with fine particles, Tribol. Int. 40 (2007) 1170-1178.

[53] F. E. Kennedy, Frictional heating and contact temperatures, in: B. Bhushan (Ed.), Modern Tribology Handbook, CRC Press LLC (2001).

[54] L. Chang, G. Zhang, H. Wang, K. Fu, Comparative study on the wear behaviour of two high-temperature-resistant polymers, Tribol. Lett. 65 (2017) 34.

[55] G. Zhang, H. Yub, C. Zhang, H. Liao , C. Coddet, Temperature dependence of the tribological mechanisms of amorphous PEEK (polyetheretherketone) under dry sliding conditions, Acta Mater. 55 (2008) 2182–2190.

[56] P. Samyna, J. Quinteliera, P. De Baetsa, G. Schoukensb, Characterization of polyimides under high-temperature sliding, Mat. Lett. 59 (2005) 2850- 2857.

[57] L. Chang, Z. Zhang, H. Zhang, A. K. Schlarb, On the sliding wear of nanoparticles filled polyamide, Compo. Sci. Technol. 66 (2006) 3188–3198.

[58] J. F. Archard, Wear theory and mechanisms, Wear control handbook, ASME, New York, 1980.

[59] T. Tevruz, Tribological behaviours of bronze-filled polytetrafluoroethylene dry journal bearings, Wear 230 (1999) 61-69.

[60] Z. Zhang, C. Breidt, L. Chang, F. Haupert, K. Friedrich, Enhancement of the wear resistance of epoxy: short carbon fibre, graphite, PTFE and nano-TiO_2, Compos. A 35 (2004) 1385-1392.

[61] C. J. Hooke, S. N. Kukureka, P. Liao, M. Rao, Y. K. Chen, The friction and wear of polymers in non-conformal contacts, Wear 200 (1996) 83-94.

[62] C. C. Lawrence, T. A. Stolarski, Rolling contact wear of polymers: a preliminary study, Wear 132 (1989) 83-91.

[63] S. Bahadur, D. Gong, The role of copper compounds as fillers in the transfer and wear behaviour of polyetheretherketone, Wear 154 (1992) 151-165.

[64] W. Österle, A. I. Dmitriev, B. Wetzel, G. Zhang, I. Häusler, B. C. Jim, The role of carbon fibres and silica nanoparticles on friction and wear reduction of an advanced polymer matrix composite, Mat. Des. 93 (2016) 474-484.

[65] G. Zhang, C. Zhang, P. Nardin, W.-Y. Lia, H. Liao, C. Coddet, Effects of sliding velocity and applied load on the tribological mechanism of amorphous poly-ether–ether–ketone (PEEK), Tribology international 41 (2008) 79–86.

[66] P. B. J. Briscoe, Y. Lin Heng, T. A. Stolarski, The friction and wear of poly(tetrafluoroethylene)-poly (etheretherketone) composites: An initial appraisal of the optimum composition, Wear 108 (1986) 357-374.

[67] G.Zhang, L.Chang, A. K.Schlarb, The roles of nano-SiO_2 particles on the tribological behaviour of short carbon fibre reinforced PEEK, Compo. Sci. Technol. 69 (2009) 1029-1035.

[68] M. A. Chowdhury, M. M. Helali, The effect of amplitude of vibration on the coefficient of friction for different materials, Tribo. Int. 41 (4) (2008) 307-314.

[69] M. A. Chowdhury, M. M. Helali, The effect of frequency of vibration and humidity on the coefficient of friction, Tribol. Int. 39 (2006) 958-962.

[70] D. M. Nuruzzaman, M. A. Chowdhury, Ch 14, Friction and wear of polymer and composites, pp. 300-330.

[71] Q.-H. Wang, Q.-J. Xue, W.-M. Liu, J.-M. Chen, Effect of nanometer SiC filler on the tribological behaviour of PEEK under distilled water lubrication, J. App. Pol. Sci. 78 (2000) 609-614.

[72] Y. Yamamoto, M. Hashimoto, Friction and wear of water lubricated PEEK and PPS sliding contacts. Part 2. Composites with carbon or glass fibre, Wear 257 (2004) 181–189.

[73] Y. Yamamoto, T. Takashima, Friction and wear of water lubricated PEEK and PPS sliding contacts, Wear 253 (2002) 820–826.

[74] T. A. Stolarski, Tribology of poly ether ether ketone, Wear 158 (1992) 71–78.

[75] H. Unal, A. Mimaroglu, Influence of test conditions on the tribological properties of polymers, Ind. Lub. Tribol. 55(4) (2003) 178-183.

[76] M. M. Gauthier, Engineered materials handbook, ASM international (desk edition) (1995).

[77] G.T. Wang, H.Y. Liu, Z.Z Yu, Y.W. Mai, Evaluation of methods for stiffness predictions of polymer/clay nanocomposites, J. Reinfor. Plas. Compo. 28 (2009) 1625-1649.

[78] J. Liu, H. J. Sue, Z.J. Thompson, F. S. Bates, M. Dettlof, G. Jacob, Nano-cavitation in self-assembled amphiphilic block copolymer-modified epoxy, Macromolecules 41 (2008) 7616-7624.

[79] J. K. Chen, G. T. Wang, Z. Z. Yu, Z. P. Huang, Y. W. Mai, Critical particle size for interfacial debonding in polymer/nanoparticle composites, Compos. Sci. Technol. 70 (2010) 861-872.

[80] K. Friedrich, M. Evstatiev, S. Fakirov, O. Evstatiev, M. Ishii, M. Harrass, Microfibrillar reinforced composites from PET/PP blends: processing, morphology and mechanical properties, Compo. Sci. Technol. 65 (2005) 107-116.

[81] J. Wang, B. Chen, N. Liu, G. Han, F. Yan, Combined effects of fiber/matrix interface and water absorption on the tribological behaviours of water-lubricated polytetrafluoroethylene-based composites reinforced with carbon and basalt fibres, Compo. A, 59 (2014) 85-92.

[82] H. Pelletier, V. L. Houerou, C. Gauthier, R. Schirrer, Scratch experiments and finite element simulation: friction and nonlinearity effects, In: S. k. Sinha, B. J. Briscoe (eds.) Polymer tribology, London, UK, Imperial College Press, Ch. 4 (2009) 108-140.

[83] A. Golchin, K. Friedrich, A. Noll, B. Prakash, Tribological behaviour of carbon-filled PPS composites in water lubricated contacts, wear 328-329 (2015) 456-463.

[84] D. Zhang, H. Qia, F. Zhao, G. Zhang, T. Wang, Q. Wang, Tribological performance of PPS composites under diesel lubrication conditions, Tri. Int. 115 (2017) 338-347.

[85] E. L. Yang, J. P. Hirvonen, R. O. Toivanen, Effect of temperature on the transfer film formation in sliding contact of PTFE with stainless steel, Wear 146 (1991) 367–376.

[86] R. Pudjoprawoto, P. Dougherty, F. C. Higgs, A volumetric fractional coverage model to predict frictional behaviour for in situ transfer film lubrication, Wear 304 (2013)173-182.

[87] G. Zhang, T. Burkhart, B. Wetzel, Tribological behaviour of epoxy composites under diesel-lubricated conditions, Wear 307 (2013)174-181.

[88] Q. Zhao, S. Bahadur, A study of the modification of the friction and wear behavior of polyphenylene sulfide by particulate Ag_2S and PbTe fillers, Wear 217 (1998) 62–72.

[89] C. Lhymn, Lubricated wear of fiber-reinforced polymer composites, Wear 122 (1988) 13-31.

[90] E. Y. A. Wornyoh, C. F. Higgs, An asperity-based fractional coverage model for transfer films on a tribological surface, Wear 270 (2011)127-139.

[91] C. F. Higgs, E. Y. A. Wornyoh, An in-situ Mechanism for self-replenishing powder transfer films: experiments and modelling, Wear 264 (2008) 131-138.

[92] R. Browning, G. Lim, A. Moyse, L. Sun, H.-J. Sue, Effects of slip agent and talc surface treatment on the scratch behaviour of TPOs, Poly. Eng. Sci. 46 (2006) 601-608.

[93] H. Jiang, R. Browning, H.-J. Sue, Understanding of scratch induced damage mechanisms in polymers, Pol. 50 (2009) 4056-4065.

[94] H. Unal, A. Mimaroglu, U. Kadioglu, H. Ekiz, Sliding friction and wear behaviour of polytetrafluoroethylene and its composites under dry conditions, Mat. Des. 25 (2004) 239-245.

[95] S. Bahadur, Y. Zheng, Mechanical and tribological behaviour of polyester reinforced with short glass fibres, Wear 137 (1990) 251-266.

[96] S. Bahadur, V. K. Polineni, Tribological studies of glass fabric-reinforced polyamide composites filled with CuO and PTFE, Wear 200 (1996) 95-104.

[97] E. Santner, H. Czichos, Tribology of polymers, Tribo. Int. 22(2) (1989) 103-109.

[98] J. SEPPALA, M. HEINO, C. KAPANEN, Injection-Moulded Blends of a Thermotropic Liquid Crystalline Polymer with Polyethylene Terephthalate, Polypropylene, and Polyphenylene Sulfide, J.Apple. Polym. Sci. (1992) 44:1051.

[99] Y. Sirong, Y. Zhongzhen, M. Yiu-Wing, Effects of SEBS-g-MA on tribological behaviour of nylon 66/organoclay nanocomposites, Tribo. Int. 40 (2007) 855-862.

[100] H. Liu, G. Wang, Y. Mai, Y. Zeng, On the fracture toughness of nano particle modified epoxy, Composites Part B, 42 (2011), pp. 2170-2175

[101] A. Borruto, G. Crivellone, F. Marani, Influence of surface wettability on friction and wear tests, Wear 222 (1998) 57–65.

[102] A. Wang, S. Yan, B. Lin, X. Zhang, X. Zhou, Aqueous lubrication and surface microstructures of engineering polymer materials (PEEK and PI) when sliding against Si3N4, Friction 5(4) (2017) 414–428.

[103] N. Chen, N. Maeda, M. Tirrell, J. Israelachvili, Adhesion and friction of polymer surfaces: The effect of chain ends, Macromolecules 38 (2005) 3491-3503.

[104] Arash Golchin, Tribological behavior of polymers in lubricated contacts, PhD thesis, 2013, Department of Engineering Sciences and Mathematics, Luleå University.

[105] H. Zhao, Y. Feng, J. Guo, Polycarbonateurethane films containing complex of copper (II) catalyzed generation of nitric oxide, J. App. Pol. Sci. 122 (2011) 1712-1721.

[106] T. Tevruz, Tribological behaviours of carbon-filled polytetrafluoroethylene dry journal bearings, Wear 221 (1998) 61-68.

[107] H. Pihtili, N. Tosun, Investigation of the wear behaviour of a glass fibre-reinforced composite and plain polyester resin, Compo. Sci. Technol. 62 (2002) 367-370.

[108] F Hakami, A Pramanik, N Ridgway, AK Basak, Developments of rubber material wear in conveyer belt system, Tribo. Int. 111 (20017) 148-158.

[109] Q. Xue, Q. Wang, Wear mechanisms of polyetheretherketone composite filled with various kinds of SiC, Wear 213 (1997) 54–58.

[110] X. S. Xing, R. K. Y. Li, Wear behavior of epoxy matrix composites filled with uniform sized sub-micron spherical silica particles, Wear 256 (2004) 21–26.

[111] M. Z. Rong, M. Q. Zhang, H. Liu, H. M. Zeng, B. Wetzel, K. Friedrich, Microstructure and tribological behavior of polymetric nanocomposites, Industrial Lubrication and Tribology 53 (2001) 72–77.

[112] K. Friedrich, Particulate dental composites under sliding wear conditions, Journal of Materials Science: Materials in Medicine 4 (1993) 266–272.

[113] S. Guang, M. Q. Zhang, M. Z. Rong, B. Wetzel, K. Friedrich, Friction and wear of low nanometer Si_3N_4 filled epoxy composites, Wear 254 (2003) 784–796.

[114] S. Guang, M. Q. Zhang, M. Z. Rong, B. Wetzel, K. Friedrich, Sliding wear behavior of epoxy containing nano-Al_2O_3 particles with different pretreatments, Wear 256 (2004) 1072–1081 .

[115] C. K. Lam, K. T. Lau, Tribological behavior of nanoclay/epoxy composites, Materials Letters 61 (2007) 3863–3866.

[116] K. Friedrich, R. Walter, H. Voss, J. Karger-Kocsis, Effect of short fiber reinforcement on fatigue crack propagation and fracture of PEEK matrix composites, Composites 17 (1986) 205–216.

[117] J. Karger-Kocsis, K. Friedrich, Effect of temperature and strain rate on fracture toughness of PEEK and its short glass fiber composites, Polymer 27 (1986) 1753–1760.

[118] B. Wetzel, F. Haupert, K. Friedrich, M. Q. Zhang, M. Z. Rong, Impact and wear resistance of polymer nanocomposites at low filler content, Polymer Engineering and Science 42 (2002) 1919–1927.

[119] Q. B. Guo, K. T. Lau, M. Z. Rong, M. Q. Zhang, Optimization of tribological and mechanical properties of epoxy through hybrid filling, Wear 269 (2010) 13–20.

[120] A. J. Kinloch, R. Mohammed, A. Taylor, C. Eger, S. Sprenger, D. Egan, The effect of silica nano-particles and rubber particles on the toughness of multiphase thermosetting epoxy polymers, Journal of Materials Science 40 (2015) 5083-5086.

[121] K. Friedrich, Erosive wear of polymer surfaces by steel ball blasting, Journal of Materials Science 21 (1986) 3317–3332.

[122] M. H. Cho, S. Bahadur, Study of the tribological synergistic effects in nano CuO filled and fiber reinforced polyphenylene sulfide composites, Wear 258 (2005) 835–845.

[123] Y. L. Liang, R. A. Pearson, The toughening mechanism in hybrid epoxy–rubber nano-composites (HESRNs), Polymer 51 (2010) 4880-4890.

[124] Z. Zhang, C. Breidt, L. Chang, K. Friedrich, Wear of PEEK composites related to their mechanical performances, Tribology International 37 (2004) 271–277.

[125] G. T. Wang, On fracture toughness and fatigue resistance of polymer/nanoparticle composites, Phd thesis, The University of Sydney (2010).

[126] J. C. Halpin, J. L. Kardos, The Halpin–Tsai equations – a review, Polymer Engineering and Science 16(5) (1976) 344-352.

[127] C. Gao, G. Guo, F. Zhao, T. Wang, B. Jim, B. Wetzel, G. Zhang and Q. Wang, Tribological behaviors of epoxy composites under water lubrication conditions, Tribology international 95 (2016) 333–341.

[128] Y. J. Zhong, G.Y. Xie, G.X. Sui, R. Yang, Poly (ether ether ketone) composites reinforced by short carbon fibres and zirconium dioxide nanoparticles: mechanical properties and sliding wear behaviour with water lubrication, Journal of Applied Polymer Science 119 (2011) 1711–1720.

[129] Q. Wang, J. Xu, W. Shen, W. Liu, An investigation of the friction and wear properties of nanometer Si_3N_4 filled PEEK, Wear 196 (1996) 82-86.

[130] X. Shao, W. Liu, Q. Xue, The tribological behavior of micrometer and nanometer TiO_2 particle-filled poly (phthalazine ether sulfone ketone) composites, Journal of Applied Polymer Science 92 (2004) 906-914.

[131] T.Y. Tsui, J. Vlassak, W.D. Nix, Indentation plastic displacement field: Part I. The case of soft films on hard substrates, Journal of materials research 14(6) (1999) 2196–2203.

[132] G. Ellis, M. Naffakh, C. Marco and P. H. Hendra, Fourier transform Raman spectroscopy in the study of technological polymers Part 1: poly (aryl ether ketones), their composites and blends, Spectrochim. Acta, Part A, 1997, 53, 2279–2294.

[133] A. K. Basak, L. Zhang, Deformation of Ti-Based bulk metallic glass under a cutting tip, Tribology Letters 66 (1) (2018) 27-35.

[134] J. Coates, Interpretation of infrared spectra- a practical approach in encyclopedia of analytical chemistry, John Wiley & Sons, Chichester, pp. 10815–10837 (2000).

[135] B. Stuart, Infrared spectroscopy: Fundamentals and applications, John Wiley and Sons, Chichester, pp. 45-47 (2004).

[136] I. Hutchings, R. Winter, J. Field, Solid particle erosion of metals: the removal of surface material by spherical projectiles, in: Pro. Roy. Soc. of London A: Mathematical, Physical and Engineering Sciences. The Royal Society, 1976.

[137] Y. Ben-Ami, A. Uzi, A. Levy, Modelling the particles impingement angle to produce maximum erosion, Powder Technol. 301 (2016) 1032–1043.

[138] G. Sheldon, A. Kanhere, An investigation of impingement erosion using single particles, Wear 21 (1) (1972) 195–209.

[139] S. Biswas, K. Williams, M. Jones, Development of a constitutive model for erosion based on dissipated particle energy to predict the wear rate of ductile metals, Wear 404–405 (2018) 166–175.

[140] I. Finnie, Erosion of surfaces by solid particles, Wear 3 (2) (1960) 87–103.

[141] J. Bitter, A study of erosion phenomena part I, Wear 6 (1) (1963) 5–21.

[142] J. Bitter, A study of erosion phenomena: part II, Wear 6 (3) (1963) 169–190.

[143] H. C. Meng, K. C. Ludema, Wear models and predictive equations: their form and content, Wear 181-183 (1995) 443-457.

[144] S. K. Rhee, Wear equation for polymers sliding against metal surfaces, Wear 16 (1970) 431-445.

[145] J. F. Archard, Contact and rubbing of flat surfaces, J. Appl. Phys. 24 (1953) 981–988.

[146] E. Rabinowicz, Friction and Wear of Materials, Wiley, 1965.

[147] J. F. Archard, W. Hirst, The wear of metals under unlubricated conditions, Proc. R. Soc. A 236 (1956) 397–410.

[148] H. Blok, The flash temperature concept, Wear 6 (1963) 483-494.

[149] A.W. Glaeser, Design of plain bearings for heavy machinery, ASTM STP 1105 (1991) 12-29.

[150] E. Hombogen, The role of fracture toughness in the wear of metals, Wear 33 (1975) 251-259.

[151] A. G. Evans, D. B. Marshall, Wear mechanism in ceramics, in Fundamentals of friction and wear of materials, D. A. Rigney (Ed.) ASM, 439 (1981).

[152] A. Shebani, C. Pislaru, Wear measuring and wear modelling based on Archard, ASTM, and neural network models, Int. J. Mecha. Mechatro. Eng. 9 (1) (2015) 177-182.

[153] Standard Test Method for Wear Testing with a Pin-on-Disk Apparatus, ASTM Publishing, 4.02, USA, 95 (2000).

[154] N. X. Randall, Tribological characterization of biomaterials, Materials for Medical Devices, ASM, ASM Handbook, ASM International Press, 23, Switzerland, 148 (2007).

[155] H. Czichos, Influence of adhesive and abrasive mechanisms on the tribological behaviour of thermoplastic polymers, Wear 88(1) (1983) 27–43.

[156] K. Kato, Koshi Adachi, Wear Mechanisms, (Chapter 7) in Modern tribology handbook, Ed. B. Bhushan, CRC press, London, 2001, ISBN 0-8493-8403-6.

[157] K. Hokkirigawa, K. Kato, An experimental and theoretical investigation of ploughing, cutting and wedge formation during abrasive wear, Tribo. Int. 21 (1) (1988) 51-57.

[158] T. E. Fischer, M. P. Anderson, S. Jahanmir, Influence of fracture toughness on the wear resistance of yttria-doped zirconium oxide, J. Am. Ceram. Soc. 72 (2) (1989) 252-257.

[159] Z. Zhang, K. Friedrich, K. Velten, Prediction of tribological properties of short fibre composites using artificial neural networks, Wear 252 (2002) 668-675.

[160] Z. Zhang, K. Friedrich, Artificial neural networks applied to polymer composites: a review, Compo. Sci. Technol. 63 (2003) 2029-2044.

[161] H. El Kadi, Y. AI-Assaf, Energy-Based fatigue life prediction of fibreglass/epoxy composites using modular neural network, Composite 57 (2002) 85-89.

[162] B. Briscoe, Wear of polymers: an essay on fundamental aspects. Tribol. Int. **14**(4),

[163] J. K. Lancaster, Abrasive wear of polymers. Wear **14**(4), 223–239 (1969).

List of publications based on this work

Journal Article:

A. Kurdi, H. Wang, L. Chang, Effect of nano-sized TiO_2 addition on tribological behavior of poly ether ether ketone composite, Tribology International, 117 (2018) 225–235.

A. Kurdi, W.H. Kan, L. Chang, Tribological behaviour of high performance polymers and polymer composites at elevated temperature, Tribology International, 130 (2019) 94-105.

A. Kurdi, L. Chang Recent Advances in High Performance Polymers - Tribological Aspects, Lubricants, 7(1) (2019) 2-31.

Conference Paper

A. Kurdi, L. Chang, Comparative tribological and mechanical property analysis of nano-silica and nano-rubber reinforced epoxy composites. 2ed International Conference on Material Engineering and Application (ICMEA 2017), August 2017, Shanghai, China: Applied Mechanics and Materials ISSN: 1662-7482, Vol. 875, pp 53-60